



**SEISMIC AND SEQUENCE STRATIGRAPHY OF THE EARLY
CRETACEOUS ECHUCA SHOALS FORMATION, NORTHERN
CASWELL SUB-BASIN, BROWSE BASIN, AUSTRALIA**

**Amir Hidayat, BSc
(University of Pembangunan Nasional)**

**This thesis is submitted in partial fulfillment of the requirements for the
Master of Science in Petroleum Geoscience**

**Australian School of Petroleum,
The University of Adelaide**

November, 2007

ABSTRACT

The Early Cretaceous Echuca Shoals Formation is known as one of the potential source rock intervals in the northern Caswell Sub-basin. Even though hydrocarbons have been discovered in this formation in the adjacent Yampi Shelf Sub-basin, no hydrocarbons have been found in the northern Caswell Sub-basin. Of 12 wells encountered the Echuca Shoals Formation in this sub-basin, only three penetrated sandstone within this interval. Penetrating sand and finding traps in the Echuca Shoals Formation has become a challenge in exploring this area.

Facies analysis and sequence stratigraphic methods were used to identify reservoir sand distributions, to interpret depositional environments, and to predict stratigraphic traps. Reflection configurations from seismic data, log motifs from electric logs and core data were used to identify seismic facies. A chronostratigraphic framework was established for the formation based on spore-pollen biostratigraphy.

The Echuca Shoals Formation in the northern Caswell Sub-basin can be divided into two stratigraphic sequences. Sequence 1 was deposited as lowstand fans and lowstand wedges in a deepwater environment and consists of five channels and five lobes. The channels have a southeast-northwest orientation with an average width to thickness ratio of 1:17. Sequence 2, which was also deposited as lowstand fans and lowstand wedges in a deepwater environment, consists of four channels and four lobes. The channels in Sequence 2 also have a southeast-northwest orientation with an average width to thickness ratio of 1:21.

Terminal pinchouts of channels and lobes may represent stratigraphic traps in the area. The results of this work indicate that in the study area there are seven potential candidates for stratigraphic traps in the Echuca Shoals Formation.

STATEMENT OF CONFIDENTIALITY

Due to a confidentiality agreement between Chevron Australasia Strategic Business Unit and the Australian School of Petroleum, this thesis is not available for public inspection or borrowing until 5 November 2010.

ACKNOWLEDGEMENTS

Alhamdulillah, thanks to Allah SWT for health and opportunity that was given while I am studying in Adelaide.

I would like to thank my advisors R. Bruce Ainsworth, Tobias H.D. Payenberg and Boyan K. Vakarelov for the discussion and their input during the completion of my project. I would like to thank Andrew Mitchell and all ASP staff for their help.

I would like to express my appreciation to Jimmy Dolan, Chris Davin, and management of Chevron Indonesia Co. who provided the financial support during my study. It is a great opportunity for me to pursue my Master's Degree at Australian School of Petroleum, the University of Adelaide.

Thank to Justyn Wood, Joe Ponthier, Mike Barrett, Mike Wilson and the team from Chevron Australasia Strategic Business Unit who helped in providing thesis data and preparing facility while I was in Perth.

Thanks to my friends at Reservoir Analog Research Group for the discussion and great time. Thanks to Kerrie Deller for the discussion and the books. Thanks to all my class mates at ASP (Irma, Chris, Tim, Jess, Wendy, Efthy, Matt, and Blaise) for their help during my study and wonderful time in the class and field trips.

I am especially grateful for patience and understanding from my wife, Ida and my son, Dzaki. Their support has been a great help for me in finishing my study.

TABLE OF CONTENTS

Abstract	i
Statement of Confidentiality.....	ii
Acknowledgements	iii
Table of Contents	iv
List of Figures and Tables	vi
Chapter 1 Introduction	
1.1 Rationale	1
1.2 Objectives.....	1
1.3 Study Area Location	2
1.4 Previous Studies	4
1.5 Work Flows.....	5
Chapter 2 Regional Setting	
2.1 Structural Evolution of the Browse Basin	6
2.2 Tectonostratigraphic Framework.....	11
2.3 Paleogeography	13
2.4 Petroleum Systems	13
2.4.1 Source Rocks.....	13
2.4.2 Reservoir.....	13
2.4.3 Trap Types.....	14
2.4.4 Migration	14
2.4.5 Seal.....	14
2.5 Exploration History	16
Chapter 3 Sedimentology and Sequence Stratigraphy	
3.1 Sedimentology.....	17
3.1.1 Core Description	17
3.1.2 Biostratigraphy	17
3.1.3 Depositional Processes and Models.....	17
3.2 Sequence Stratigraphy.....	20
3.3 Deepwater Sequence Stratigraphy Model.....	22

Chapter 4 Methodology	
4.1 Database	25
4.2 Wireline Log Interpretation	29
4.3 Well to Seismic Tie.....	36
4.4 Seismic Interpretation.....	38
4.5 Geometry Interpretation	40
Chapter 5 Results	
5.1 Sequence 1	42
5.2 Sequence 2	48
Chapter 6 Interpretation and Discussion	
6.1 Sequence 1	52
6.2 Sequence 2	61
Chapter 7 Play Analysis	
7.1 Sequence 1	65
7.2 Sequence 2	69
7.3 Summary	70
Chapter 8 Conclusion and Recommendations	
8.1 Conclusions.....	72
8.2 Recommendations	73
References	74

LIST OF FIGURES AND TABLES

Figure 1.1 Location of the study area which is 740 km south-west of Darwin.	2
Figure 1.2 Location of the study area, Northern Caswell Sub-basin dictated by red arrow.	3
Figure 2.1 Schematic cross-sections illustrating major basin-forming events in the Browse Basin (Struckmeyer et al., 1998).	7
Figure 2.2 Structural elements of the Browse Basin region with Palaeozoic and Jurassic faults (Struckmeyer et al., 1998).	9
Figure 2.3 Major Palaeozoic zones of the Browse Basin overlain on satellite gravity image (Sandwell & Smith, 1995).	10
Figure 2.4 Tectonostratigraphic and petroleum system summary chart for the Browse Basin (Blevin, et al., 1998a).	12
Figure 2.5 Paleogeographic map of Valanginian to Barremian (Longley et al., 2002).	15
Figure 3.1 Classification of deep-marine systems based on sediment volume, grain size and the nature of supplying system (after Richards and Bowman, 1998).	19
Figure 3.2 Five architectural elements of deep-marine clastic systems (after Richards et al., 1998).	20
Figure 3.3 Concept of depositional sequence (Mitchum et al, 1977)	21
Figure 3.4 Block diagrams showing early relative lowstand in sea-level and deposition of lowstand fan (a) and lowstand wedge (b) (Posamentier and Vail, 1988).	23
Figure 4.1 Seismic lines and wells used in this study.	26
Figure 4.2 Good quality seismic data from 130-03.	27
Figure 4.3 Poor quality seismic data from BBHR-175-15B.	27
Figure 4.4 Well correlation from Crux-1 to Buccaneer-1 wells to show distribution the Echuca Shoals Formation in the study area.	30
Figure 4.5 Well correlation from Argus-1 to Productus-1 wells to show distribution the Echuca Shoals Formation in the study area.	31
Figure 4.6 Sequence stratigraphy of Kalyptea-1ST1, Asterias-1, and Productus-1 wells	32
Figure 4.7 Sequence stratigraphy of Gryphaea-1 to Adele-1 wells	33
Figure 4.8 Sequence stratigraphy of Echuca Shoals-1 to Crux-1 wells	34

Figure 4.9 Log responses (Gamma Ray and Resistivity) in Point source mud/sand rich sub-marine system (Richards and Bowman, 1998).	35
Figure 4.10 Amplitude, frequency, and phase spectrum for an extracted wavelet (blue color) using autocorrelation method and trapezoid model wavelet (red color).	37
Figure 4.11 Sonic log, density log, RC series, seismic data and synthetic seismogram for Heywood-1 well. Strong event at 2240 and at 2100 msec correlate very well with the synthetic; however, the synthetic does not match at 2320 msec (red arrow).	37
Figure 4.12 Seismic profile illustrating seismic facies of channel-levee systems and condensed sections and erosional sequence boundary (Weimer, 1991).	39
Figure 4.13 Seismic section line at BBHR 175-12 shows the seismic facies of channel-levee systems in the study area. The seismic was flattened at Base Barremian horizon.	39
Figure 4.14 Graph showing the relationship of channel width to depth (aspect ratio) in deepwater environments (Clark and Pickering, 1996). A red line shows 1:20 aspect ratio.	40
Figure 4.15 Time-depth curves of wells in the study area.	41
Figure 5.1 Seismic line BBHR 175-11 (a) uninterpreted (b) interpreted showing seismic stratigraphic interpretation.	44
Figure 5.2 TWT map of the base of Valanginian horizon. Dashed line shows the zero edge of the Echuca Shoals Formation. Contour interval 100 msec.	45
Figure 5.3 TWT map of the base of Barremian horizon. Dashed line shows the zero edge of the Echuca Shoals Formation. Contour interval 100 msec.	46
Figure 5.4 Isochron map of Sequence 1 (red arrow showing paleodirection of sediment supply). Contour interval 25 msec.	47
Figure 5.5 TWT map of Base Aptian horizon. Dashed line shows the zero edge of the Echuca Shoals Formation. Contour interval 100 msec.	50
Figure 5.6 Isochron map of Sequence 2 (red arrow showing paleodirection of sediment supply). Contour interval 25 msec.	51
Figure 6.1 Electric-log characteristic in mud/sand rich submarine fan systems (Modified after Richards and Bowman, 1998).	54
Figure 6.2 Seismic section line 119-09 (a) uninterpreted and (b) interpreted, showing mound feature interpreted as lobes. The line is flattened at base Barremian.	55
Figure 6.3 Seismic section line BBHR-175-10 (a) uninterpreted (b) interpreted showing divergent shape, interpreted as a channel-levee.	56

Figure 6.4 Seismic section line 119-10 (a) uninterpreted and (b) interpreted, showing clinoform unit, interpreted as a lowstand wedge.	58
Figure 6.5 Paleogeographic map of Sequence-1.	59
Figure 6.6 Sequence 1 channel-levee and fan based on seismic facies interpretation.	60
Figure 6.7 Sequence 2 channel-levee and fan based on seismic facies interpretation.	62
Figure 6.8 Paleogeographic map of Sequence 2.	63
Figure 6.9 Schematic depositional model of the study area.	64
Figure 7.1 Seismic section showing the Scott Reef-Brecknock structural trend, this structural trend is the boundary of the Echuca Shoals Formation.	68
Figure 7.2 Schematic of hydrocarbon expulsion in Sequence 1. Black arrows show the migration direction.	69
Table 3.1 Core description of part of the Echuca Shoals Formation at Kalyptea-1ST1 well.	18
Table 4.1 Seismic surveys that were used in the study area.	25
Table 4.2 Wells used in this study. See figure 4.1 for well locations.	28
Table 6.1 Measurement of geometry features from seismic data.	57
Table 7.1 The coordinates of the potential stratigraphic traps	66

CHAPTER 1 INTRODUCTION

1.1 Rationale

The Browse Basin has recently become an exploration area that is attractive for both big and small oil companies. This was triggered by significant oil and gas field discoveries, improved drilling technology, and high oil and gas prices. The Browse Basin is one of the largest basins in Australia with large hydrocarbon reserves. As of January 2005, reserves in the Browse Basin were estimated as follows: 25.9 TCF of gas, 13.6 MMbbls of oil, 438.2 MMbbls of LPG and 543.4 MMbbls of condensate (Geoscience Australia, 2006).

The Echuca Shoals Formation in the northern Caswell Sub-basin, Browse Basin, is known for its source-rock potential (Blevin et al., 1998b). In another sub-basin (Yampi Shelf), hydrocarbon reservoirs were discovered in the Echuca Shoals Formation when Gwydion-1 (1995) and Cornea-1 (1997) were drilled. Meanwhile, from 19 wells drilled in the northern Caswell Sub-basin, two wells did not penetrate the Echuca Shoals Formation since the formation was not deposited due to a paleogeographic high; three wells did not penetrate the formation because the well depth was too shallow; and 12 wells encountered the Echuca Shoals Formation. From these 12 wells, only three penetrated sandstone within this interval. Therefore, it is a challenge for explorationists to predict the distribution of reservoir sand in this area.

This thesis will utilize seismic and sequence stratigraphic methods as tools to assist with exploration strategies by improving understanding and definition of the reservoir sands in the Echuca Shoals Formation in the northern Caswell Sub-basin, Browse Basin.

1.2 Objectives

The main objectives of this thesis were to build a seismic and sequence stratigraphic framework for the Echuca Shoals Formation and to predict its reservoir sand distribution, detailed as follows:

- Define the depositional environment of the Echuca Shoals Formation (Valanginian to Barremian age).
- Interpret the lithology of the Echuca Shoals Formation based on seismic facies analysis, well log, core and cuttings interpretations.

- Construct a paleogeographic map of the Echuca Shoals Formation.
- Propose drilling targets based on potential stratigraphic trapping configurations.

This study will integrate 2-D seismic data, core data, well log data, and biostratigraphic data.

1.3 Study Area Location

The study area is located in the northern part of the Caswell Sub-basin which is one of the major depocenters of the Browse Basin. It covers an area of approximately 9,500 km², with water depths of 142-572 m. The Browse Basin is a Paleozoic to Cainozoic depocentre located in the southern Timor Sea region of the Australian North West Shelf and is approximately 740 km south-west from Darwin (Figure 1.1). The Browse Basin covers 140,000 km², with water depths of 100-1500 m and contains over 10 km of sediment (Symonds et al., 1994). The Browse Basin is a northeast–southwest trending extensional basin that was part of the Westralian Superbasin during the Carboniferous to Early Permian (Yeates et al., 1987). It is bounded to the southeast by the Yampi and Leveque shelves. The western part is bounded by the Scott Plateau and the northeast part is bounded by the Ashmore Platform (Hocking et al., 1994). Hocking et al. (1994) divided the Browse Basin into the Caswell, Barcoo, Seringapatam Sub-basins and the adjacent Scott Plateau (Figure 1.2).

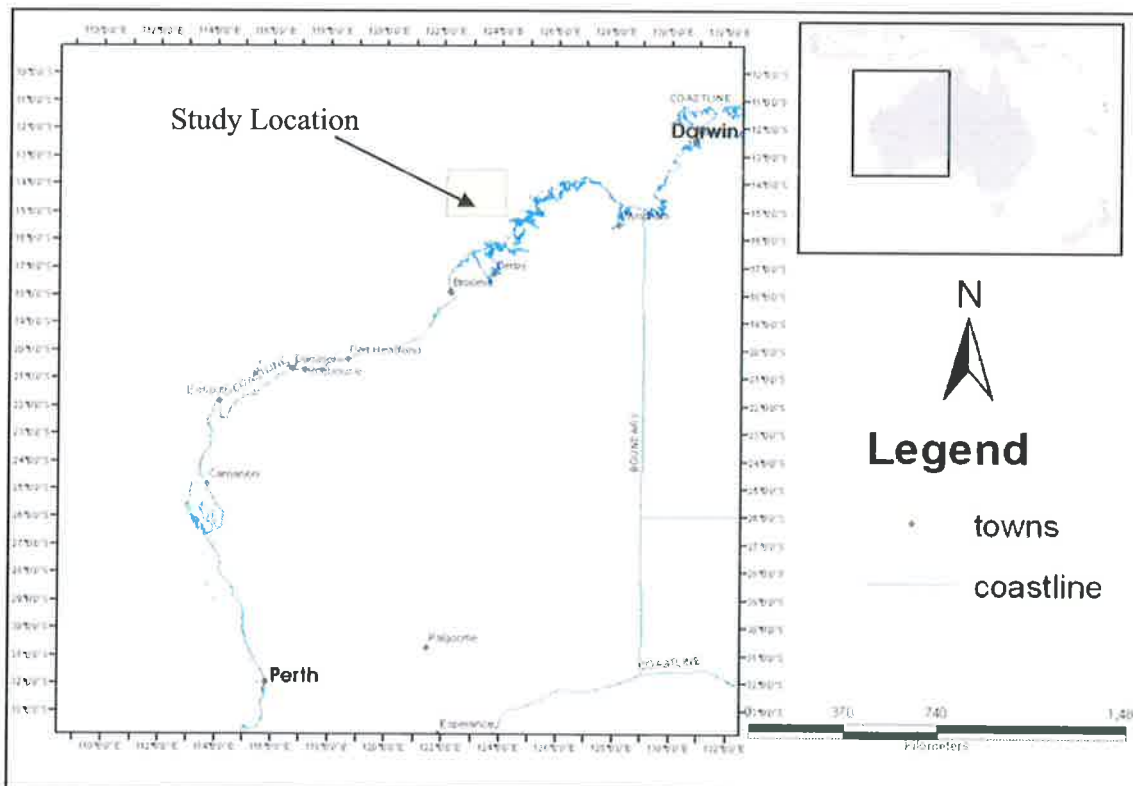


Figure 1.1 Location of the study area which is 740 km south-west of Darwin.

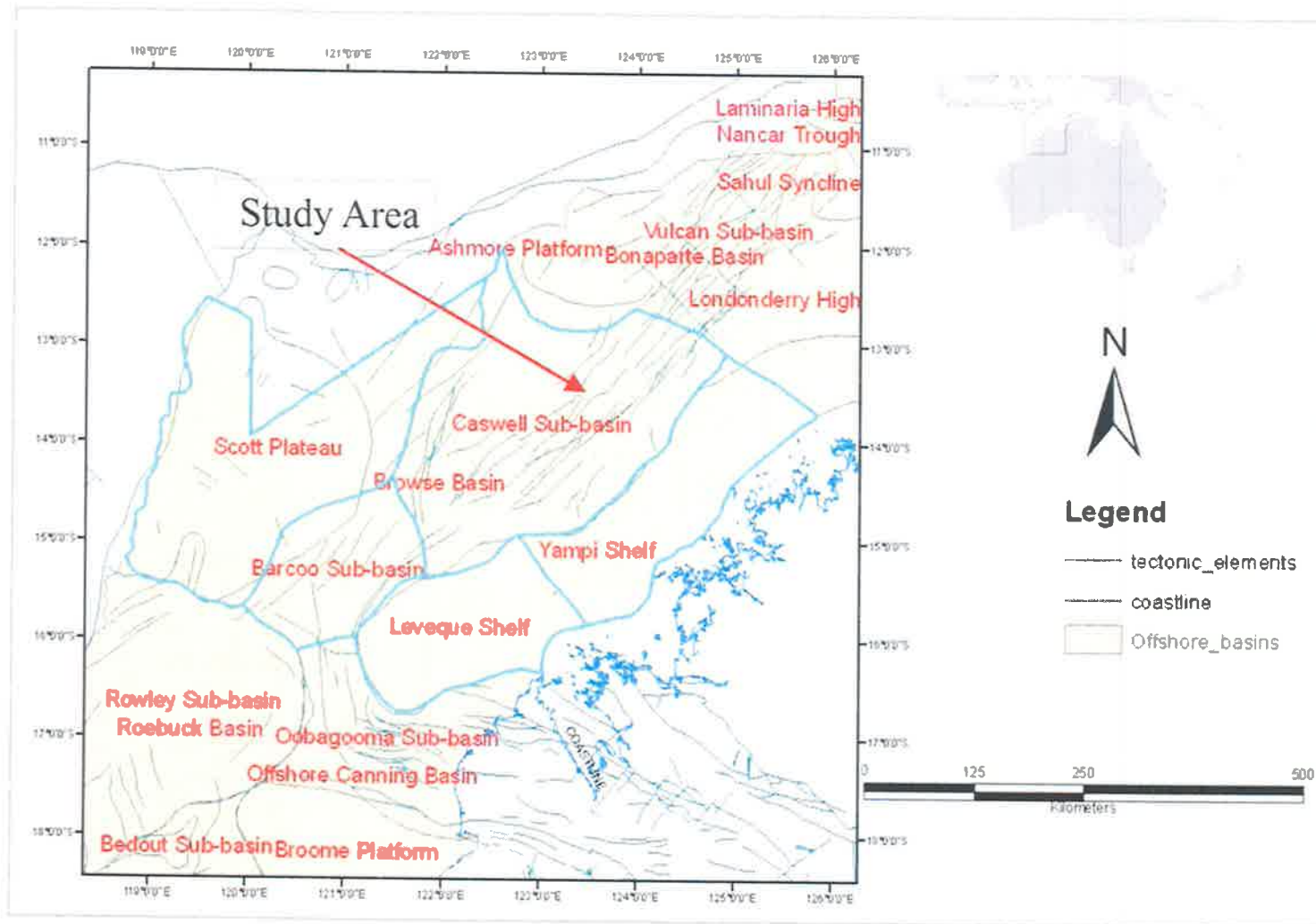


Figure 1.2 Location of the study area, Northern Caswell Sub-basin dictated by red arrow.

1.4 Previous Studies

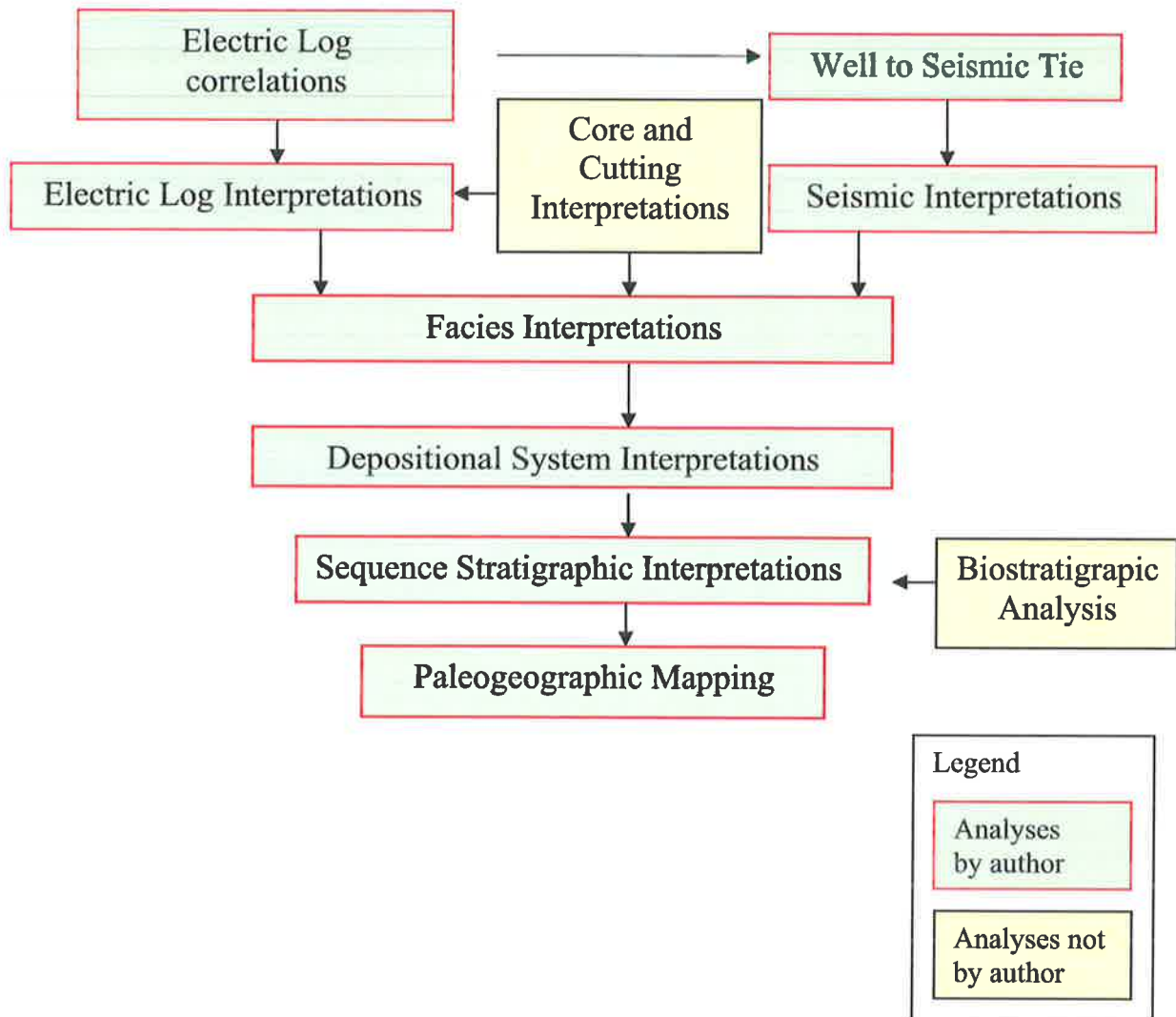
Many authors have published studies on the petroleum system of the Browse Basin. Maung et al. (1994) reviewed the petroleum potential of the Browse Basin and identified structural and stratigraphic play types based on interpretation of seismic data. Symonds et al. (1994) investigated the deep structure of the Browse Basin using the seismic dataset acquired by the Australian Geological Survey Organisation (AGSO) in 1993. A regional tectonostratigraphic framework and petroleum system study of the Browse Basin was then undertaken by AGSO in 1996-1997 and the results were published by Blevin et al. (1998a). Meanwhile, Struckmeyer et al. (1998) published a paper on the structural evolution based on deep seismic data acquired in 1996.

Blevin et al. (1998b) studied the geochemical composition of oil samples to understand the petroleum system for Lower Cretaceous age reservoirs in the Browse Basin after oil discoveries at Cornea-1 and Gwydion-1 in the eastern part of the basin. The Browse Basin had been considered to be gas prone until the oil discovery in Gwydion-1 well (1995). Spry and Ward (1997) of BHP Petroleum discussed the Gwydion discovery in the APPEA Journal.

Fluid inclusion studies were conducted by Brincat et al. (2004) in order to evaluate the oil potential in the Caswell Sub-basin. Hoffman and Hill (2004) published their work on the structural-stratigraphic evolution and hydrocarbon prospectivity of the deep-water Browse Basin. Kennard et al. (2004) modeled the subsidence and thermal history from 33 wells and 25 depocentre sites to examine the generation and expulsion history of Jurassic and Early Cretaceous petroleum systems in the Browse Basin.

1.5 Work Flow

The chart below shows the workflow used in this study.



CHAPTER 2 REGIONAL SETTING

2.1 Structural Evolution of the Browse Basin

The structural evolution of the Browse Basin has been discussed by Symonds et al. (1994) and Struckmeyer et al. (1998). Hoffman and Hill (2004) also discussed the structural and stratigraphic evolution of the Browse Basin in the deepwater part. Based on the interpretation of deep seismic data acquired by the Australian Geological Survey Organisation (AGSO) in 1993, Symonds et al. (1994) proposed that the architecture of Browse Basin mainly resulted from Late Devonian-Early Carboniferous northeast-southwest extension, northwest to north Mid Carboniferous-Early Permian regional extension and Mid Carboniferous-Early Permian lower crustal/upper mantle pure shear extension. Later structural events were the Late Permian-Early Triassic fault reactivation and margin uplift, Middle-Late Triassic inversion and uplift, and Late Triassic fault reactivation, inversion and folding. Symonds et al. (1994) demonstrated that the distribution of the reservoir facies and the source rock has been controlled by these events.

In 1996, AGSO acquired the Browse Basin high resolution seismic grid. Based on this new data, Struckmeyer et al. (1998) identified that there have been six major phases of deformation in the Browse Basin, as summarized in Figure 2.1. These phases are:

- Middle to Upper Miocene inversion
- Upper Jurassic to Cainozoic thermal subsidence
- Lower to Middle Jurassic extension
- Upper Triassic to Lower Jurassic compression and inversion
- Upper Permian to Triassic thermal subsidence, and
- Upper Carboniferous to Lower Permian extension

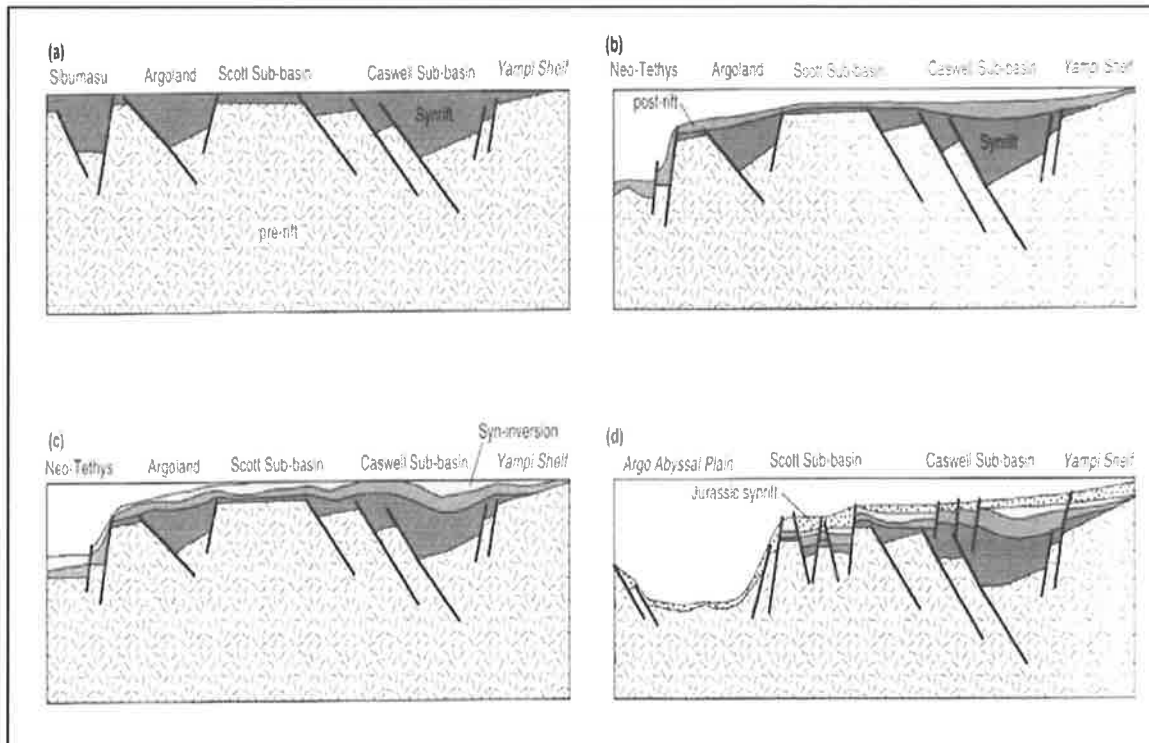


Figure 2.1 Schematic cross-sections illustrating major basin-forming events in the Browse Basin (sections are not to scale): a) Upper Carboniferous to Lower Permian extension; b) Upper Permian to Middle Triassic thermal subsidence; c) Upper Triassic inversion; and d) Lower to Middle Jurassic extension (Struckmeyer et al., 1998)

The Browse Basin was initiated by north-northwest extension during the Carboniferous to Early Permian. This event resulted in large-displacement faults (5 – 8 km throw) that have a predominant northeast-southwest trend. The major displacement faults (Basset, Brewster, Caswell, and Barcoo faults) controlled the sedimentary fill (Figure 2.2). The upper crustal faulting produced half-graben basin geometries in the basin and compartmentalized the Browse Basin into its two major sub-basins, the Caswell and Barcoo Sub-basins. The major rifting phase that occurred during the Late Carboniferous to Permian was followed by a reduction in tectonic subsidence rates in the Browse Basin (Struckmeyer et al., 1998).

In the Late Triassic, a major compressional tectonic event occurred. The Palaeozoic and Triassic strata were inverted and this inversion resulted in the formation of anticlines and synclines within the hanging walls of the Palaeozoic faults. The inversion was marked by a regional unconformity (Struckmeyer et al., 1998).

The Early Jurassic extensional phases caused numerous smaller scale faults which resulted in the collapse of many Triassic anticlines and the erosion of Upper Triassic strata. The Jurassic faults typically have a northeast-southwest trend, parallel to the trend of Palaeozoic faults and Triassic inversion structures (Struckmeyer et al., 1998) (Figure 2.2).

The Late Jurassic rifting event caused reactivation of older structures in the Yampi Shelf and Prudhoe Terrace. In the Late Mesozoic to Cainozoic, accommodation space was controlled by thermal subsidence, minor reactivation events and changes in eustasy and sediment supply (Struckmeyer et al., 1998).

In the Middle of the Late Miocene, inversion structures formed along Palaeozoic faults trends in the Barcoo Sub-basin and small-scale extensive normal faulting in the northern Caswell Sub-basin. Struckmeyer et al. (1998) demonstrated that the Caswell Sub-basin depocenter was delineated by a major Paleozoic fault based on a satellite gravity image (GEOSAT) overlain on the Browse Basin (Sandwell and Smith, 1995) (Figure 2.3).

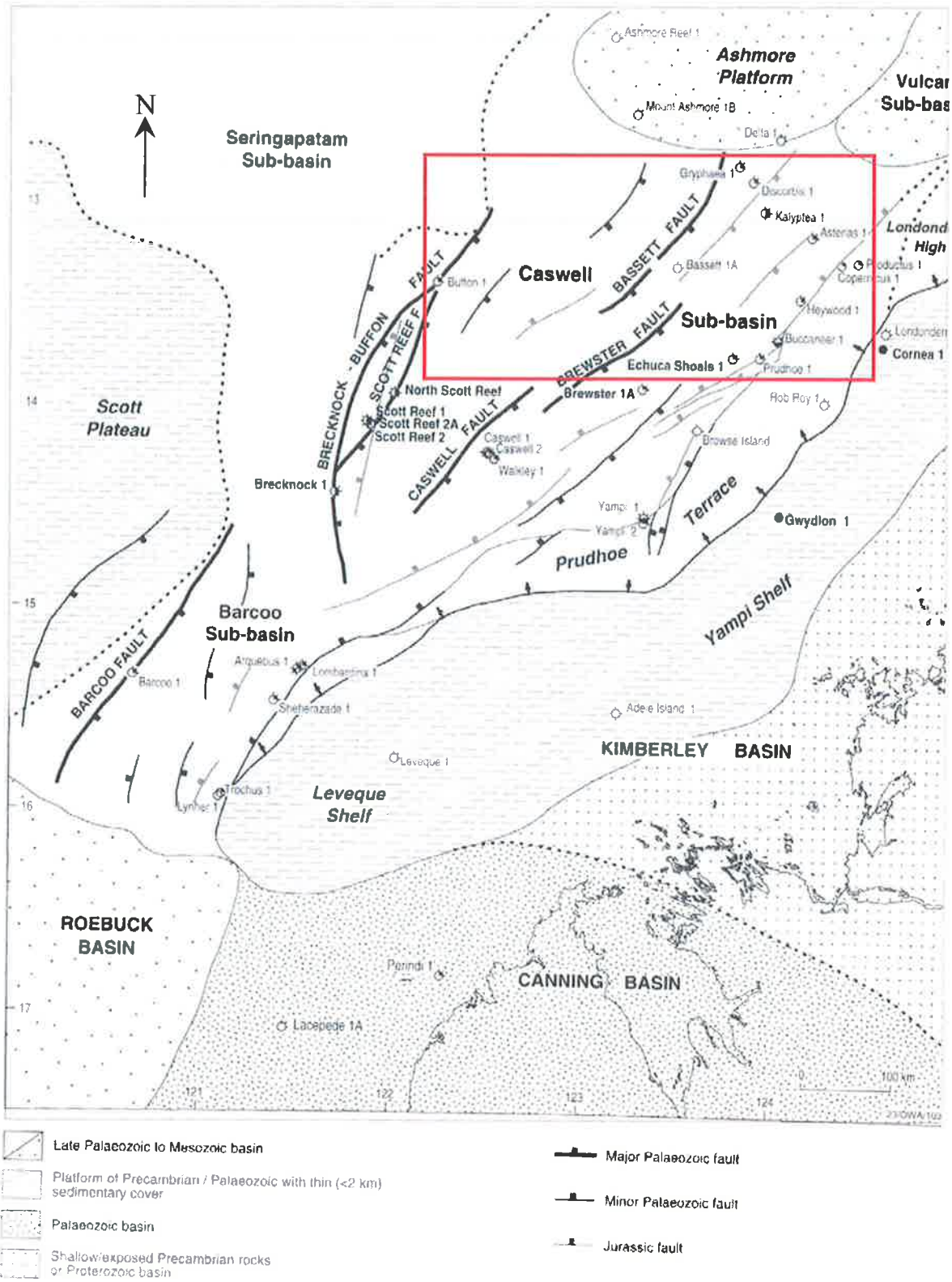


Figure 2.2 Structural elements of the Browse Basin with Palaeozoic and Jurassic faults (Struckmeyer et al., 1998). Red box shows location of study area.

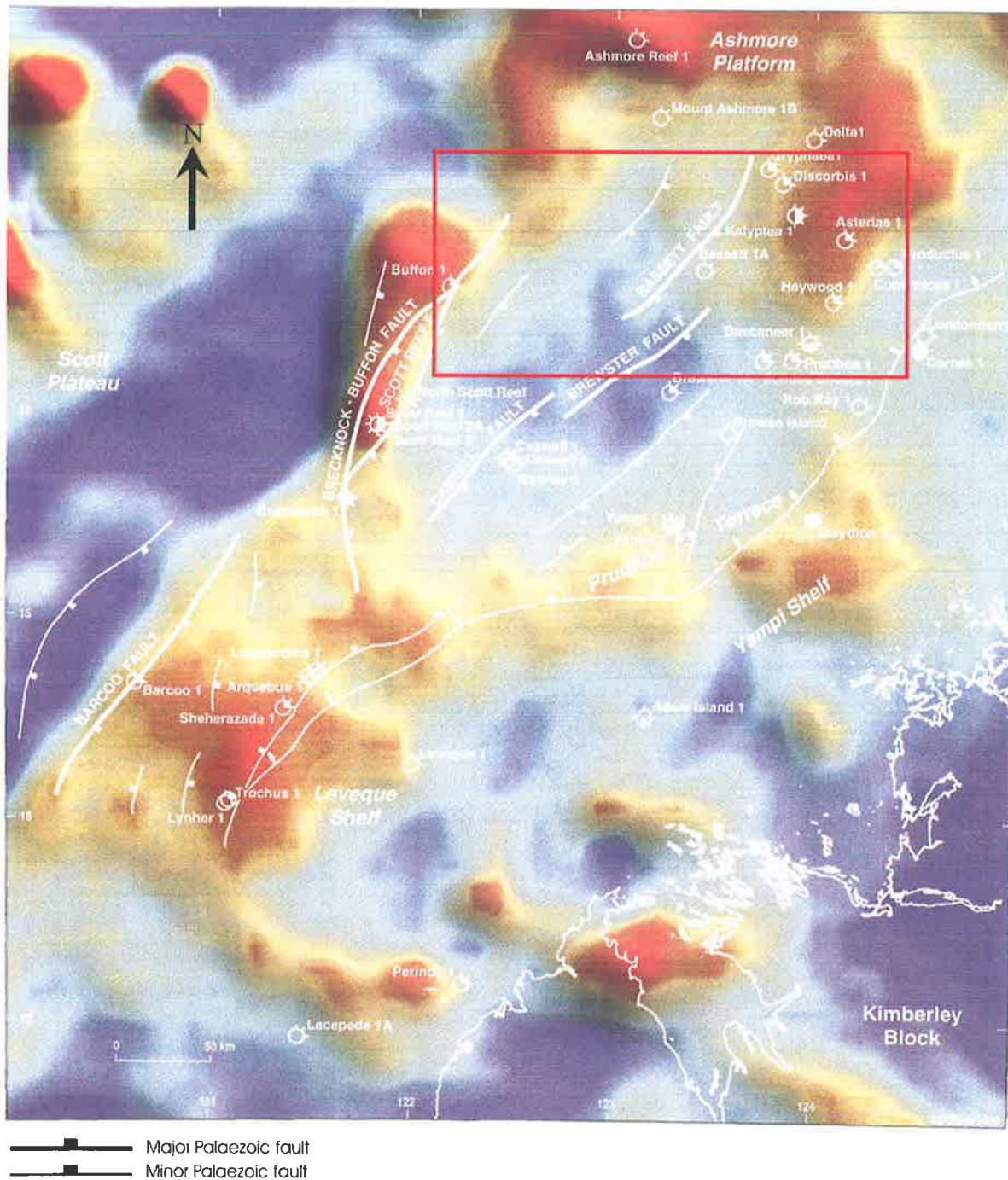


Figure 2.3 Major Palaeozoic zones of the Browse Basin overlain on satellite gravity image (Sandwell and Smith, 1995). Red box shows location of study area.

2.2 Tectonostratigraphic Framework

A stratigraphic study by Blevin et al. (1998a) resulted in establishment of a tectonostratigraphic framework ranging in age from Carboniferous to Late Tertiary (Figure 2.4). The study mapped twenty-two megasequences and supersequences (BB1 to BB22), correlated to the six tectonic phases described by Struckmeyer et al. (1998).

As explained in a previous section, half-grabens were generated in the Browse Basin during the extension-1 phase. Since the sediments in the deepest part of the half grabens have not been penetrated by any wells; the age of the oldest part of the succession is still speculative (Blevin et al., 1998a). The Carboniferous section is generally fluvio-deltaic in nature and the Lower Permian is marine (primarily limestones and shales). The Upper Permian section consists of transgressive sandstones overlain by limestone. The oldest Triassic sequence found in the Browse Basin (eg. Echuca Shoals-1) consists of marine claystones. The most commonly intersected Triassic facies in this basin is a shallow marine succession which consists of limestone grading into siltstones and shales (Blevin et al., 1998a).

The Early to Middle Jurassic was a period of high sediment influx during which a fluvio-deltaic depositional system extended across the basin. The strata intersected in wells are made up of stacked channel sands and/or coarsening-upward prograding deltaic sands, interbedded with finer-grained prodelta to delta plain siltstones and shales. The Upper Jurassic succession is predominantly fluvio-deltaic, and relatively thin across most of the central and western basin (Blevin et al., 1998a).

The Lower Cretaceous succession consists of an upward gradation of lowstand, transgressive and highstand depositional packages. Facies within the lowstand systems tracts include slope fans, prograding fluvio-deltaic, and shallow marine shelfal facies (Blevin et al., 1998a). In the Caswell Sub-basin the sediment infills up to 425 m during the Valangian to Aptian (Hoffman and Hill, 2004). The Turonian to Early Tertiary records the transition from a transgressive to a regressive stacking pattern.

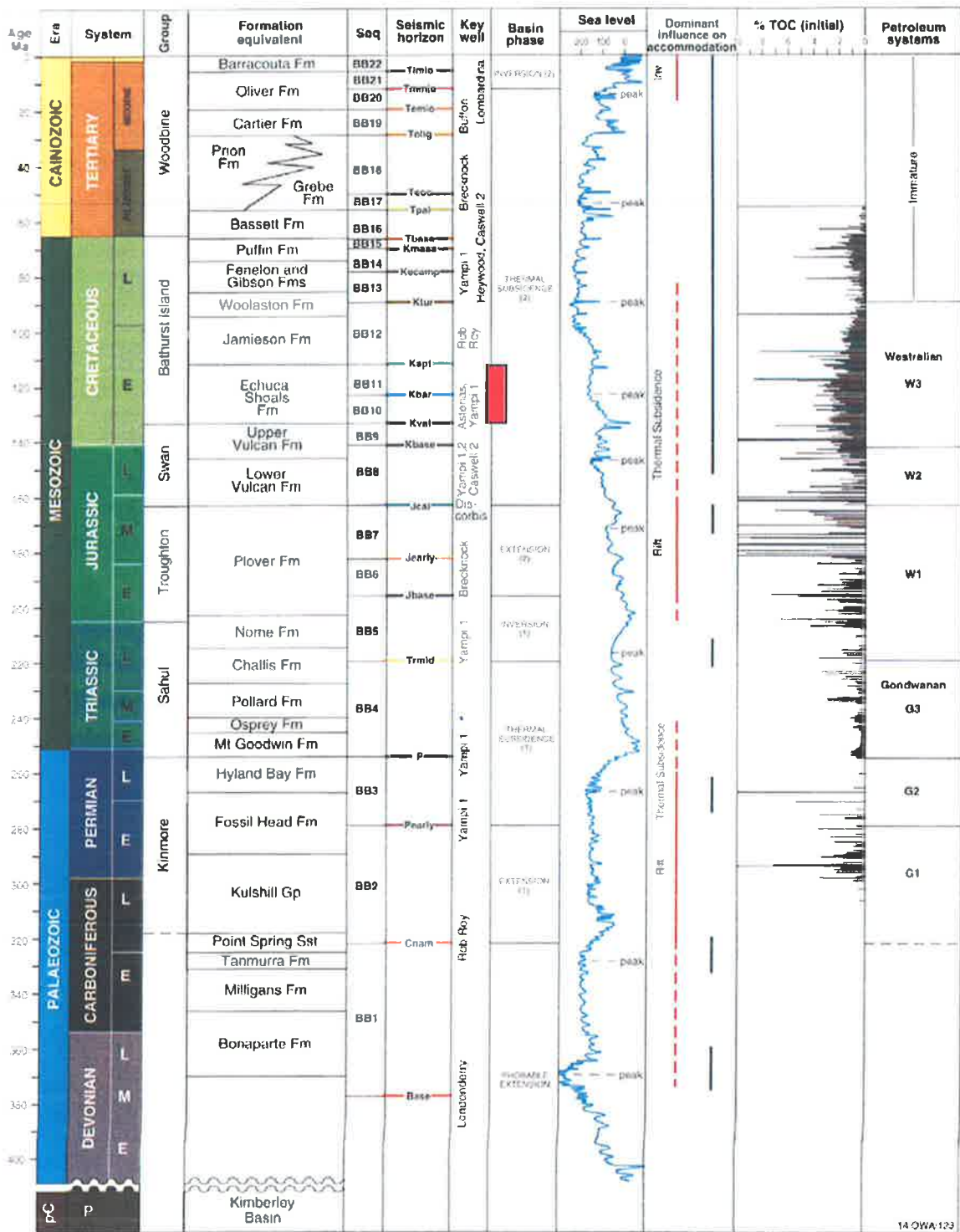


Figure 2.4 Tectonostratigraphic and petroleum system summary chart for the Browse Basin (Blevin, et al., 1998a). Red bar shows location of study interval.

2.3 Paleogeography

Bradshaw et al. (1998) noted that isostatic flexural modeling in the Browse Basin has shown that upper crustal extension alone can not account for the amount of accommodation space created and filled during the Jurassic. Bradshaw et al. (1998) proposed that the thermal anomaly under the Browse Basin was due to a slower rate of cooling resulting in subsidence and sedimentation being “suspended” until the latest Upper Jurassic and Lower Cretaceous, when higher rates of sedimentation and thermotectonic subsidence developed. The Browse Basin contains the thickest Cretaceous depocentre of the North West Shelf, as would be expected with the lower crust extended (Bradshaw et al., 1998). Longley et al. (2002) drew a paleogeographic map of the North West Shelf in the Valanginian to Barremian interval showing the regional paleodirection of sediment supply (Figure 2.5).

2.4 Petroleum Systems

2.4.1 Source Rocks

Based on oil-oil correlations, Blevin et al. (1998b) recognized two populations of oils in the Browse Basin. Population A (Cornea 1, Gwydion 1, Caswell 2 and Kalyptea1ST1) belongs to source rocks of Valanginian to Barremian age, while population B (Scott Reef 1, North Scott Reef 1, and Brecknock 1) still needs further work to determine the age of the source rocks. In the Echuca Shoals Formation, the maturity increased from oil and wet gas to dry gas to the northwest of the Caswell Sub-basin (Kennard et al., 2004). Blevin et al. (1998b) described many intervals in the Upper Jurassic to Lower Cretaceous successions that were considered to have potential oil source rocks (e.g. hydrogen index values of >200 mg hydrocarbons/g TOC) and contain less than 2% TOC. At these low to moderate TOC degrees, if the source rock generated oil, it will stay within the source rock and at higher maturity will subsequently crack to gas. In the Lower Cretaceous system, the maturation was driven by the overburden of Aptian to Tertiary age strata rocks (Blevin et al., 1998b).

2.4.2 Reservoirs

Sand-prone reservoir facies of the Barremian transgressive and lowstand successions are proven reservoir intervals at Londonderry-1 and Gwydion-1. The oil and gas reservoirs in Gwydion-1 have porosities of 24-27% (Spry and Ward, 1997). These facies contain quartzose sands and greensands which are best developed along the Prudhoe Terrace and Yampi Shelf

(Blevin et al., 1998b). The Barremian sands are also developed in Asterias-1, Kalyptea-1, and Crux-1 wells in the northern part of Caswell Sub-basin.

2.4.3 Trap Types

Structural traps of tilted fault blocks and compactional drapes over fault blocks represent the proven trap style in the central and western part of the Browse Basin (Bishop, 1999). Besides structural traps, stratigraphic traps are also present in the Lower Cretaceous. Examples of those are the lowstand fans and onlapping transgressive facies across the Yampi Shelf and Prudhoe Terrace (Blevin et al., 1998b).

2.4.4 Migration

Spry and Ward (1997) noted that in the eastern part of the Browse Basin, hydrocarbon migration paths appear to be initially vertical up the basin margin fault system and then lateral within the sand units of Cretaceous age. The western part of the Browse Basin is more gas prone, while the eastern margin has potential for liquid hydrocarbon exploration.

2.4.5 Seal

The highstand shales which were deposited in the Upper Triassic are potential seal and source facies (Blevin et al., 1998a). Blevin et al. (1998a) noted that in the Lower Jurassic, the interbedding of prodelta and coastal plain facies has created a number of reservoir and seal pairs. The sealing potential has been proven at Brecknock-1 and North Scott Reef-1. In the Echuca Shoals Formation, rapid flooding followed by deposition of highstand shales in Valanginian to Aptian package is interpreted as a potential seal in the Browse Basin (Blevin et al., 1998b).

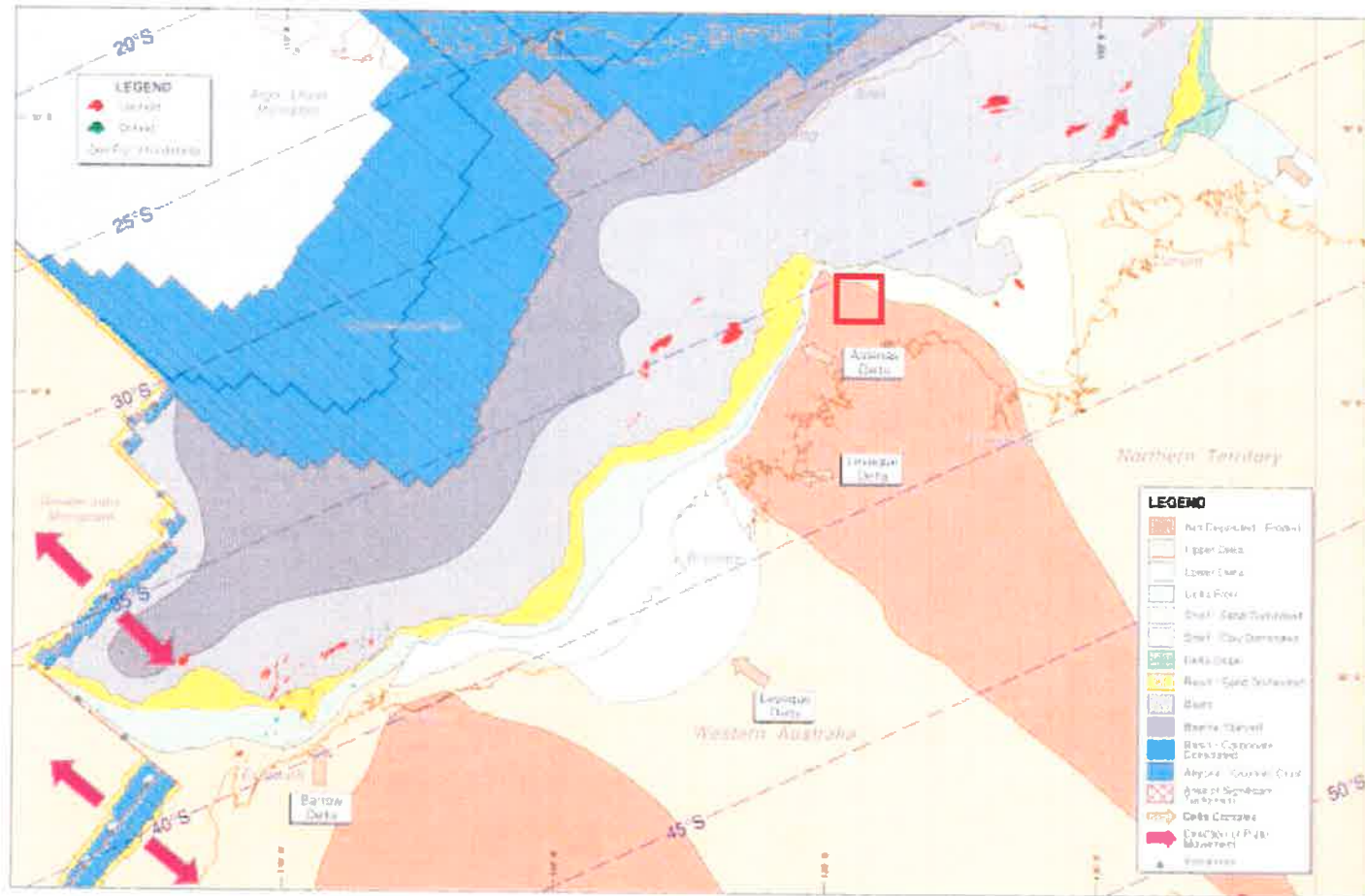


Figure 2.5 Paleogeographic map of Valanginian to Barremian (Longley et al., 2002). Red box shows location of study area.

2.5 Exploration History

The first well drilled in the Browse Basin, Leveque-1, was a failure. The first discovery of gas was made at Scott-Reef in 1971. Other gas discoveries like Brecknock-1 (1979), Brewster-1A (1980), North Scott Reef-1 (1982) and Echuca Shoal-1(1983), confirmed this to be a gas-prone basin. In 1983 Caswell-2 was drilled with minor oil shows from thin Late Jurassic and Early Cretaceous sediments and high gas readings within the Late Jurassic and Early Cretaceous sediments. Oil potential in the Browse Basin was confirmed by the oil discoveries on the Yampi Shelf in Gwydion-1 (1995) and Cornea-1 in 1997. Gwydion-1 penetrated four separate hydrocarbon zones in Albian to Barremian age sandstone. The well penetrated an oil sand between 809.5 m and 819 m (Spry and Ward, 1997). Significant gas discoveries were made in the central Caswell Sub-basin (Dinichthys-1, Gorgonichthys-1, and Titanichthys-1) and the northeastern part of the Browse Basin (Crux-1) in 2000.

CHAPTER 3 SEDIMENTOLOGY AND SEQUENCE STRATIGRAPHY

3.1 Sedimentology

3.1.1 Core Description

Core data from the Echuca Shoals Formation is available only for Kalyptea-1ST1. The core depth is from 4160–4170.5 mKB. Core description was done by B. Messent of BHP Petroleum (March 1990). Based on this core description the depositional environment for the Echuca Shoals Formation in the study area has been interpreted as a lower fan, non channelized, deepwater environment. The top 1.8 m of the core description is shown in Table 3.1.

3.1.2 Biostratigraphy

Biostratigraphic data has been examined from 18 well reports in the northern Caswell Sub-basin. The quality of the data varies due to different spud date of the wells and the different companies that drilled the wells. The data that was used for chronostratigraphic analysis are from palynological data that characterize the Valanginian to Barremian interval. The *Systematophora areolata* pollen was used to identify the Mid-Late Valanginian. The *Senoniasphaera tabulata* was used to identify the Berriasian-Lower Valanginian whereas the *Muderongia australis* identifies the Aptian-Barremian. Challenges were encountered in the use of the data as not all wells were found to have identified these species, and hence a reliable correlation of all wells could not be performed.

3.1.3 Depositional Processes and Models

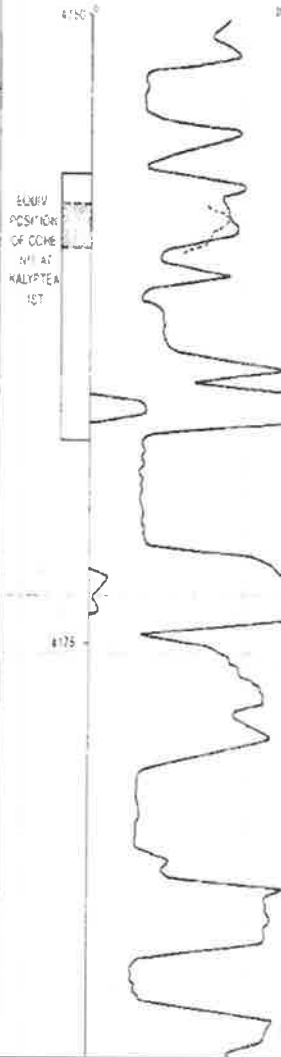
From core analysis of Kalyptea-1ST1, the Echuca Shoals Formation was interpreted to be deposited in a deepwater environment. Therefore, the depositional processes and the model that will be discussed in this section is focused on deepwater systems. There are many terminology schemes for deepwater systems. One of the schemes emphasizes marine-sediment gravity-flow processes, environments and deposits (Weimer and Slatt, 2004). Four basic types of sediment flows have been recognized based on sediment gravity flow processes: turbidity current, fluidized/liquidized flows, grain flows and cohesive flows (Richards, 1996).

Table 3.1. Core description of part of the Echuca Shoals Formation at Kalypteia-1ST1 well (Kalypteia-1ST1 well completion report)

MD (mKB)	CORE DEPTH (mKB)	GRAINSIZE (ϕ , s, vt, f)	SEDIMENTARY STRUCTURES	PETROGRAPHIC FEATURES IN HAND SPECIMEN	ENERGY LEVELS & DEPOSITIONAL ENV	STRAT	CORE ANALYSIS (% weight)					HYDROCARBON EVALUATION	
							W	V	S	F	T		
4160.3	4157.5					2 dy							
2			Generally massive thin siltstone lens (1.1cm by 2mm) occasionally present orientation parallel to bedding	CLAYSTONE: dark grey to dark green, silty in part micromicaceous, non calcareous	LOW ENERGY								
4	4155					2dy							
6			Angular claystone clasts orientated at 50° to horizontal	QTZ ARENITE: Grey to transparent, very fine to fine grained subangular with moderate sphericity. Abundant calcareous cement and fine grain glauconite grains, no visible porosity	LOW-MODERATE ENERGY								
8			Generally massive, occasional plant fragment orientated parallel to bedding Massive	CLAYSTONE: Dark grey, noncalcareous	LOW ENERGY								
			Occasional elongate siltstone lens orientated approximately parallel to bedding Reverse fault 53° displacement 20mm	CLAYSTONE: Dark grey/green, micromicaceous Trace siltsize glauconite grains predominantly in laminar lenses									
4161			Crossbedding-upper 53°, lower 30° (opposite orientation)	QTZ ARENITE: Grey, predominately quartz with up to 5% glauconite grains, fine to very fine grained subangular with slight spherical sphericity moderately well sorted, very calcareous no visible porosity	MODERATE ENERGY		0.6	2.68	0.01	0.01	0.01		
2			Generally massive with thin siltstone laminar/lenses orientated parallel to bedding Angular claystone clast orientated 45°	CLAYSTONE: Dark grey/green micromicaceous, silty in part (quartz silt grains in laminae/lenses)	LOW ENERGY								
4	4155		Plant fragments (0.5mm by 3mm) along bedding surfaces										
6			Angular claystone clasts orientated parallel to bedding	QTZ ARENITE: Predominantly quartz grains with up to 5% glauconite grains, fine to very fine grained with slight spherical sphericity, well sorted with up to 40% of sample sparry calcite cement No visible porosity	LOW-MODERATE ENERGY								
8			massive	CLAYSTONE: A/A	LOW ENERGY								
6	4155.4		massive	QTZ ARENITE: Predominantly gray quartz grained, subrounded well sorted with less than 10% calcareous silt Authigenic quartz dominant cement	LOW ENERGY								

RESIDUAL
S_w > 90%

NON CHANNELIZED
LOWER FAN
DEEP WATER



Many authors have differentiated turbidity currents into low-and high density flows. The distinction is important because it can control the final location of sand deposition within a deep marine basin (Richards et al., 1998).

The volume of sediment, the grain size distribution and the nature of the supplying system control the sand-body architecture, geometry and internal facies distribution of deep-marine turbidite systems (Reading and Richards, 1994; Richards and Bowman, 1998). Based on these parameters, four classes of deep-marine clastic systems have been identified: gravel-rich, sand-rich, mixed sand-mud and mud-rich systems (Reading and Richards, 1994; Richards et al., 1998; Richards and Bowman, 1998) (Figure 3.1).

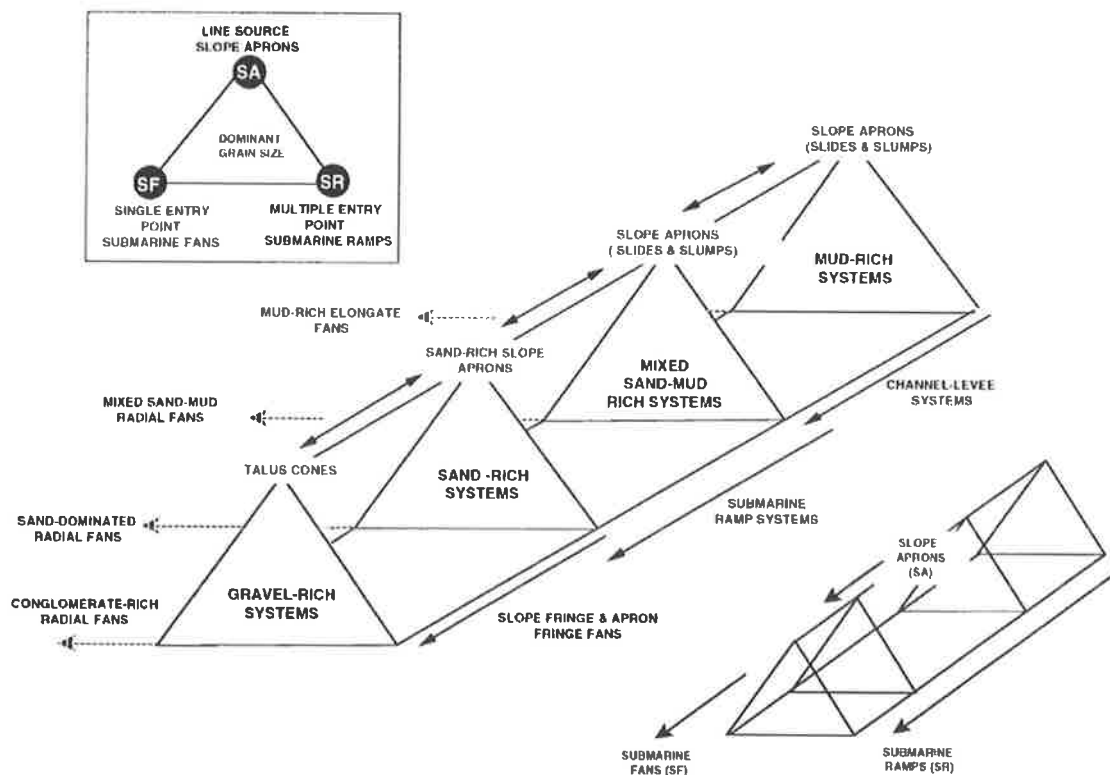


Figure 3.1 Classification of deep-marine systems based on sediment volume, grain size and the nature of supplying system (after Richards and Bowman, 1998).

Richards et al. (1998) recognized five architectural elements of deep-marine clastic systems: wedges, channels, lobes, sheets, and chaotic mounds. This identification was based on outcrop, wireline log and seismic data (Figure 3.2).

PRINCIPAL ARCHITECTURAL ELEMENTS

SYSTEM TYPE	WEDGES	CHANNELS	LOBES	SHEETS	CHAOTIC MOUNDS
GRAVEL-RICH SYSTEMS		CHUTES 			
SAND-RICH SYSTEMS		BRAIDED 	CHANNELIZED-LOBES 		
MUD/SAND-RICH SYSTEMS		CHANNEL-LEVEE 	DEPOSITIONAL LOBES 		SLUMPS & SLIDES
MUD-RICH SYSTEMS		CHANNEL-LEVEE 	DEPOSITIONAL LOBES 		SLUMPS & SLIDES

Figure 3.2 Five architectural elements of deep-marine clastic systems (after Richards et al., 1998).

3.2 Sequence Stratigraphy

Introduction

Sequence stratigraphy is a modern approach to placing the stratigraphic record in a chronostratigraphic framework (Catuneanu, 2006). In its application, sequence stratigraphy can be used as a tool to predict reservoir lithology distribution, seal distribution and trap style (Posamentier and Allen, 1999). Sequence stratigraphy can also be utilized for regional analysis by using seismic data, well logs, and biostratigraphy (Van Wagoner et al., 1990). With structural traps becoming harder to find, sequence stratigraphy can be used to help identify stratigraphic traps.

Concepts, History and Definition

The term sequence was used by Sloss (1963) to describe stratigraphic units bounded by unconformities that can be recognized in a wide area of a continent. The sequence concept was further developed through use of seismic data to interpret regional stratigraphy. P.R. Vail and his colleagues from Exxon Production Research Company recognized unconformities in seismic data and recognized their importance as chronostratigraphic surfaces. The result of their work was published in 1977 in Memoir 26 by the American Association of Petroleum Geologists. Mitchum, Vail, and Thompson (1977) defined a sequence as “a stratigraphic unit

composed of a relatively conformable succession of genetically related strata and bounded at its top and base by unconformities or their correlative conformities” (Figure 3.3). They added that the sequence is bounded not only by unconformities but also by equivalent conformities.

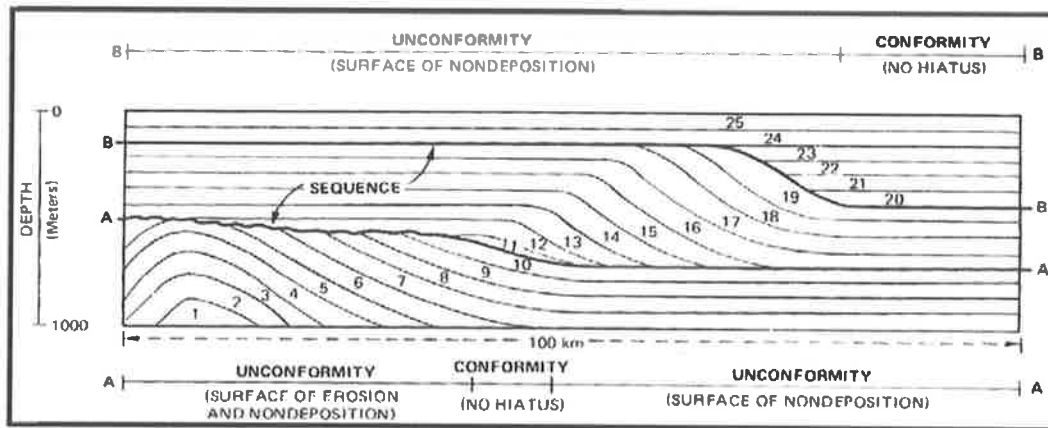


Figure 3.3 Concept of depositional sequence (Mitchum et al., 1977)

The stratal packages within sequences comprise:

Systems tracts- Systems tracts are defined as “a linkage of contemporaneous depositional systems” (Brown and Fisher, 1977). Systems tracts are distinguished based on the type of bounding surfaces, position within the sequence, and stacking patterns of parasequences and parasequence sets. Systems tracts are also characterized by geometry and facies associations (Van Wagoner et al., 1988).

Parasequence- A parasequence is “a relatively conformable succession of genetically related beds or bedsets bounded by marine flooding surfaces and their correlative surfaces” (Van Wagoner et al., 1988).

Parasequence set- A parasequence set is “a succession of genetically related parasequences which form a distinctive stacking pattern that is bounded, in many cases, by major marine flooding surfaces and their correlative surfaces” (Van Wagoner et al., 1988).

Stratigraphic surfaces comprise:

Sequence Boundary- A sequence boundary is “a single, wide-spread surface that separates all of the rocks above from all of the rocks below the boundary. The sequence boundary

commonly is marked by significant regional erosion and onlap, which exert a strong control on facies distribution” (Van Wagoner et al., 1990).

Maximum flooding surface- A maximum flooding surface is “a surface marking the end of shoreline transgression, separates retrograding strata below from prograding (highstand normal regressive) strata above” (Catuneanu, 2006).

Transgressive Surface- A transgressive surface is “initiated by the first significant flooding event” (Posamentier and Vail, 1988). The transgressive surface has a low diachroneity along dip that reflects the rates of sediment transport (Catuneanu, 2006).

3.3 Deepwater Sequence Stratigraphy Model

Vail (1987) noted that the depositional sequence consist of three systems tracts: lowstand, transgressive and highstand systems tracts.

Lowstand Systems Tract

The lowstand systems tract is “the basal (stratigraphically oldest) systems tract in the depositional sequence deposited during an interval of relative sea-level fall at the offlap break and subsequent slow relative sea level rise” (Myers and Milton, 1996). This systems tract is bounded by subaerial unconformity and marine correlative conformity at the base and at the top by the transgressive surface (Catuneanu, 2006). In deepwater environments, in basins with a shelf-slope break, the lowstand systems tract is divided into lowstand fan and lowstand wedge portions (Posamentier and Vail, 1988) (Figure 3.4). The lowstand fan is dominated by deposition of submarine fans at a time when sediments are bypassing the shelf through actively incised valley (Posamentier and Vail, 1988). The early lowstand wedge is differentiated by active leveed-channel deposition with related rhythmic turbidites (Posamentier and Vail, 1988).

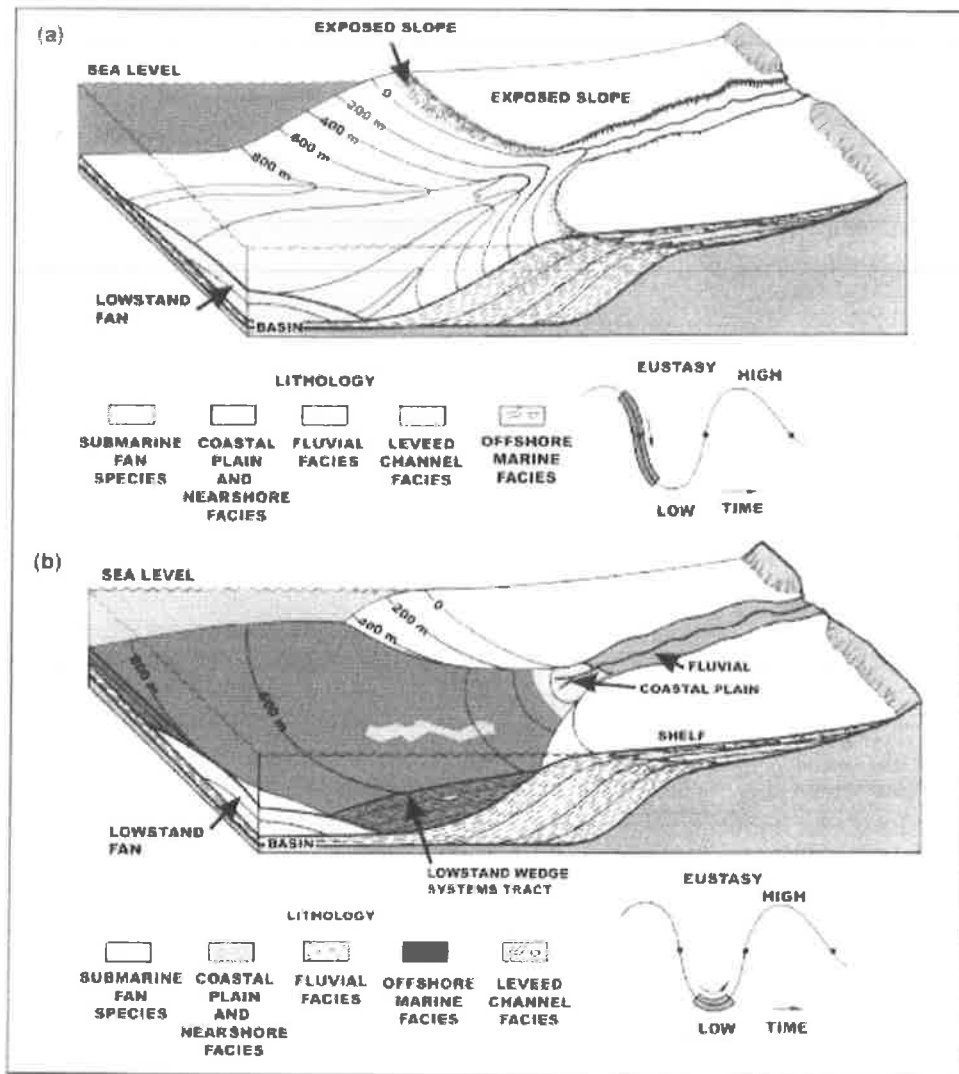


Figure 3.4 Block diagrams showing early relative lowstand in sea-level and deposition of lowstand fan (a) and lowstand wedge (b) (Posamentier and Vail, 1988).

Transgressive Systems Tract

The transgressive systems tract is “the middle systems tract in the depositional sequence deposited during that part of a relative sea-level rise cycle when topset accommodation volume is increasing faster than the rate of sediment supply” (Myers and Milton, 1996). This systems tract is bounded by the transgressive surface at the base and by maximum flooding surface at the top (Catuneanu, 2006).

Highstand Systems Tract

The highstand systems tract is “the progradational topset-clinoform system deposited after maximum transgression and before a sequence boundary, when the rate of creation of accommodation is less than the rate of sediment supply” (Myers and Milton, 1996). In deep-water environments, sedimentation during the highstand systems tract is pelagic and results in the development of a condensed section (Catuneanu, 2006).

CHAPTER 4 METHODOLOGY

4.1 Database

Seismic Data

This study uses 2D seismic data provided by Chevron Australia. The seismic data were acquired by the Australian Geological Survey Organisation (AGSO) from 1993 to 1996 (Table 4.1). Fifteen seismic lines were used in the seismic interpretation which covers an area of 100 km x 95 km. Figure 4.1 shows the seismic data set and wells used in this study. The quality of seismic data in this location varies from good to poor. The quality of the seismic lines BBHR-175-11 and BBHR-130-03 is good and easy to be interpreted (Figure 4.2). The quality of the data at line BBHR175-15B below the Basset-1 well is poor due to noise caused by a fault (Figure 4.3).

Table 4.1 Seismic surveys that were used in the study area

Survey	Vintage	Operator
AGSO marine survey 119	1993	AGSO
AGSO marine survey 130	1994	AGSO
AGSO marine survey 175	1996	AGSO

Well Data

Nineteen wells are available in the study area and all of them were used for the lithostratigraphic correlations. Based on this correlation, two wells did not encounter the Echuca Shoals Formation, because the formation was not deposited in this area as a result of a paleogeographic high. Three wells did not penetrate down into the Echuca Shoals Formation. Fifteen of the nineteen wells have checkshot data and thus were used in seismic interpretation. The log data recorded in these wells is a standard well log suite: gamma ray (GR), resistivity (RT), neutron (NPHI), density (RHOB) and sonic log (DT). A list of wells used in this study is shown in the Table 4.2.

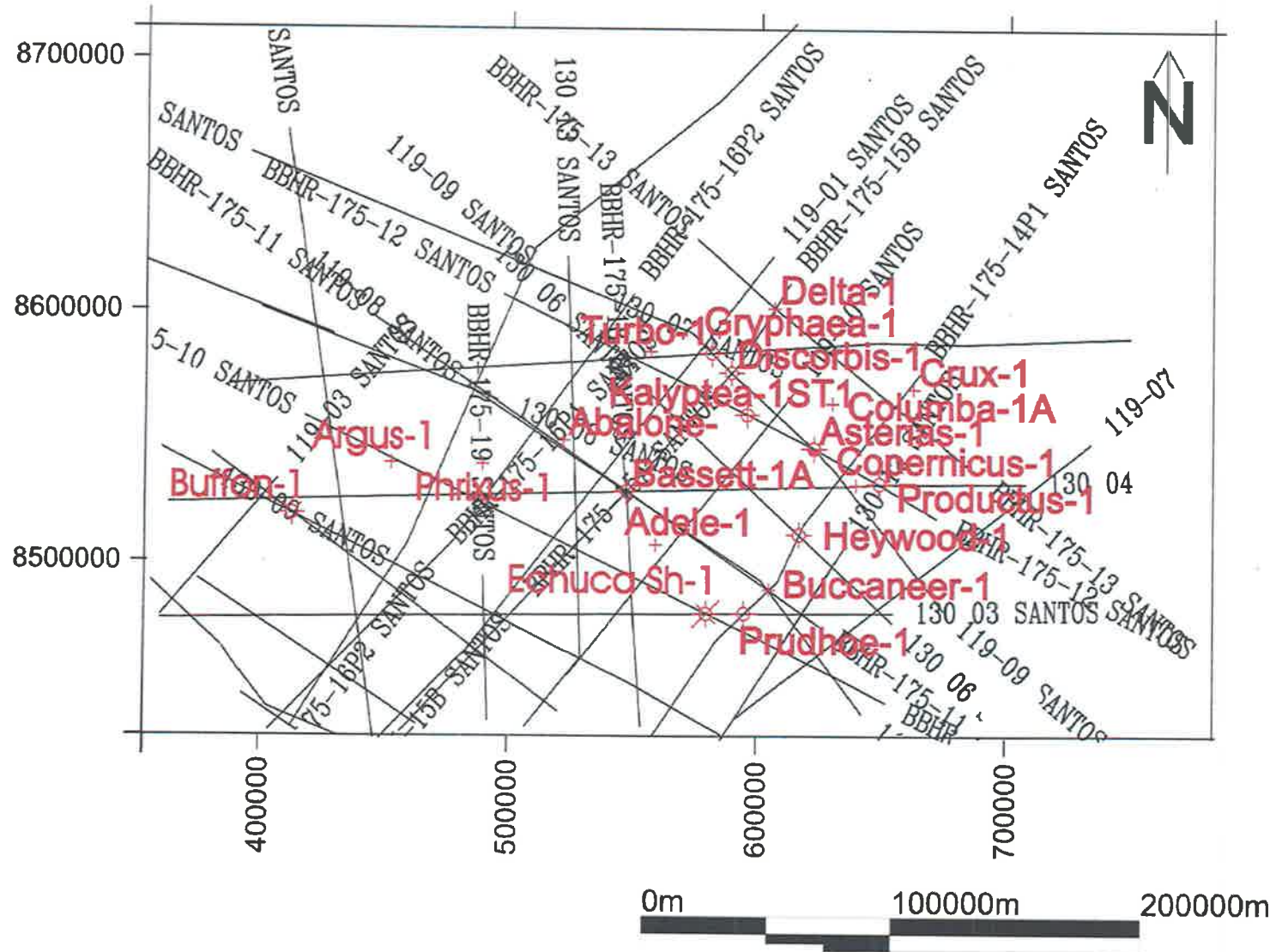


Figure 4.1 Seismic lines and wells used in this study.

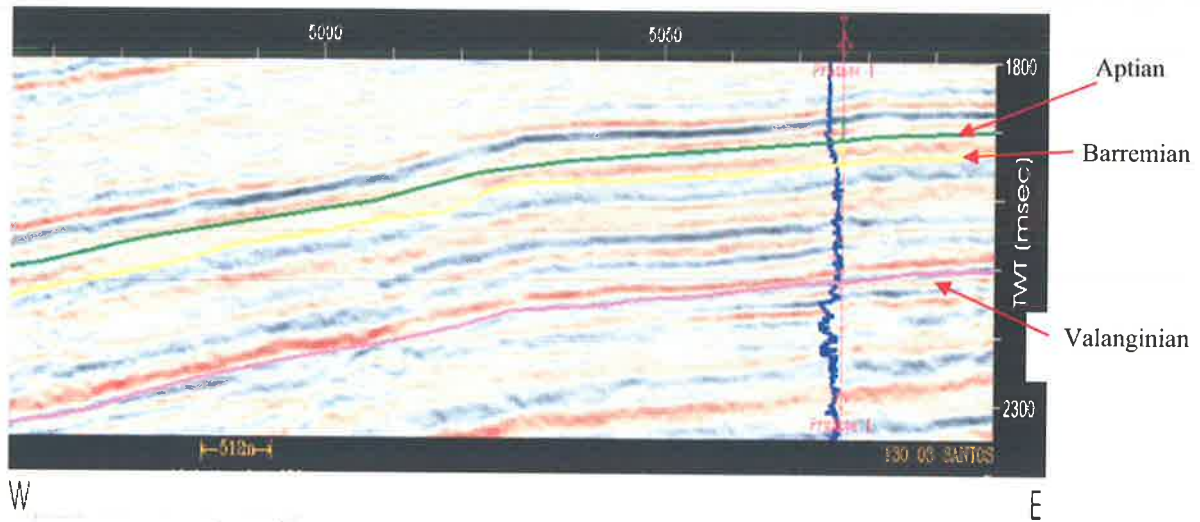


Figure 4.2 Good quality seismic data from 130-03.

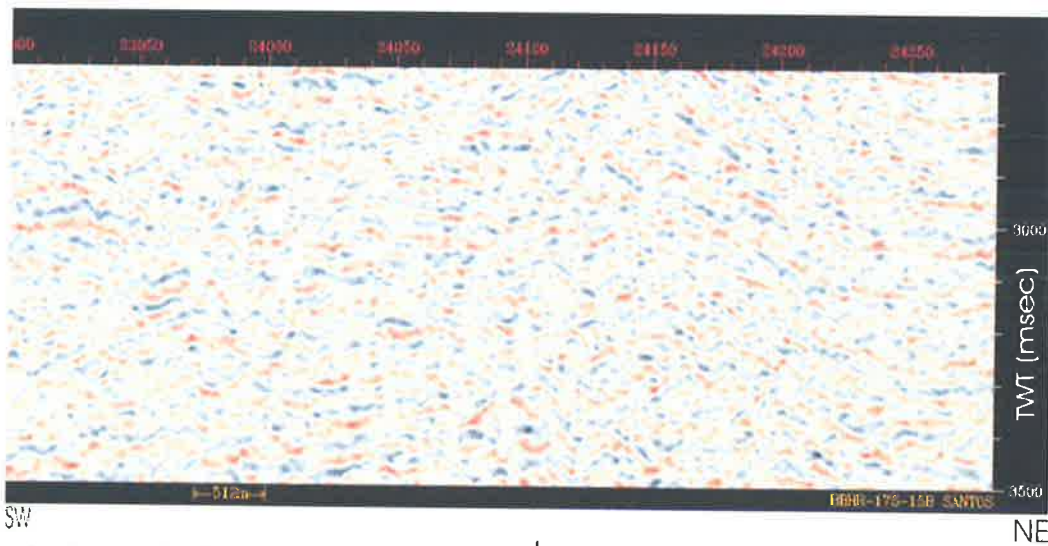


Figure 4.3 poor quality seismic data from BBHR-175-15B.

Table 4.2 Wells used in this study. See figure 4.1 for well locations.

No	Well name	Spud date	Remarks
1	Abalone-1	4 September 2000	Did not penetrate the Echuca Shoals Formation
2	Adele-1	28 July 1998	
3	Argus-1	21 June 2000	The Echuca Shoals Formation was not deposited due to paleogeographic high.
4	Asterias-1	14 June 1987	
5	Basset-1	19 June 1978	Did not penetrate the Echuca Shoals Formation
6	Buccaneer-1	26 February 1990	
7	Buffon-1	14 January 1980	The Echuca Shoals Formation was not deposited due to paleogeographic high.
8	Columba-1	20 February 1999	
9	Copernicus-1	29 September 1993	
10	Crux-1	16 April 2000	
11	Discorbis-1	8 August 1989	
12	Echuca Shoals-1	8 November 1983	
13	Gryphaea-1	16 September 1987	
14	Heywood-1	7 April 1974	
15	Kalyptea-1/ST	17 September 1988	
16	Phrixus-1	22 October 2001	Did not penetrate the Echuca Shoals Formation
17	Productus-1	12 October 1991	
18	Prudhoe-1	13 September 1974	
19	Turbo-1	26 June 2000	

4.2 Wireline Log Interpretation

Lithostratigraphic and Chronostratigraphic Correlation

In the lithostratigraphic correlation the formations that were present in the northern part of the Caswell Sub-basin were correlated from well to well. The formation names and the pick depth were obtained from well reports. The software used for this correlation was Landmark-Stratworks. The wells were correlated in strike and dip directions (Figure 4.4 and Figure 4.5). The aim of this lithostratigraphic interpretation was to define the distribution of the Echuca Shoals Formation within the area. Based on the correlation, it was deduced that the Echuca Shoals Formation was not present in Buffon-1 and Argus-1 because the formation was not deposited in those locations. The correlation results were used as a basis to understand the geological framework of the study area.

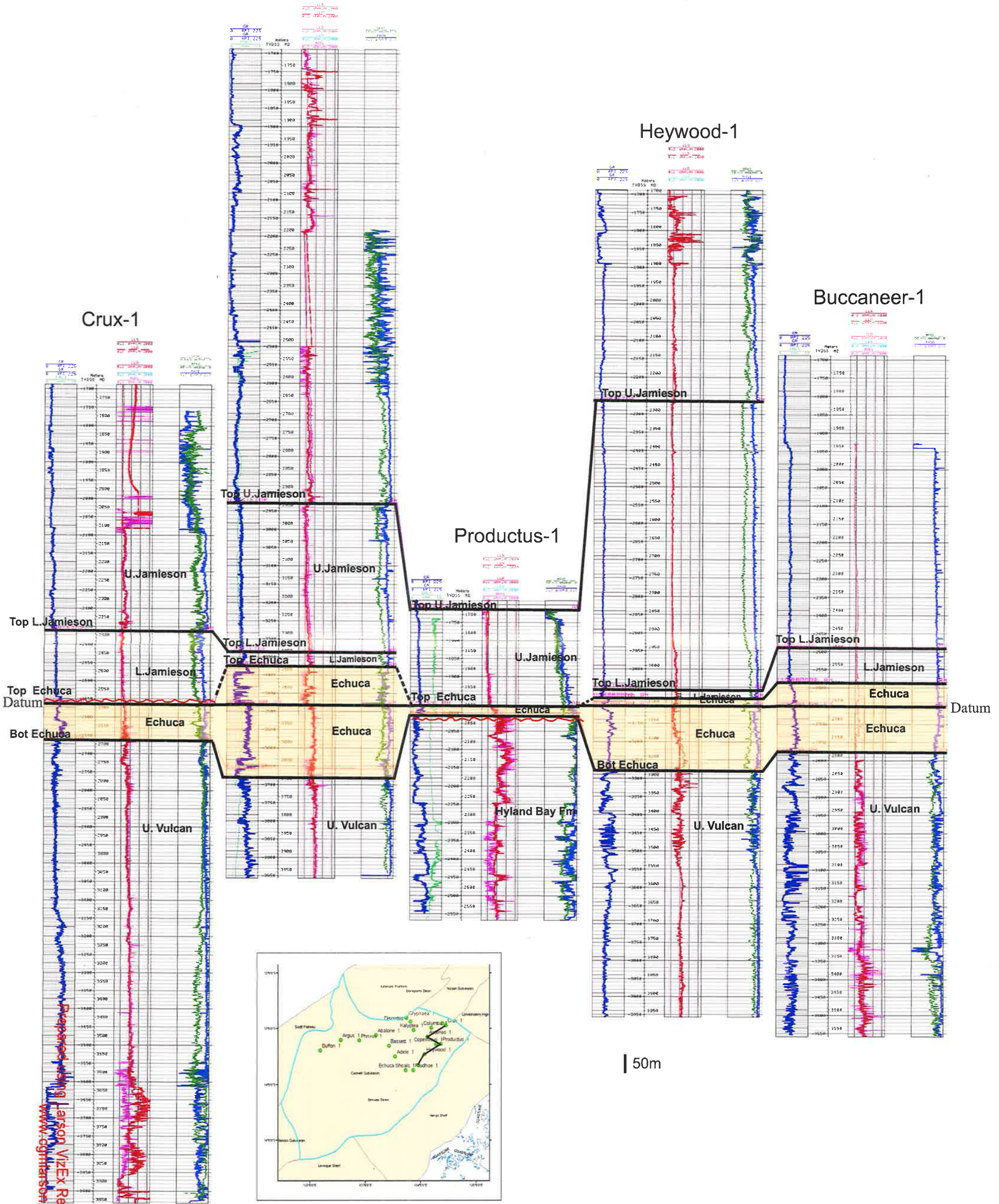
For the chronostratigraphic correlation, biostratigraphy was used to tie the correlation and sequence stratigraphy to define key stratigraphic surfaces. The zone of interest in this study is the Valanginian to Barremian interval. The Valanginian interval is determined by the presence of *Systematophora areolata* to *Senoniasphaera tabulata* spore-pollen zones. The Barremian interval is determined by the *Muderongia Australis* spore-pollen zone. After the logs were displayed at the same scale, Kalyptea-1ST1, which has core data, and Asterias-1 which has the best log motifs, were chosen as starting points for depositional dip and strike lines. The next step was hanging all of the correlation wells on a datum. The candidate maximum flooding surface above the sand at 4283 m at Kalyptea-1ST1 was chosen as a datum (Figure 4.6). The stacking patterns were marked with arrows in the well logs. The next step was to correlate the candidate surfaces (Sequence Boundary, Transgressive Surface and Maximum Flooding Surface) on the well logs. A sequence boundary can be recognized in well log by abrupt change upwards from clean, distal marine shales to very coarse, nearshore marine sands (Rider, 1996). On seismic data, the sequence boundary can be recognized from a downward shift in coastal onlap, implying a fall in relative sea-level, with exposure and erosion of the highstand topsets (Myers and Milton, 1996). A maximum flooding surface can be recognized in well log as the boundary between transgressive unit, or retrogradational parasequence set, and an overlying regressive unit, or progradational parasequence set (Myers and Milton, 1996). On seismic data, a maximum flooding surface is recognized as a surface where clinoforms downlap on to underlying topsets, which may display backsteeping and apparent truncation (Bertram and Milton, 1996). Finally, systems tracts were interpreted.

Asterias-1

Heywood-1

Buccaneer-1

Crux-1



Prepared using Parson VIZEX Reader
www.cgimhanson.com

Figure 4.4 Well correlation from Crux-1 to Buccaneer-1 wells to show distribution the Echuca Shoals Formation in the study area

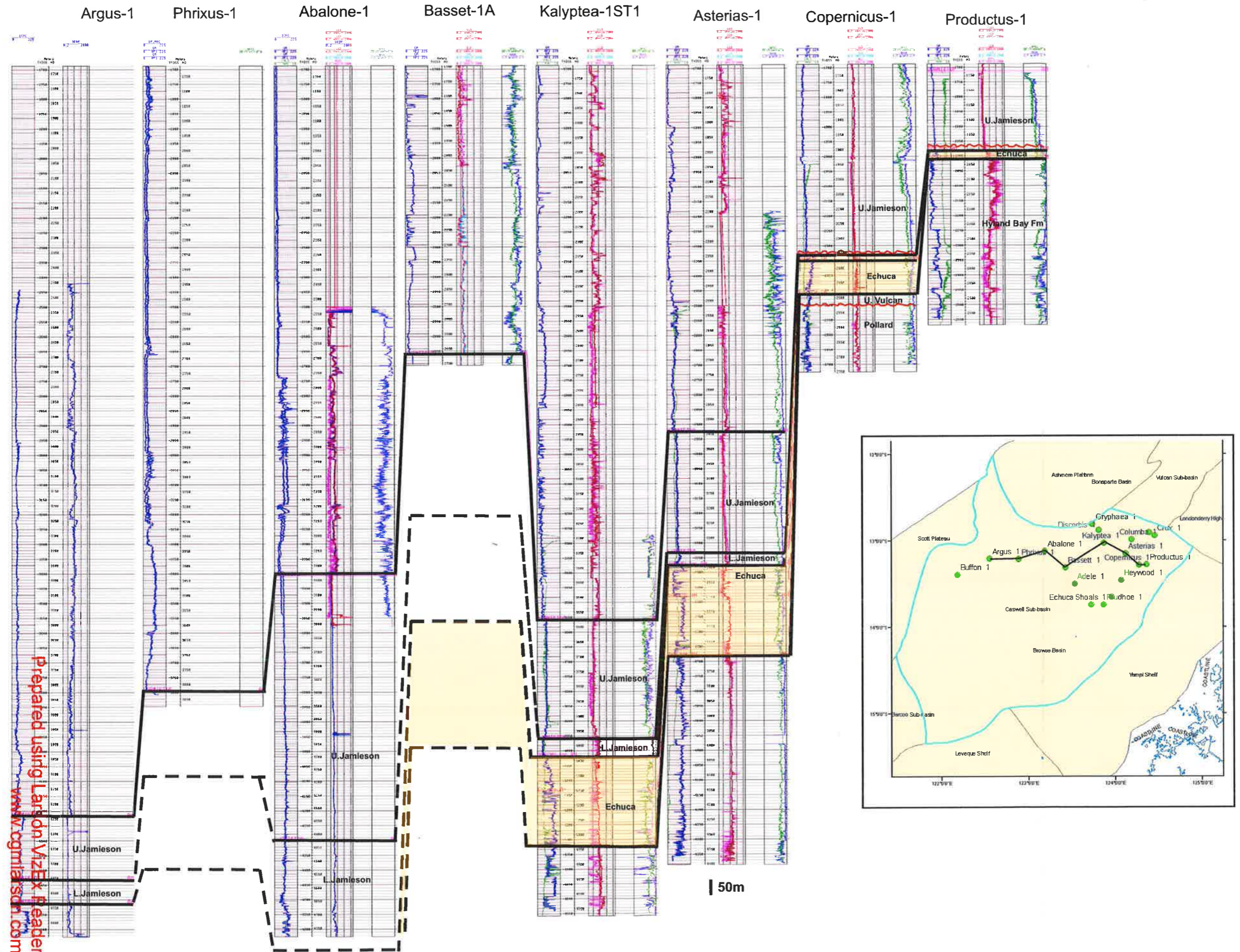


Figure 4.5 Structural correlation from Argus-1 to Productus-1 wells to show structural position of wells in the study area.

- Legend**
- Maximum Flooding Surface (MFS)
 - Transgressive Surface (TS)
 - Sequence Boundary (SB)
 - Highstand Systems Tract (HST)
 - Transgressive Systems Tract (TST)
 - Lowstand Systems Tract (LST)
 - || Core

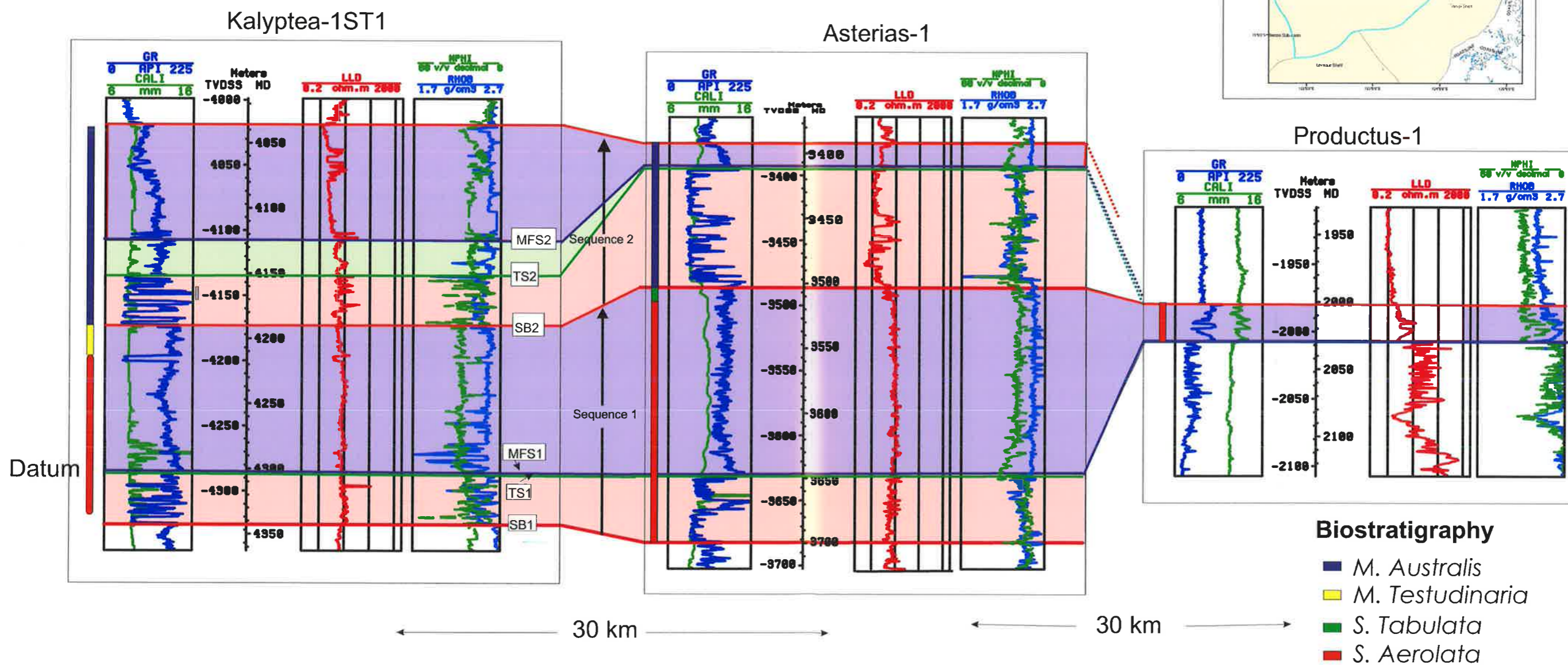
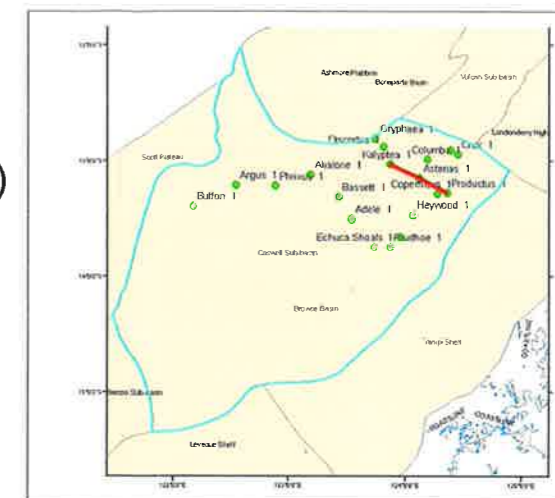


Figure 4.6 Sequence stratigraphy of Kalypteia-1ST1, Asterias-1 and Productus-1 wells

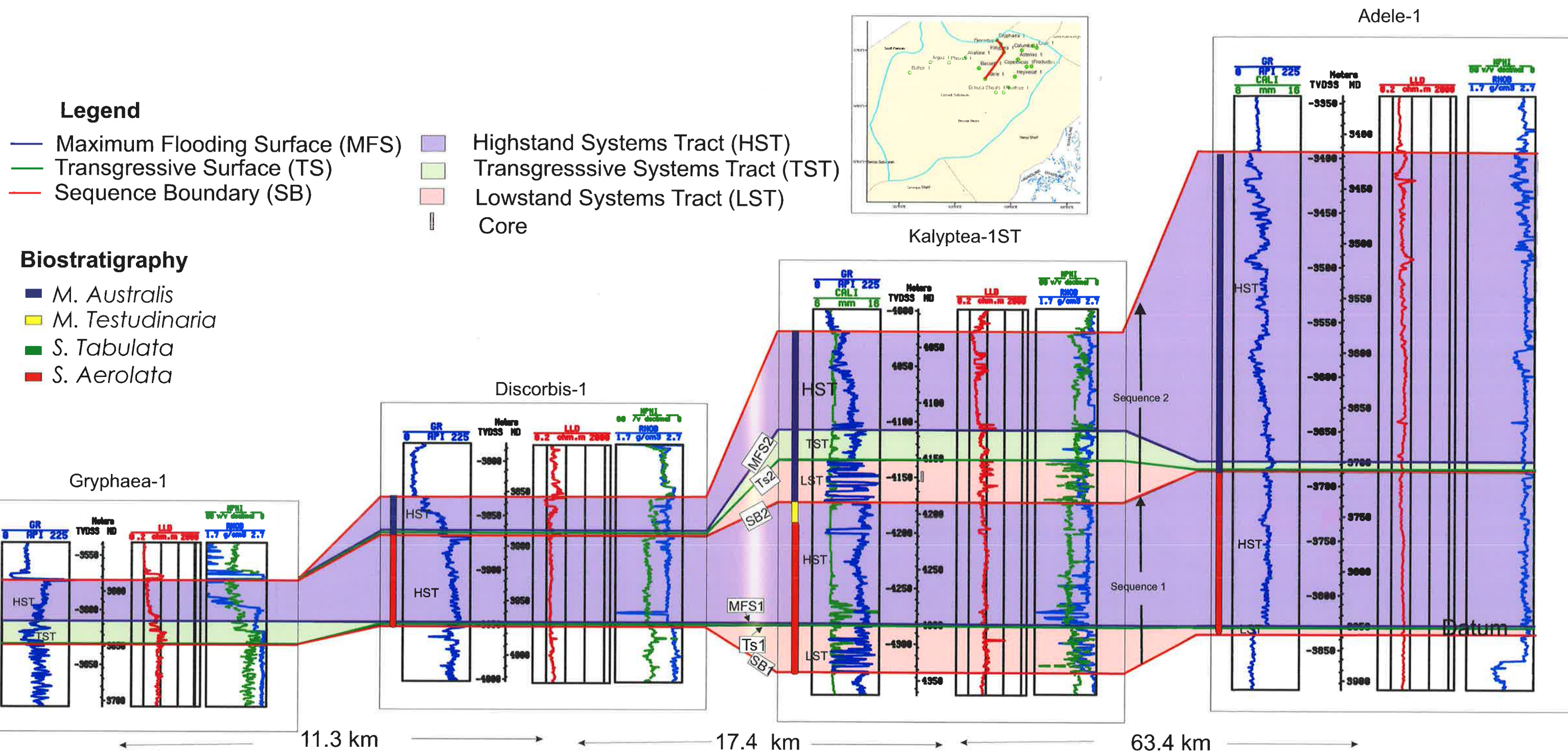


Figure 4.7 Sequence stratigraphy of Gryphaea-1 to Adele-1 wells.

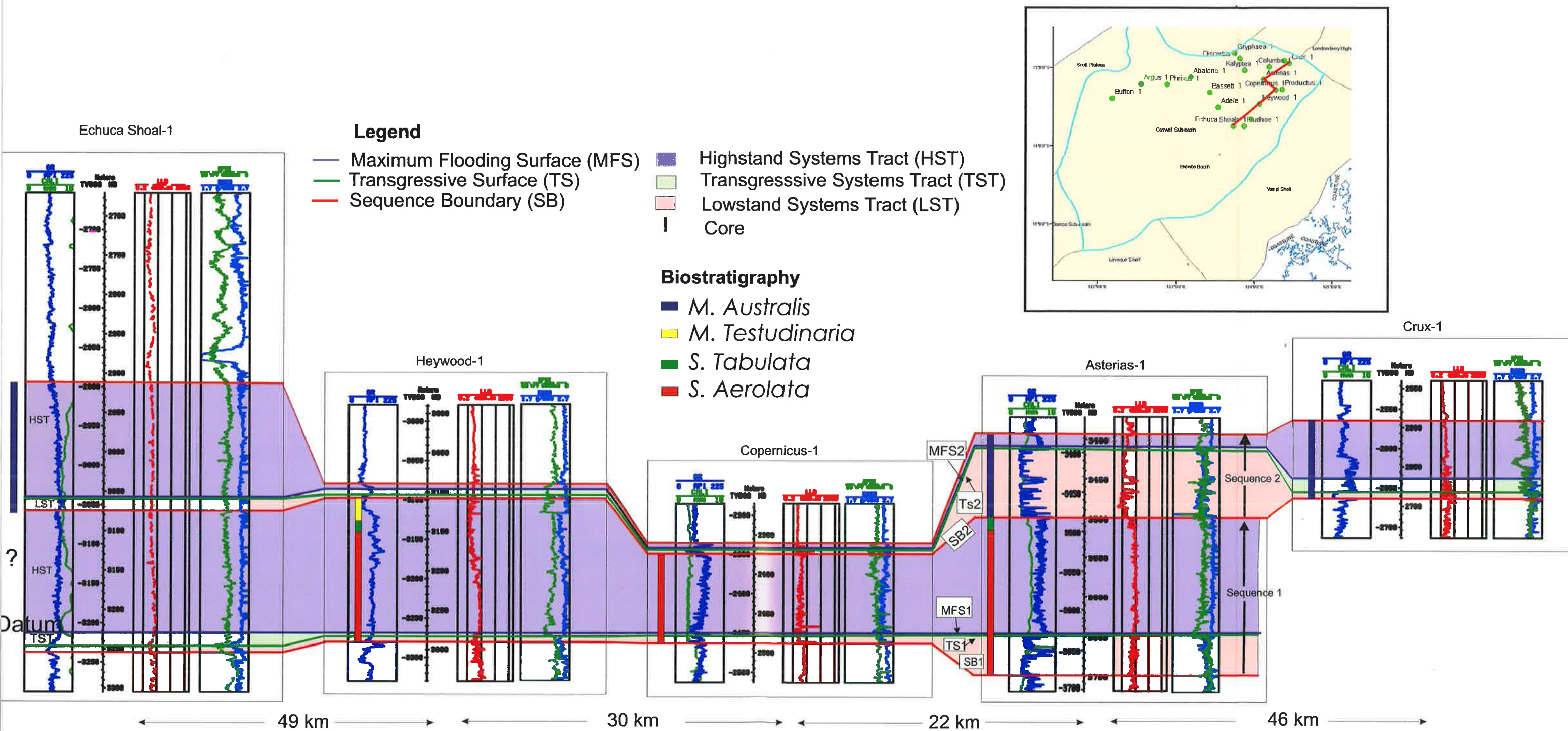


Figure 4.8 Sequence stratigraphy of Echuca Shoals-1 to Crux-1 wells.

Electro Log Facies Interpretation

The electro log facies is an interpretation of geological information that can be obtained from well logs, such as depositional system and facies (Rider, 1996). In this interpretation, as the depositional environment was determined as a deepwater environment from Kalyptea-1ST1 core analysis, the point-source mud/sand-rich sub-marine fan model (Reading and Richards, 1994) was used for the study area. The reason for applying that particular model is based on mud sand ratio within the sand bed in which the model has the percentage of the sand is between 30% and 70% (Reading and Richards, 1994). The percentage of sand in Kalyptea-1ST1 well at the Echuca Shoals Formation based on the core report at a depth of 4159 m is 60%. Richards and Bowman (1998) has described the log responses related to the point source mud/sand rich sub-marine fan model shown in Figure 4.9.

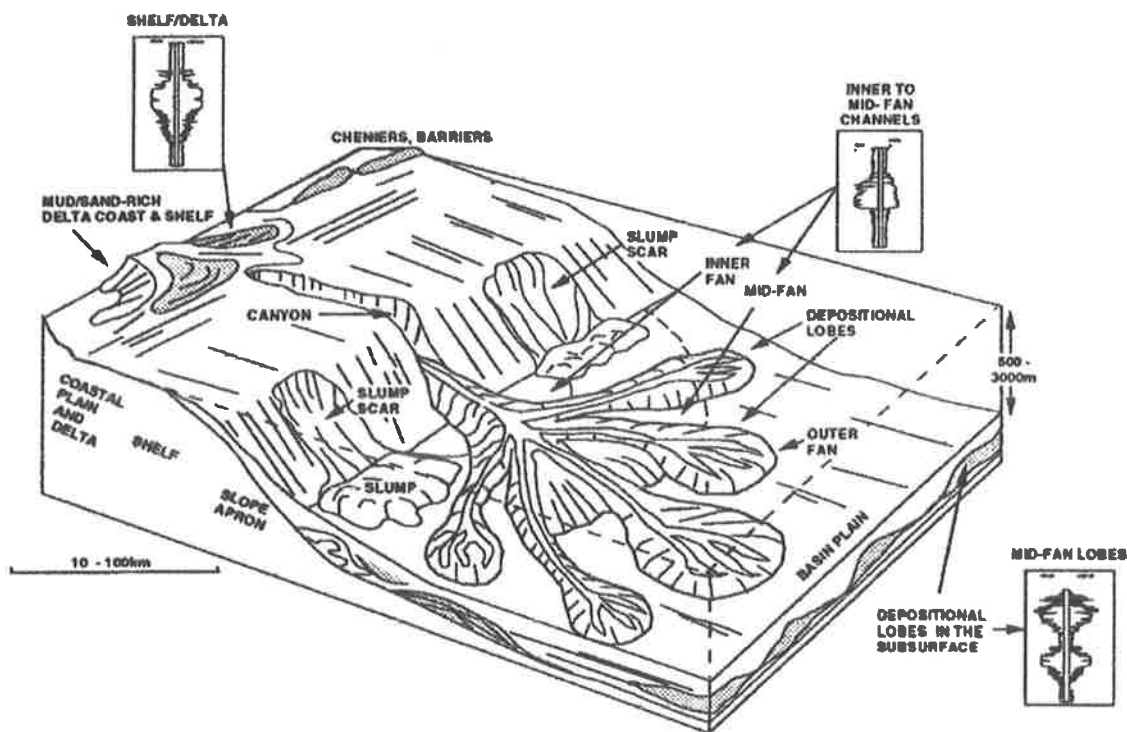


Figure 4.9 Log responses (Gamma Ray and Resistivity) in Point source mud/sand rich sub-marine system (Richards and Bowman, 1998).

4.3 Well to Seismic Tie

There are fifteen wells that have checkshot data in the study area. Checkshot data shows the relationship between time and depth at a particular well location. Therefore, a well with checkshot data acquired can be displayed directly on a seismic section and correlate a well pick to a seismic event (McQuillin et al., 1984). To ensure consistency of the checkshot data in the study area and to ensure the tie between wells and seismic, synthetic seismograms were generated using Landmark-Syntool software for three wells: Heywood-1, Asterias-1, and Kalyptea-1ST1 wells. Synthetic seismic generation uses sonic and density logs as well as checkshot data. To control the quality of the checkshot data, one can compare the velocity from the checkshot data with the velocity of the sonic log. Both velocities should have similar trends (McQuillin et al., 1984).

The synthetic seismogram is a result of a convolution between reflectivity coefficients with a wavelet. The reflectivity coefficient series at a well location is obtained from density and sonic data. The wavelet can be extracted from seismic data around the well at the zone of interest or some theoretical wavelet such as Ricker, Trapezoid or Klauder wavelet can be generated (McQuillin et al., 1984).

The synthetic seismogram for the Heywood-1 well will be discussed here. Figure 4.10 shows an extracted wavelet from the seismic data using an autocorrelation method with its frequency and phase spectrum in blue color. To generate a model wavelet, a trapezoid wavelet (red color) was generated with its frequency content matched closely to the frequency of the seismic data, as shown by the extracted wavelet. The frequency content of the seismic data is around 20-50 Hz. Figure 4.11 shows the sonic log, density log, RC and the seismic data around the well overlain with synthetic data over the area of interest. Strong seismic event at 2100 and 2240 msec correlate very well with the synthetic seismogram. However, the seismogram is not matched well with seismic events at 2180 msec and 2320 msec. These differences could be due to bad data in the sonic or density logs. Alternatively the checkshot data may need to be further edited. Edited checkshot should still be expected to have similar trend as the raw sonic data.

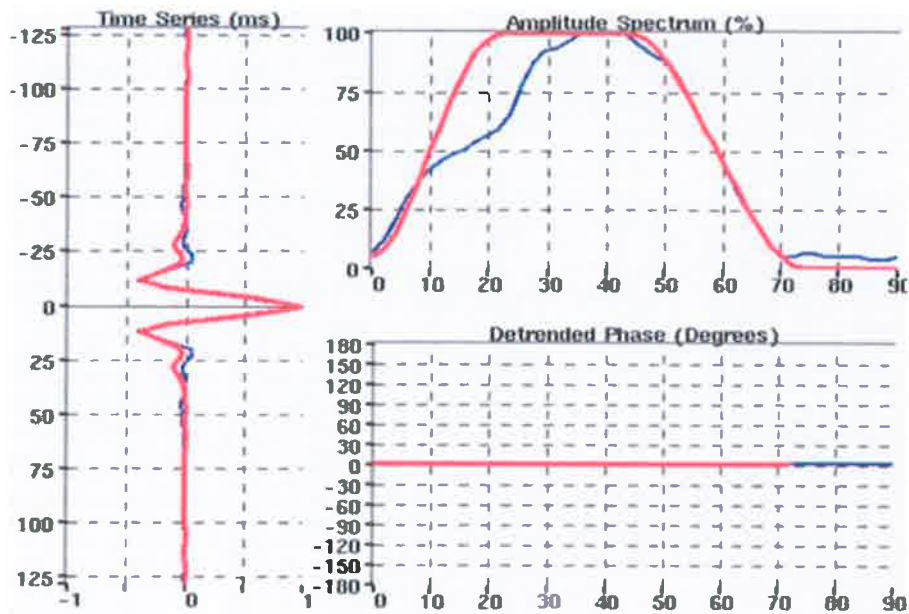


Figure 4.10 Amplitude, frequency, and phase spectrum for an extracted wavelet (blue color) using autocorrelation method and trapezoid model wavelet (red color).

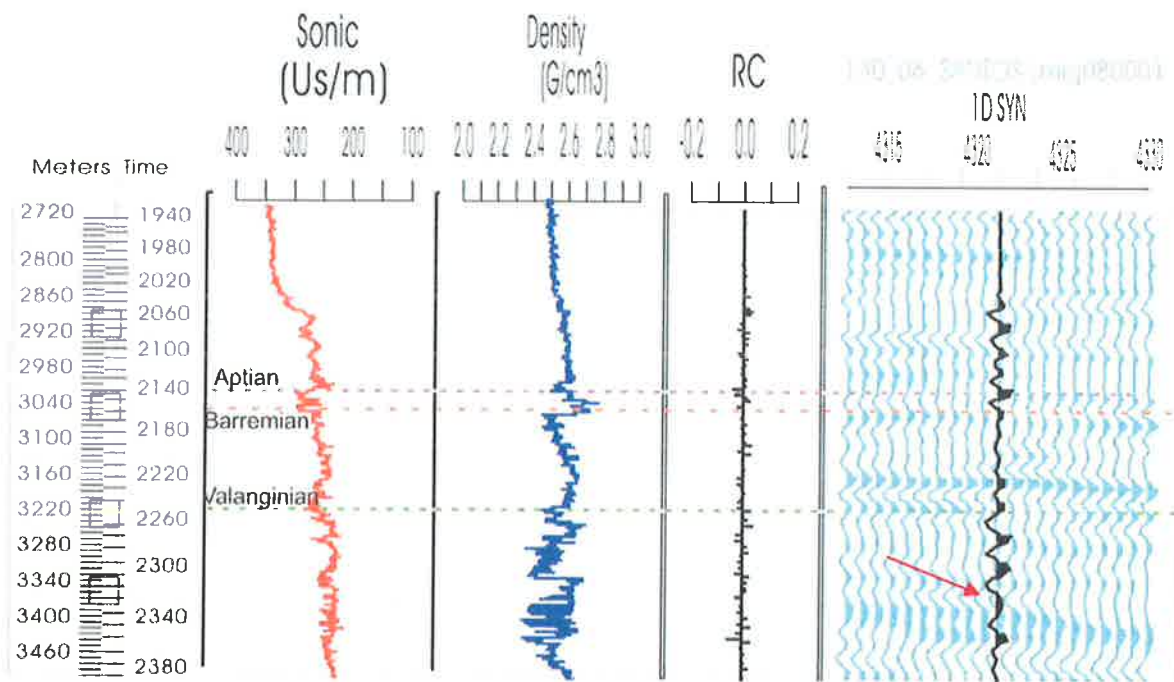


Figure 4.11 Sonic log, density log, RC series, seismic data and synthetic seismogram for Heywood-1 well. Strong event at 2240 and at 2100 msec correlate very well with the synthetic; however, the synthetic does not match at 2320 msec (red arrow).

4.4 Seismic Interpretation

Structural Mapping

Well log and sequence stratigraphic picks from the wireline log interpretation were posted on the seismic data using the time-depth relationship from available checkshot data. The well pick was associated with the nearest peak, trough or zero-crossing events on the seismic response. The event was then mapped throughout the extent of the seismic data by including the pick information from all wells.

There were three key horizons interpreted in this study in order to understand the structural geology and the depositional systems in the area. These events are Base Valanginian, Base Barremian and Base Aptian. The picking of the Base Valanginian horizon was based on the sequence boundary below the sand in the Kalyptea-1ST1 well. The picking of the Base Barremian horizon was based on the sequence boundary below the sand in the Asterias-1 well. The picking of the Base Aptian horizon was based on the maximum flooding surface in the Kalyptea-1ST1 well. Two-way time maps for those three horizons were generated and isochron maps for the Valanginian and Barremian intervals were also generated.

Two-way time maps were used to identify the structural trends in the study area. The maps were generated by gridding the horizons mapped on the 2D seismic lines. Isochron or time-thickness maps can show the variations of sediment thicknesses. The maps were generated by subtracting the top horizon from the bottom horizon and gridding the result. The maps are also used to interpret the paleo sediment supply directions (paleocurrent directions).

Seismic Facies Interpretation

Seismic facies interpretation was used to recognize the depositional components within the deepwater environment such as submarine fan and channel-levee systems. The criteria involved in recognizing submarine fans on seismic data within the lowstand-fan unit of the lowstand systems tract are described by Posamentier and Erskine (1991) as: 1. Fan pinchout geometry against bathymetric highs, which helps define the top and base of the fan interval; 2. High amplitude continuous reflections onlapping the basin margin; 3. Internal bidirectional downlap; 4. Subtle external mounding; and 5. Occurrence of overlying Type 1 unconformity and underlying lowstand-wedge deposits. Weimer (1991) stated that channels in general are characterized by a zone of stacked, subparallel high-amplitude reflections (HAR) overlain by low-amplitude, divergent reflections (DIV). These HAR are interpreted to be coarse-grained

channel-fill sediments, while the DIV are late channel-fill, fine-grained sediments. Flanking the channels are levee-overbank sediments that are characterized by low amplitude, subparallel to slightly hummocky reflections with moderate to good continuity (Figure 4.12).

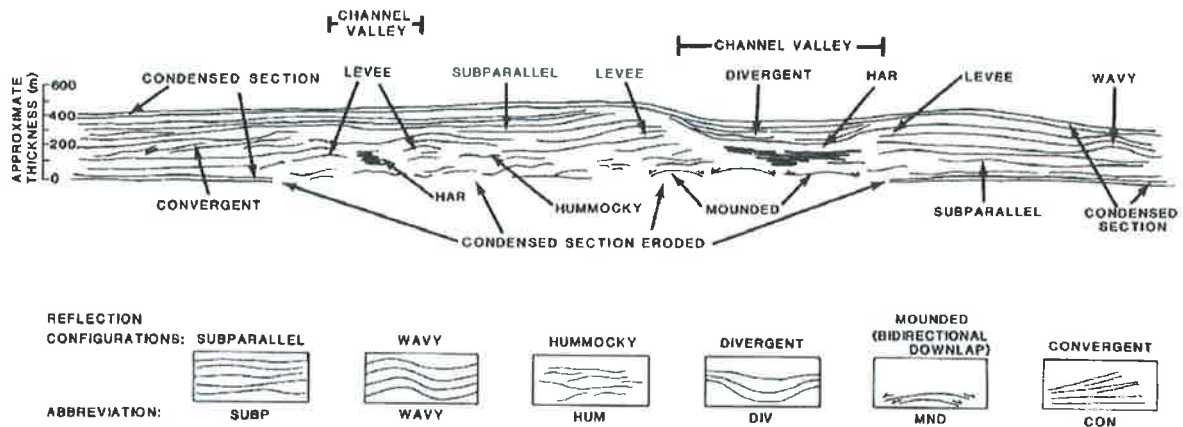


Figure 4.12 Seismic profile illustrating seismic facies of channel-levee systems and condensed sections and erosional sequence boundary (Weimer, 1991).

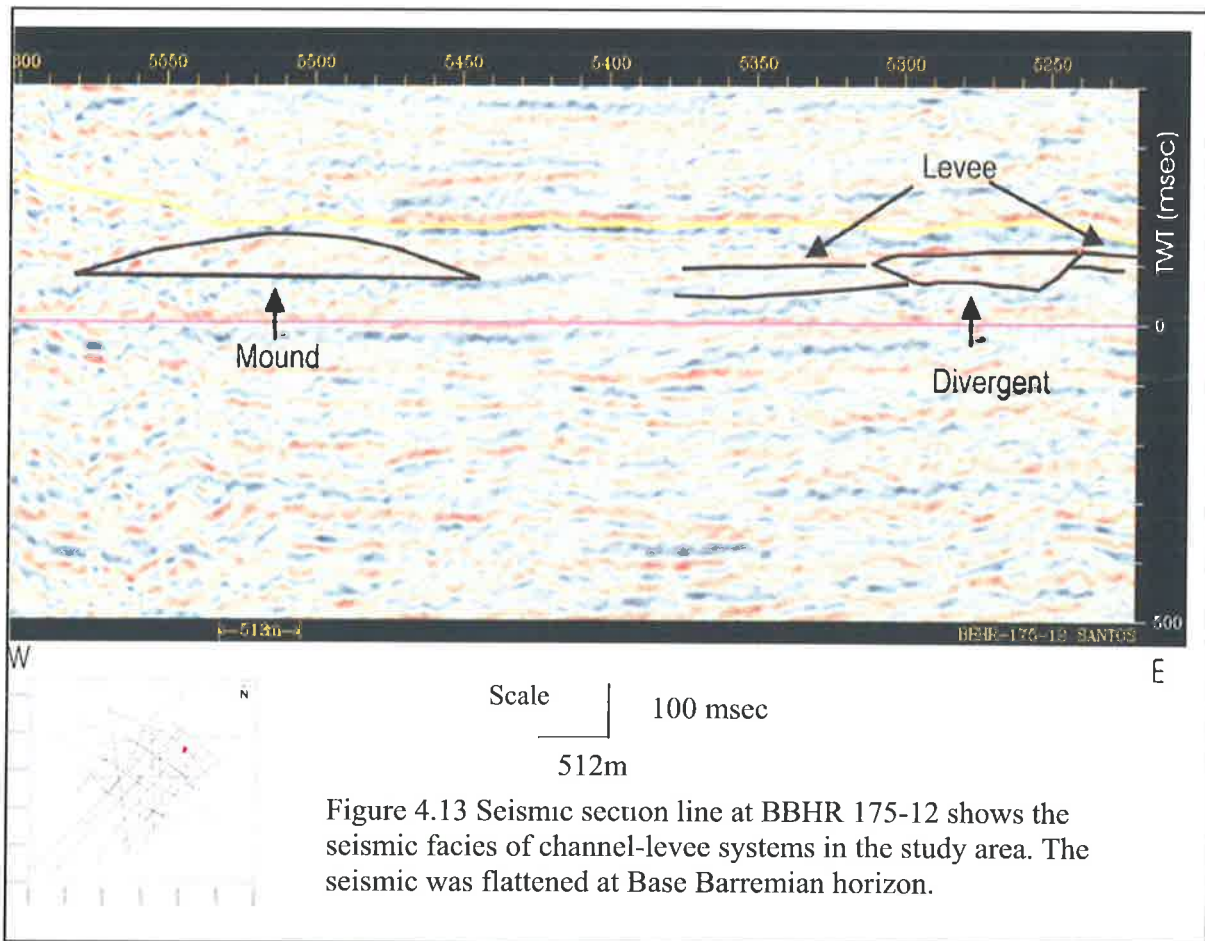


Figure 4.13 Seismic section line at BBHR 175-12 shows the seismic facies of channel-levee systems in the study area. The seismic was flattened at Base Barremian horizon.

4. 5 Geometry Interpretation

The thickness of the channel sands and the lobes that were intersected by wells were calculated directly from the logs. Widths were estimated using width to thickness aspect ratios. The average width to thickness ratio of deepwater channel sands is typically 1:20 (Clark and Pickering, 1996) (Figure 4.14). For channels and lobes that were not penetrated by a well, the thickness of the channel sands was calculated from the seismic and was converted to meters using velocity information from the nearest well (Figure 4.15). Meanwhile, the width of the channel sands in the inner and middle fan areas and the width of the lobes in the outer fan areas were measured directly from the seismic data.

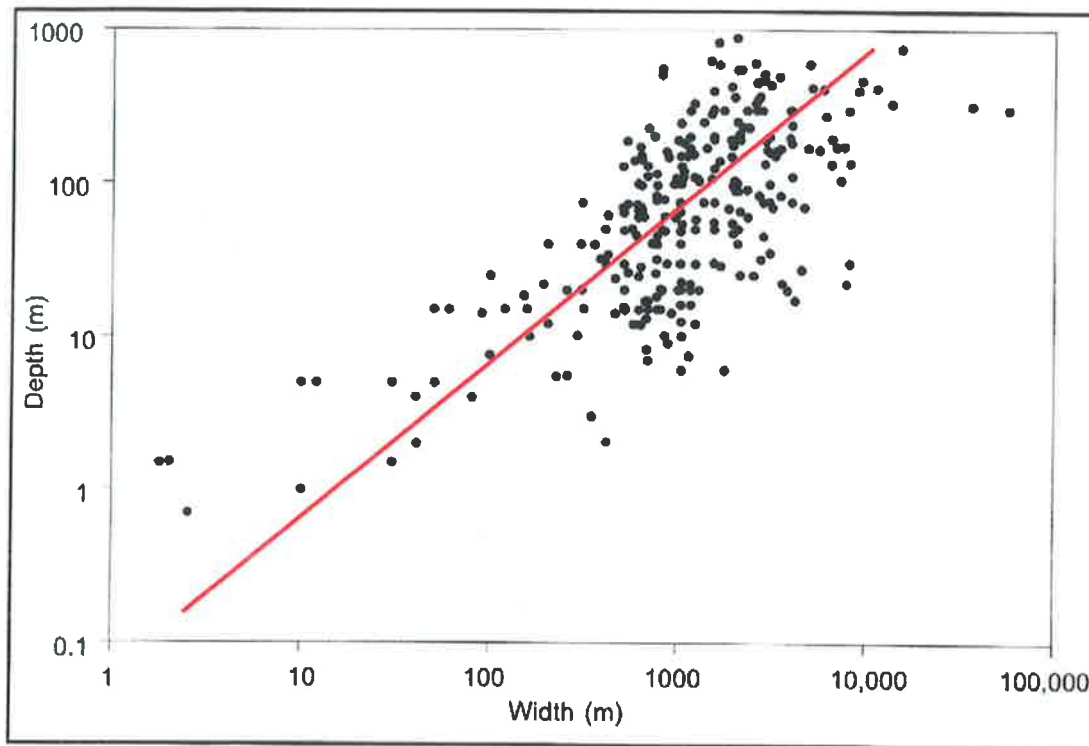


Figure 4.14 Graph showing the relationship of channel width to depth (aspect ratio) in deepwater environments (Clark and Pickering, 1996). A red line shows 1:20 aspect ratio.

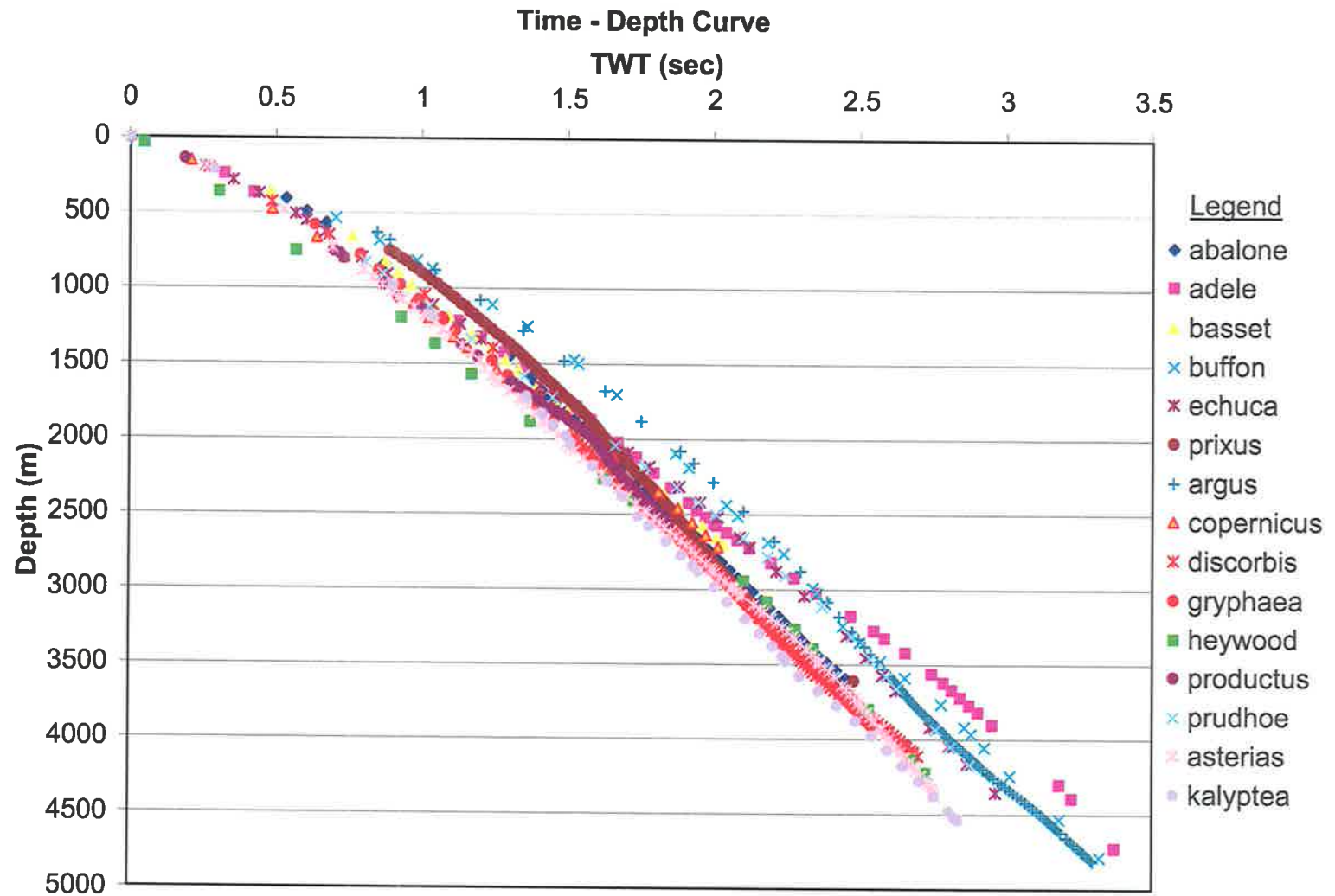


Figure 4.15 Time-depth curves of wells in the study area.

CHAPTER 5 RESULTS

The Echuca Shoals Formation is divided into two sequences based on sequence stratigraphic analysis of 14 well logs in the northern Caswell Sub-basin.

5.1 Sequence 1

Sequence 1 is separated from Sequence 2 by a sequence boundary that is recognized in well logs as a sharp upward decrease in the gamma ray logs in the Asterias-1 and Kalyptea-1ST1 wells (Figure 4.6). The maximum flooding surface in Sequence 1 is recognized by the highest value of gamma ray and can be recognized as continuous high to moderate amplitude on the seismic reflection (Figure 5.1).

Age

Sequence 1 consists of sand and shale lithology. It was deposited during Valanginian to Hauterivian times (135-125 Ma). This age is implied by the presence of *Senoniasphaera tabulata* and *Systematophora aerolata* pollen.

Seismic and Electric-log Facies

Based on reflection configuration, the seismic facies that can be recognized in Sequence 1 are mound, clinoform, divergent and hummocky reflection. The clinoforms are observed in the southern part of the study area, whereas the mounds are present in the northern part of the study area. The gamma ray log in Asterias-1 shows a blocky shape at a depth of 3630-3682 m. In Kalyptea-1ST1, a gamma ray log has a bell serrated shape at a depth of 4280-4320 m (Figure 4.6). For other wells, the gamma ray logs that have a high API unit value are indicated as shale.

Systems Tracts

Sequence 1 is divided into three systems tracts: lowstand systems tract, transgressive systems tract and highstand systems tract. The base of the lowstand systems tract is indicated by the candidate sequence boundary below the sand at Asterias-1, Kalyptea-1ST and Buccaneer-1. In seismic cross section, the lowstand systems tract is indicated by onlapping reflections (Figure 5.1). The thickest lowstand systems tract is present at Asterias-1 where it has a thickness of 50

m. The lowstand systems tract did not develop at Discorbis-1 and Adele-1 wells. At these wells, the candidate sequence boundary coincides with the transgressive surface and the maximum flooding surface. The transgressive systems tract in Sequence 1 is indicated by fining upward and only develops at the Gryphaea-1 where it is 10 m thick and Echuca Shoals-1 where it is 30 m thick. The highstand systems tract is indicated by prograding deposits overlain by a condensed section. The thickest highstand systems tract is present at Asterias-1 where it is 150 m thick and the thinnest is present at Productus-1 well where it is only 28 m due to erosion. The highstand systems tract is indicated by downlapping reflections in seismic cross section (Figure 5.1).

Distribution

Based on chronostratigraphic electric log correlation, Sequence 1 is present in 14 wells in the northern Caswell Sub-basin. Sequence 1 thickest is in Asterias-1 where it is 200 m thick and thinnest in Productus-1, where it is 50 m thick. Sand lithology is present in Kalyptea-1ST1 where it is 40 m thick, Asterias-1 where it is 50 m thick, and Crux-1 where it is 10 m thick.

Based on seismic mapping of the base of the Valanginian and the base of the Barremian, Sequence 1 is interpreted to be absent in the western part of the northern Caswell Sub-basin (Figure 5.2 and Figure 5.3).

Based on isochron mapping, Sequence 1 has a maximum thickness of 275 msec (approximately 400 m). The thickest area surrounds the Basset-1, Adele-1 and Echuca Shoals-1 wells. The isochron also shows the thinning of the sequence to the east, to the west and to the north of the study area (Figure 5.4).

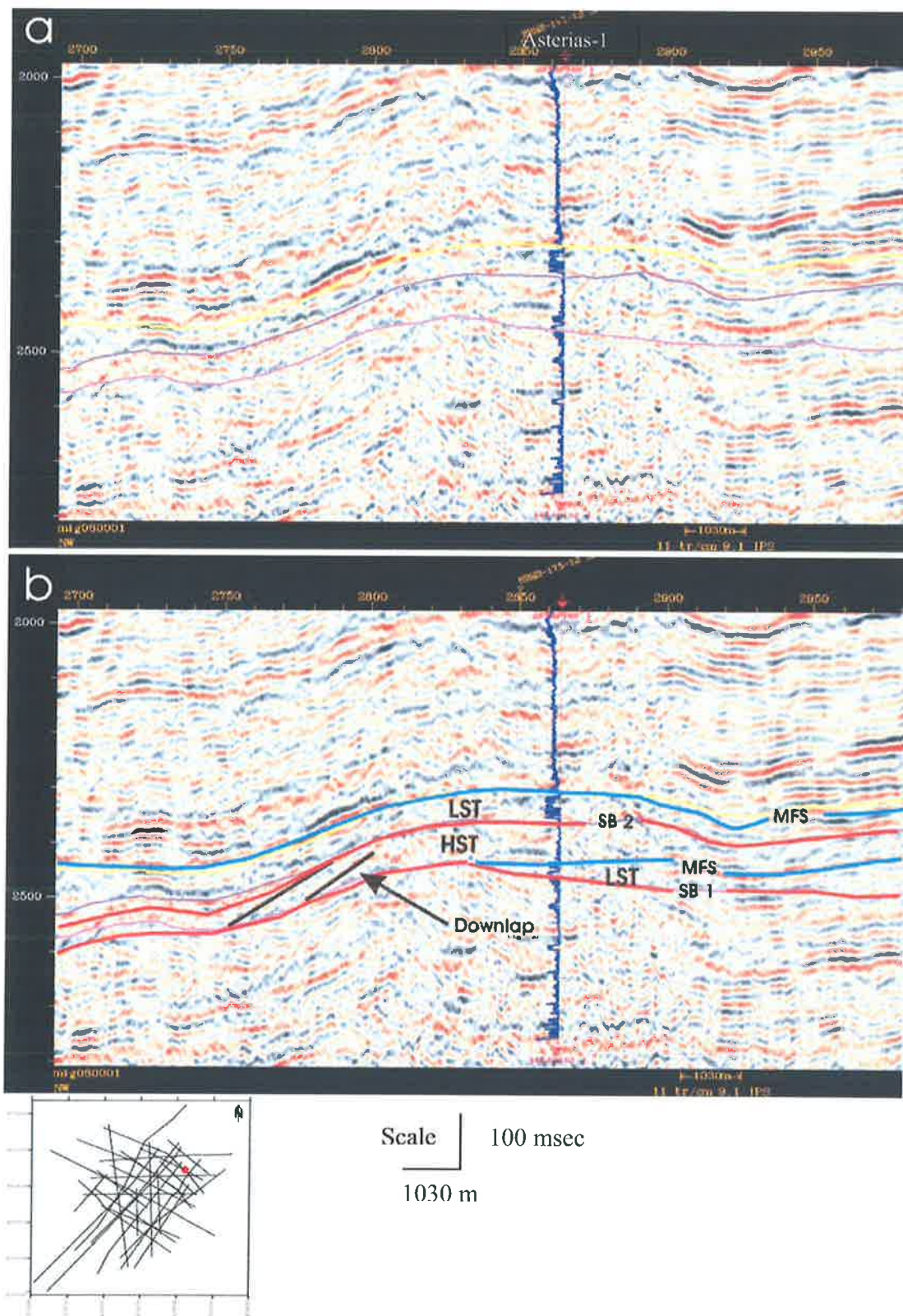


Figure 5.1 Seismic line BBHR 175-12 (a) uninterpreted (b) interpreted, showing seismic stratigraphic interpretation.

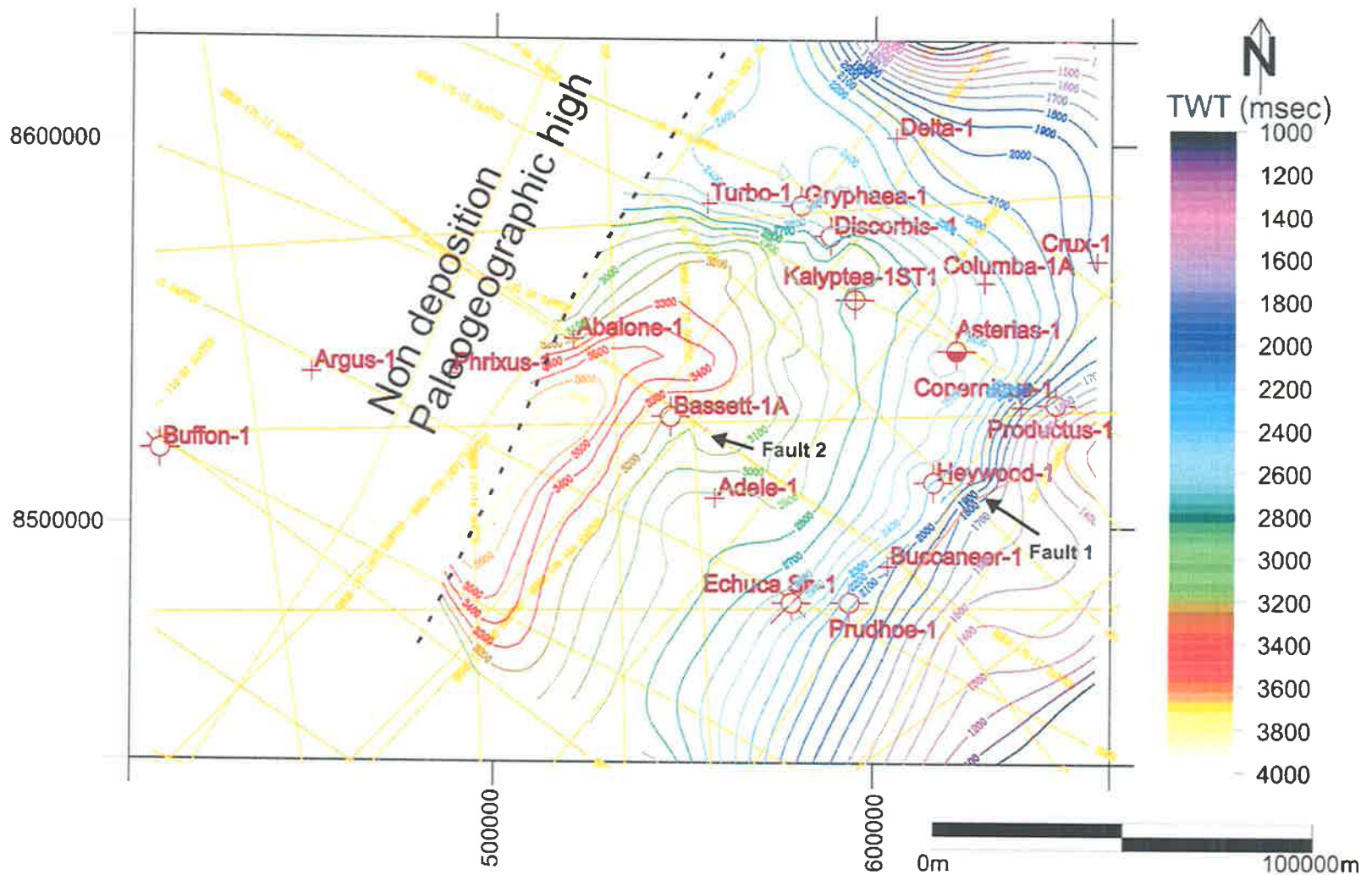


Figure 5.2 TWT map of the base of Valanginian horizon. Dashed line shows the zero edge of the Echuca Shoals Formation. Contour interval 100 msec.

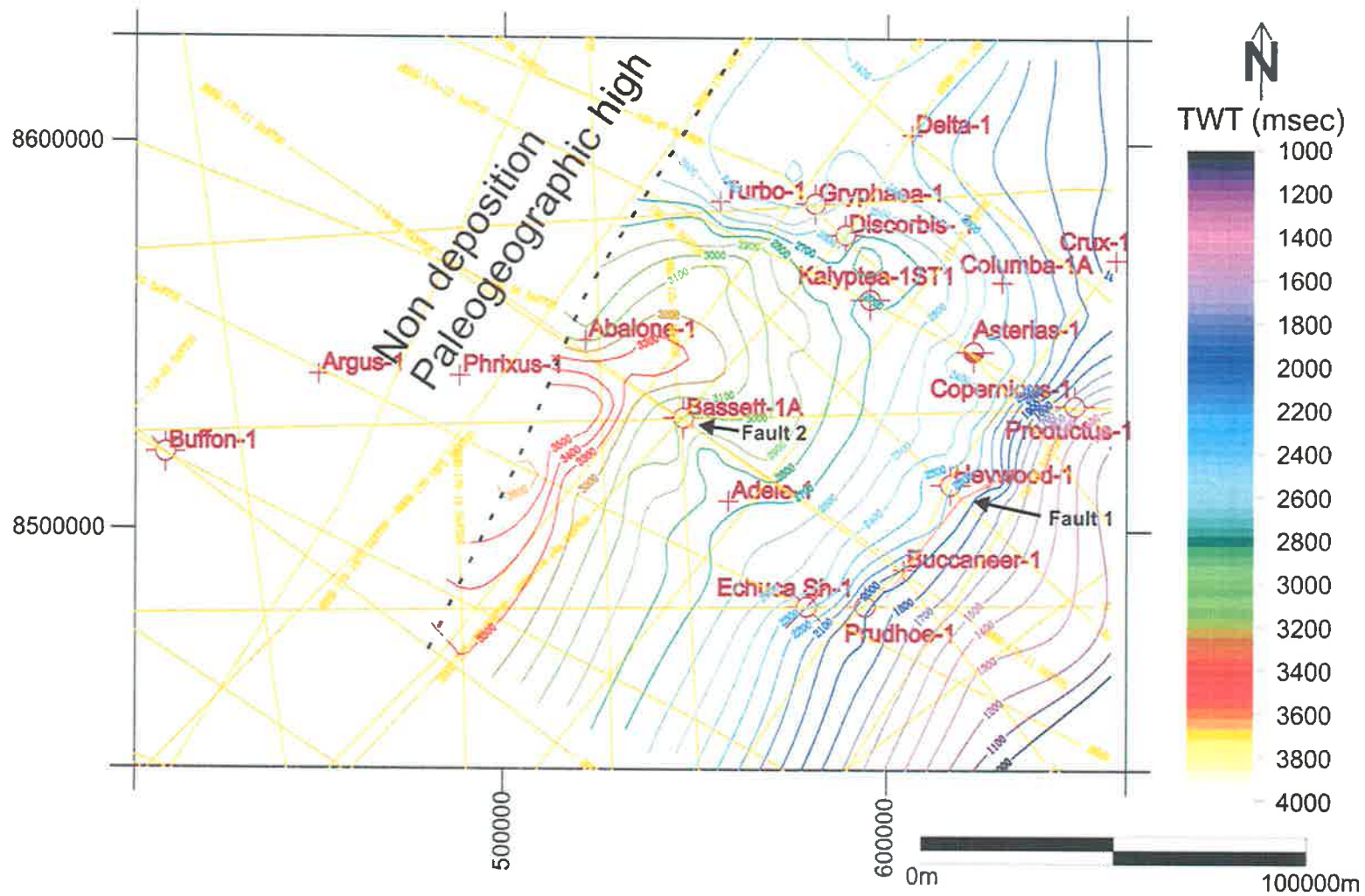


Figure 5.3 TWT map of the base of Barremian horizon. Dashed line shows the zero edge of the Echuca Shoals Formation. Contour interval 100 msec.

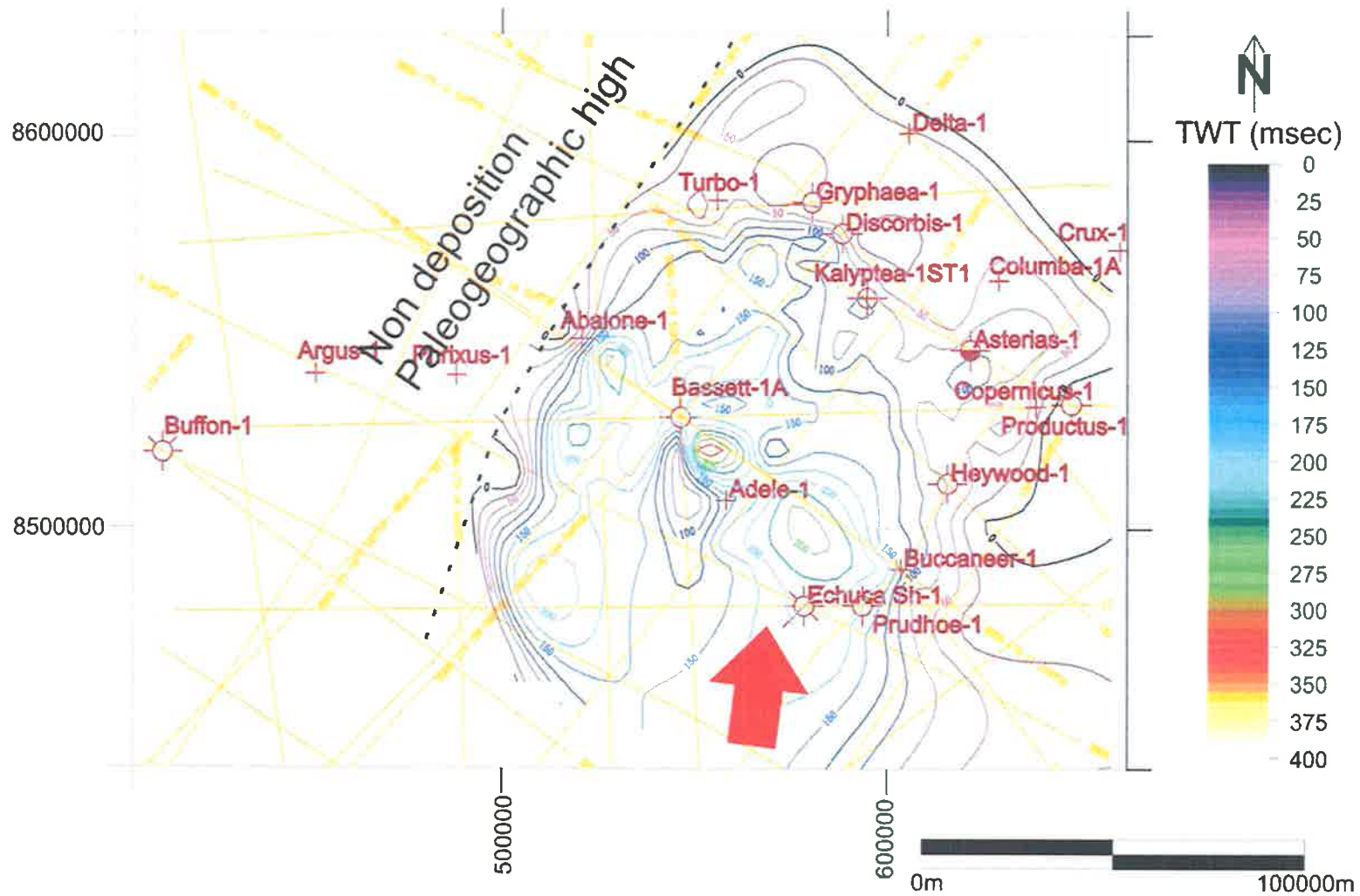


Figure 5.4 Isochron map of Sequence 1 (red arrow showing paleodirection of sediment supply).
Contour interval 25 msec.

5.2 Sequence 2

Age

Sequence 2 consists of sand and shale lithology. It was deposited in Barremian age (125-115 Ma) and is recognized by the presence of *Muderongia australis* pollen.

Seismic and Electric-log Facies

The seismic reflection configurations of mounded, divergent and clinoform types are present in Sequence 2. The clinoform configurations are present in the southern part of the study area, whereas the mounded configurations are present in the northern part of the study area (Figure 6.2 and 6.4). Log motifs in Kalyptea-1ST1 show a serrated belly shape at a depth of 4135 - 4172 m, whereas a serrated blocky shape is present at Asterias-1 at the depth 3395 - 3480 m (Figure 4.6). The blocky shape is present at Crux-1 from a depth of 3050 - 3060 m (Figure 4.8).

Systems Tracts

Sequence 2 is divided into three systems tracts: lowstand systems tract, transgressive systems tract and highstand systems tract. The lowstand systems tract in Sequence 2 is indicated by a candidate sequence boundary that is recognized by a sharp base below the sand in Asterias-1 and Kalyptea-1 (Figure 4.6). The lowstand systems tract thickness in Kalyptea-1ST1, Asterias-1, and Heywood-1 is 38 m, 80 m and 28 m respectively. The transgressive systems tract is indicated by a fining upward unit developed in Kalyptea-1ST1 where it is 28 m thick, and Heywood-1 where it is 5 m thick. The transgressive systems tract did not develop in the other wells and at those wells the transgressive surface coincides with maximum flooding surface. The maximum flooding surface is the base of the highstand systems tract in Sequence 2. The highstand systems tract developed in Kalyptea-1ST1 where it is 85 m thick, Asterias-1 where it is 18 m thick and Echuca Shoals-1 where it is 350 m thick. In seismic cross sections the maximum flooding is recognized by high to moderate continuous amplitude.

Distribution

From chronostratigraphic log correlation, Sequence 2 is observed in ten wells in the northern Caswell Sub-basin. Sequence 2 is thickest in Adele-1 (290 m) and thinnest in Copernicus-1, where it is 15 m thick. Sand is present in Asterias-1 where it is 80 m thick and Kalyptea-1 where it is 35 m thick. Sequence 2 was not deposited in Crux-1, Productus-1 and Turbo-1.

Based on horizon mapping of the Base Aptian, Sequence 2 become thins to the north, east and west of the northern Caswell Sub-basin (Figure 5.5). Based on isochron mapping, Sequence 2 has a maximum thickness of 125 msec (approximately 170 m). The thickest section is present around the Basset-1 and Adele-1 wells (Figure 5.6).

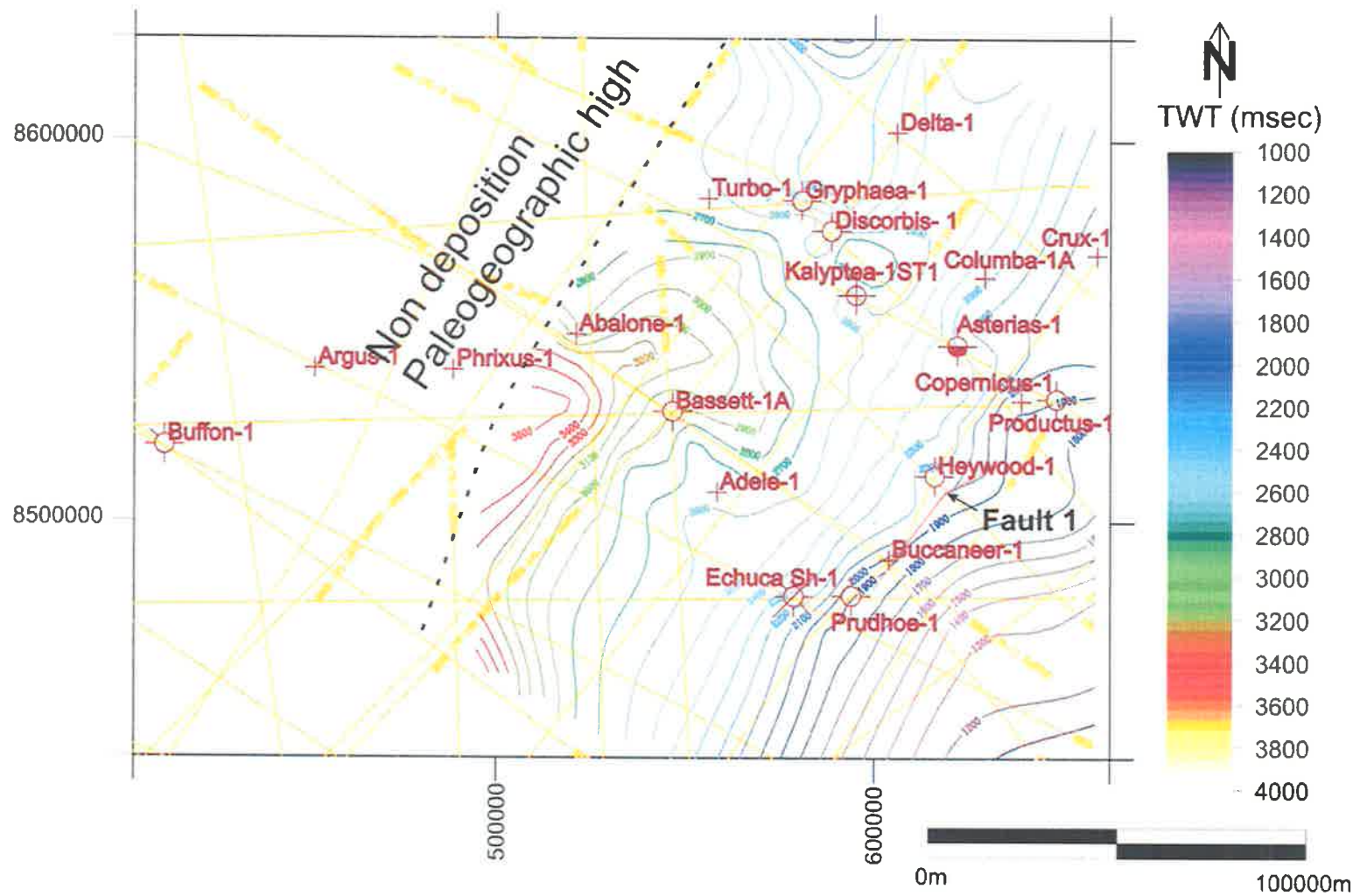


Figure 5.5 TWT map of Base Aptian horizon. Dashed line shows the zero edge of the Echuca Shoals Formation. Contour interval 100 msec.

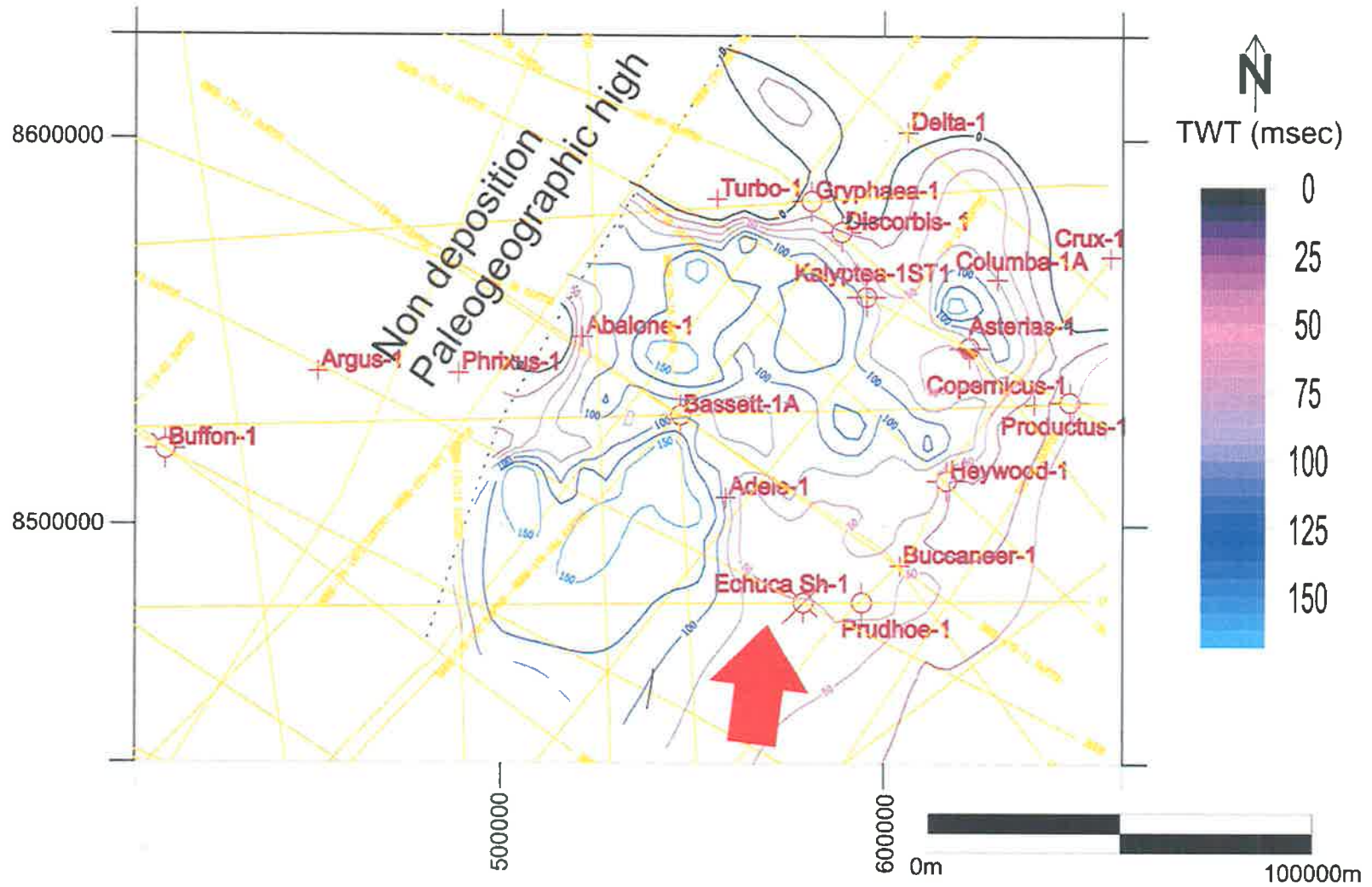


Figure 5.6 Isochron map of Sequence 2 (red arrow showing paleodirection of sediment supply). Contour interval 25 msec.

CHAPTER 6 INTERPRETATION AND DISCUSSION

6.1 Sequence 1

Seismic and Electric-log Facies Analysis

Core interpretation of the Echuca Shoals Formation at Kalyptea-1ST1 by B. Messent (March, 1990) interpreted that the formation was deposited in a deepwater, lower fan environment. Sand/mud ratio in a sand bed from core data between 4159 and 4159.3 m is 60%. Based on this ratio, the Echuca Shoals Formation was categorized as a point source mud/sand rich submarine fan according to the classification by Richards and Bowman (1998). Based on log motif interpretation, the sand in Asterias-1 at a depth of 3630-3682 m was classified as midfan channel, whereas the sand in Kalyptea-1ST1 at a depth of 4280-4320 m was classified as outer fan (Figure 6.1).

Based on seismic facies analysis, five channels and five lobes were interpreted in the study area. The mound shape observed in Sequence-1 has been interpreted as lobes (Figure 6.2). The divergent shape has been interpreted as channel-levee (Figure 6.3). Channel width in the study area for Sequence 1 varies from 500 to 1100 m. The average width to thickness ratio channels in Sequence 1 is 1:17. The result of the width to thickness ratio calculation of each channel and lobe measured from seismic data is listed in Table 6.1. The shape of channel fill in mud/sand rich systems usually is sinuous (Weimer and Slatt, 2004).

Depositional system and Paleogeography

The isochron map of the base Valanginian (Figure 5.4) shows that the thickest accumulation is in the south and it thins to the north, east, and west of this area. These isochron features suggest that the paleodirection of the sediment supply for Sequence 1 is from the south-east toward the north-west of the area. The source of the sediment supply is possible from Asterias Delta which exists at the south of the study area (Figure 2.5).

The paleogeography of the Sequence 1 has been divided into lowstand fan and lowstand wedge. The clinoform unit which exists in the southern part of the study area indicates a potential lowstand wedge of the lowstand depositional system in a deepwater environment

(Figure 6.4). The clinoforms in this study area have a vertical range from 100 to 200 msec in TWT. Using velocity in the area of 2700 m/sec, the thickness of the clinoforms ranges from 135-270m. The distribution of the lowstand wedge is around Echuca Shoals-1, Adele-1, and Prudhoe-1 wells (Figure 6.5). The lowstand fan was indicated by the presence of lobes in the northern part of the study area.

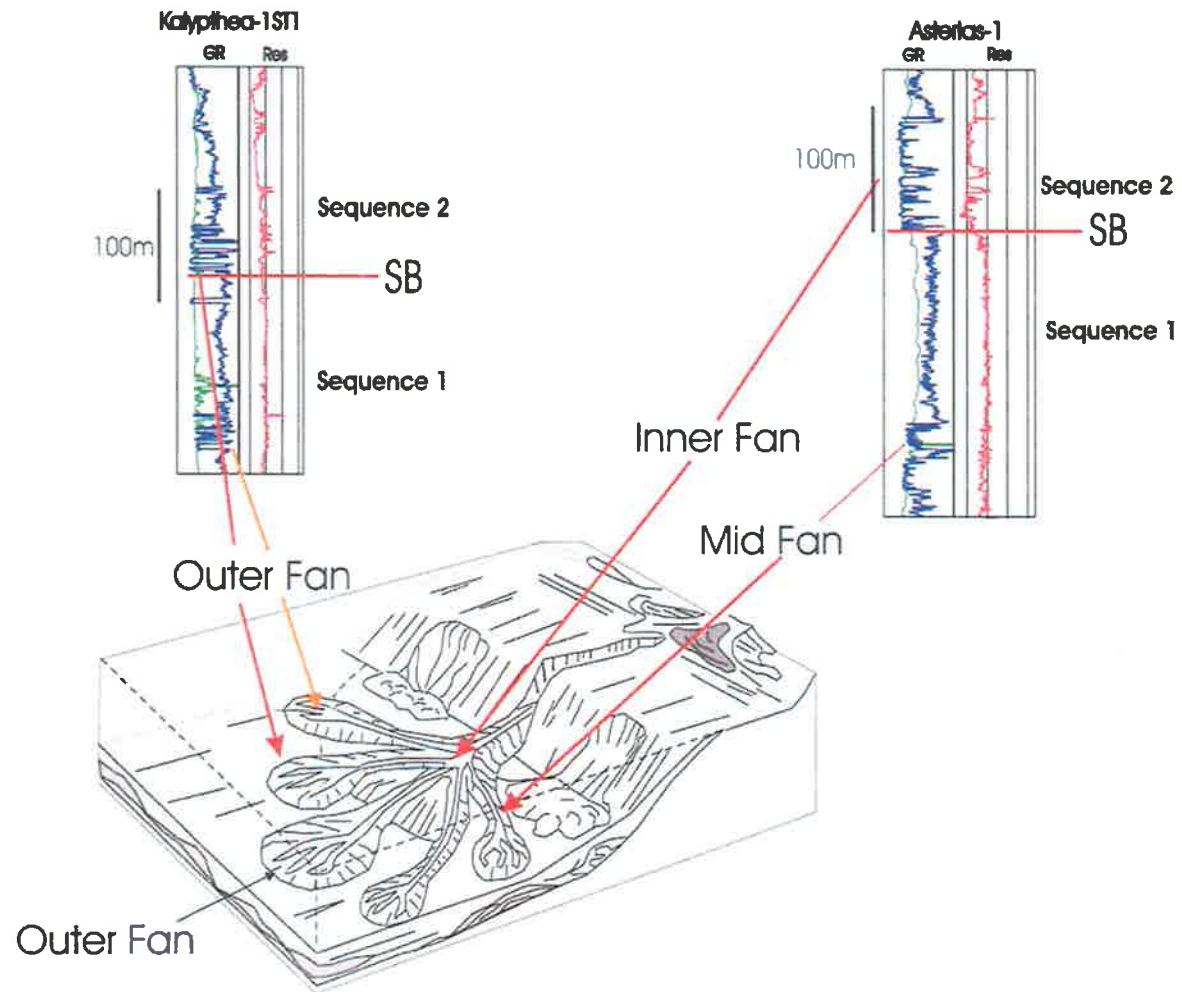
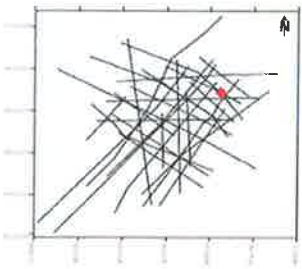
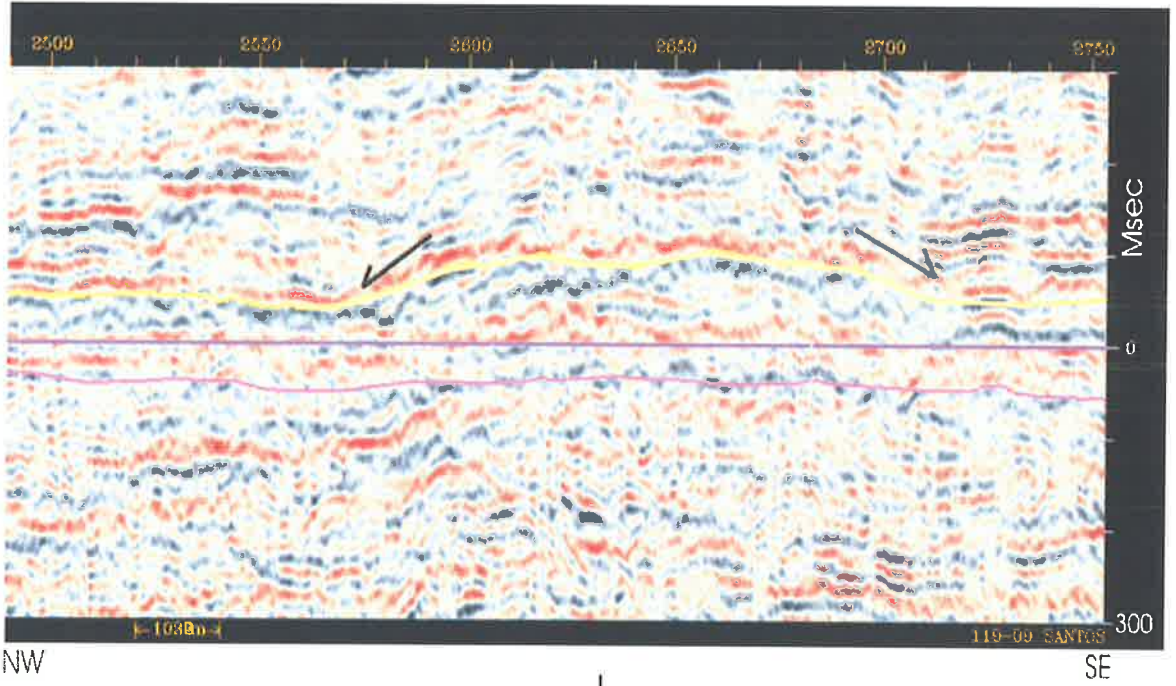
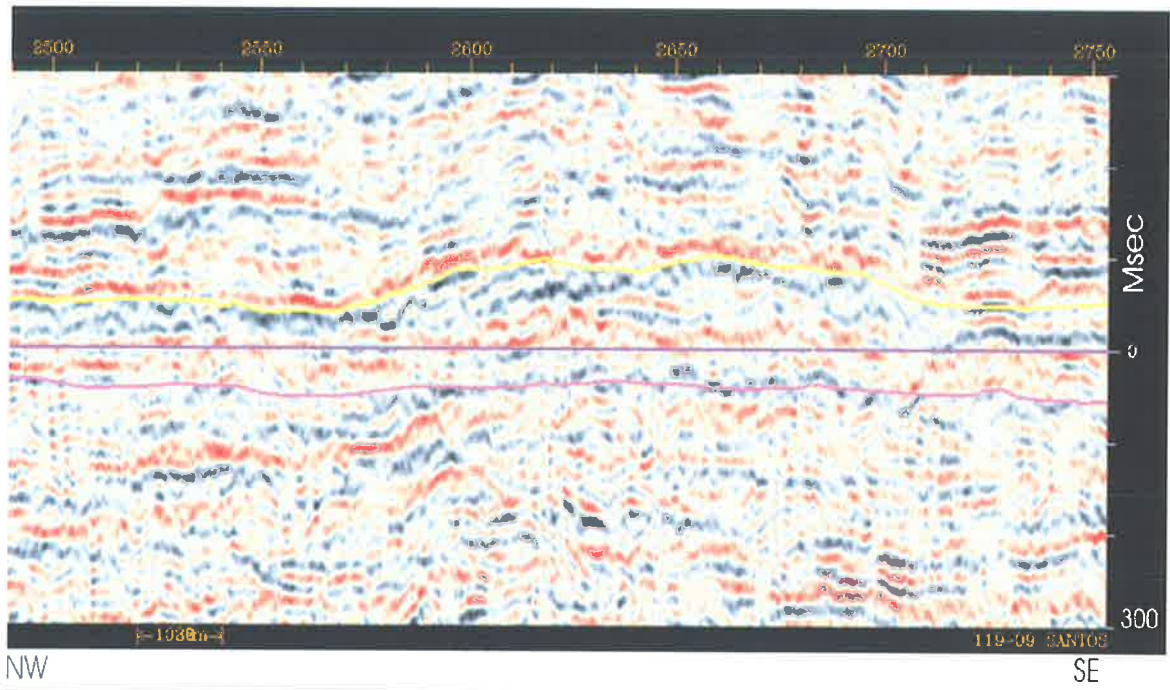


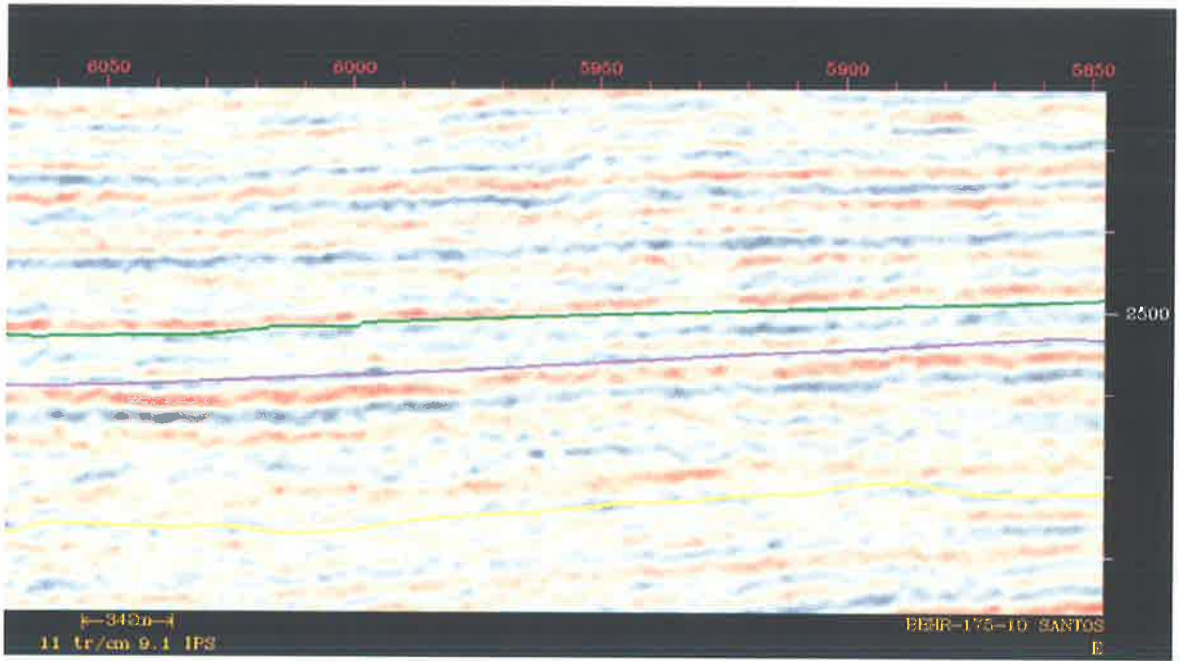
Figure 6.1 Electric-log characteristic in mud/sand rich submarine fan systems (Modified after Richards and Bowman, 1998).



Scale
 100 msec
 1030 m

Figure 6.2 Seismic section line 119-09 (a) uninterpreted and (b) interpreted, showing a mound feature interpreted as lobes. The line is flattened at base Barremian.

a



b

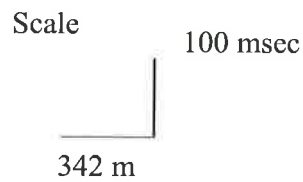
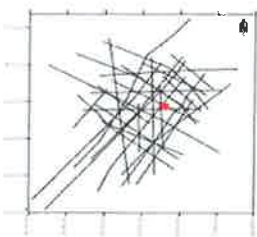
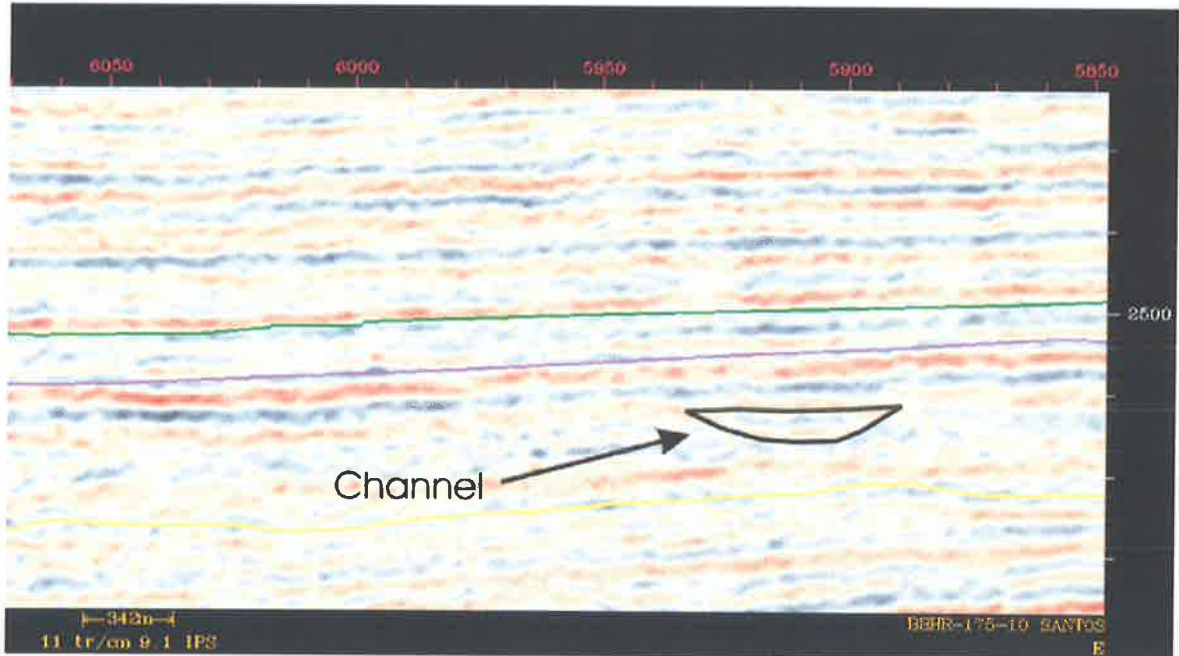
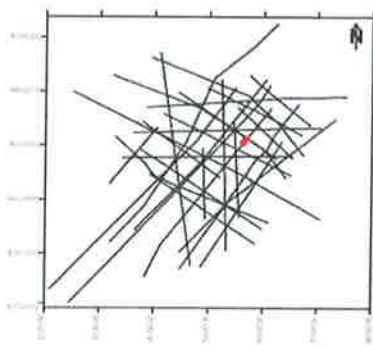
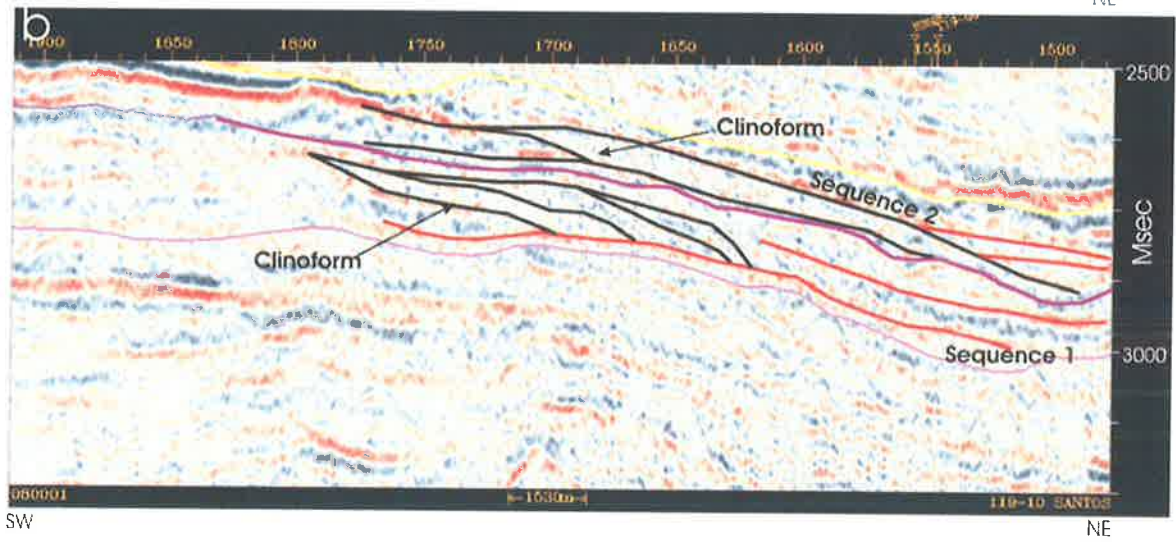
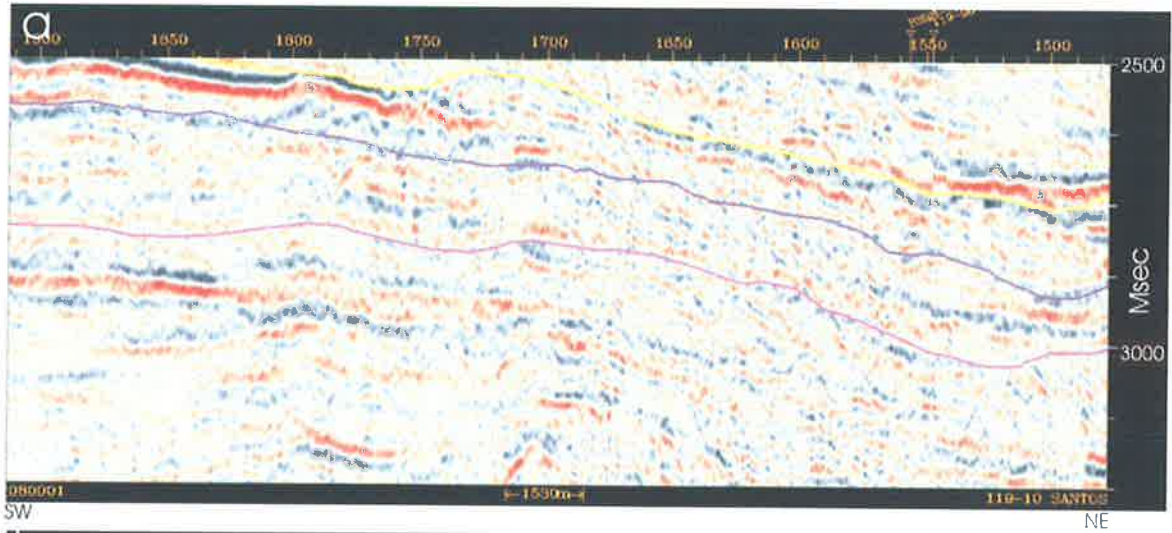


Figure 6.3 Seismic section line BBHR-175-10 (a) uninterpreted (b) interpreted showing divergent shape, interpreted as a channel.

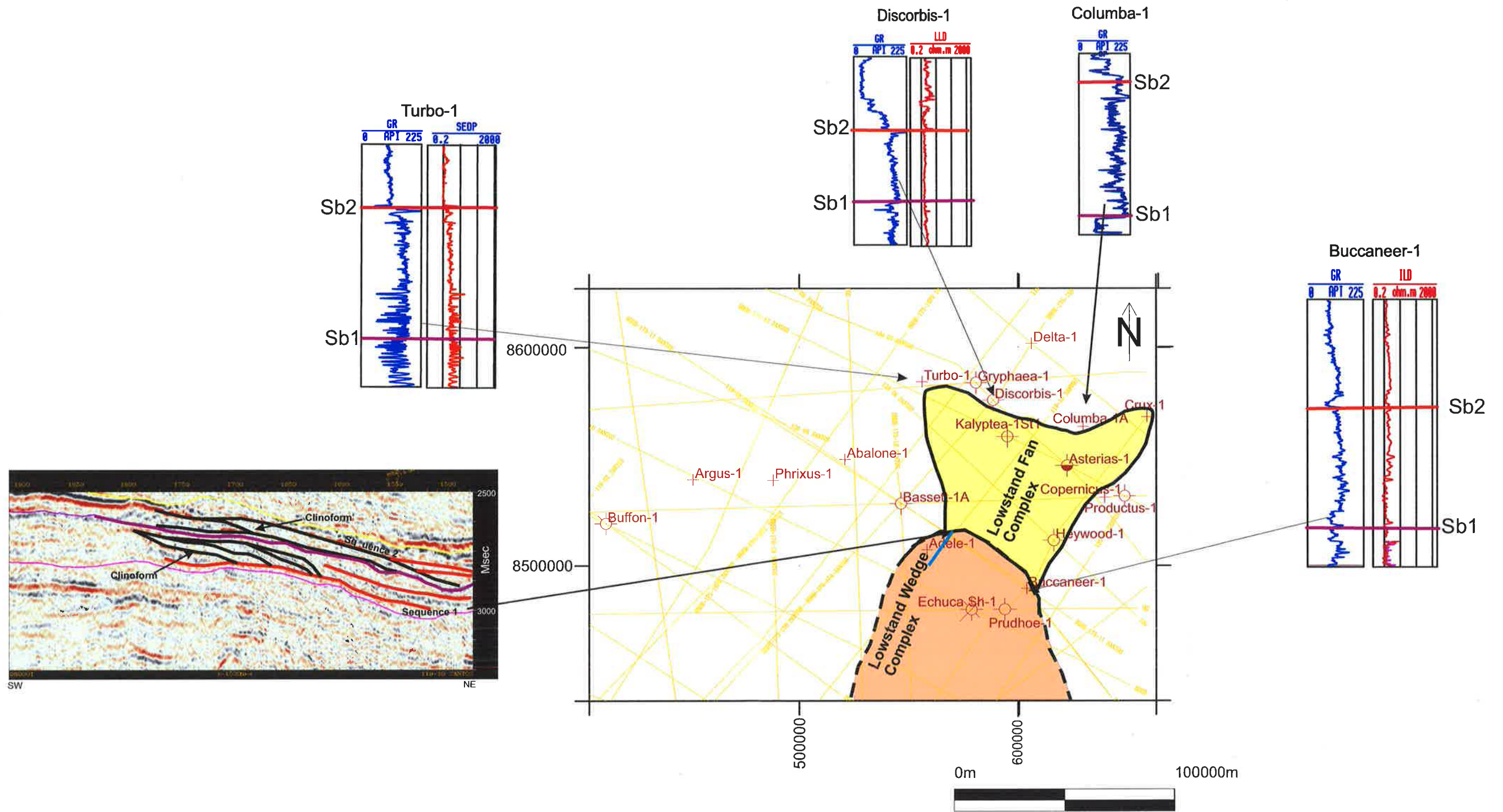
Table 6.1 Measurement of geometry features from seismic data.

	Seismic line	Shot Point	Width (m)	Thickness TWT(msec)	Thickness (m)	Width/Thick Ratio	Interp	
Sequence 1 Age : Valanginian - Hauterivian	BBHR 175-11	10900	532	26	32	16.63	Channel	
	BBHR 130-06	2250	527	28	39	13.51	Channel	
	BBHR 130-04	1650	889	32	44	20.20	Channel	
	BBHR 175-12	3131	1170	29	42	27.86	Channel	
	BBHR 130-06	2500	940	48	72	13.06	Channel	
	BBHR 130-04	1920	916	37	56	16.36	Channel	
	BBHR 119-09	2983	1131	34	51	22.18	Channel	
	BBHR 175-12	5000	936	48	75	12.48	Channel	
	BBHR 130-04	4450	597	38	49	12.18	Channel	
	BBHR 175-11	10450	452	36	49	9.22	Channel	
	BBHR 175-10	5900	710	38	54	13.15	Channel	
	BBHR 130-04	2850	1106	44	58	19.07	Channel	
	BBHR 130-06	4450	612	34	46	13.30	Channel	
	BBHR 175-10	5200	707	20	26	27.19	Channel	
	BBHR 175-11	9250	1014	36	47	21.57	Channel	
							17.20	Average
Sequence 2 Age : Barremian	BBHR 130-06	2500	952	42	60	15.87	Channel	
	BBHR 130-04	1920	1160	37	52	22.31	Channel	
	BBHR 130-04	2160	1050	41	60	17.50	Channel	
	BBHR 130-06	3400	1528	35	51	29.96	Channel	
	BBHR 175-12	5600	1416	40	63	22.48	Channel	
	BBHR 175-15B	27100	839	24	38	22.08	Channel	
	BBHR 130-06	4100	1920	69	110	17.45	Channel	
	BBHR 175-11	9250	771	29	37	20.84	Channel	
	BBHR 175-10	6300	820	29	37	22.16	Channel	
							21.18	Average
	BBHR 119-09	2650	1769	37	55	32.16	Lobe	
BBHR 119-09	2650	4110	46	70	58.71	Lobe		
						45.43	Average	



Scale
 100 msec
 1530m

Figure 6.4 Seismic section line 119-10 (a) uninterpreted and (b) interpreted, showing clinoform unit, interpreted as a lowstand wedge.



Legend

- Lowstand fan complex
- Lowstand wedge complex

Figure 6.5 Paleogeographic map of Sequence 1

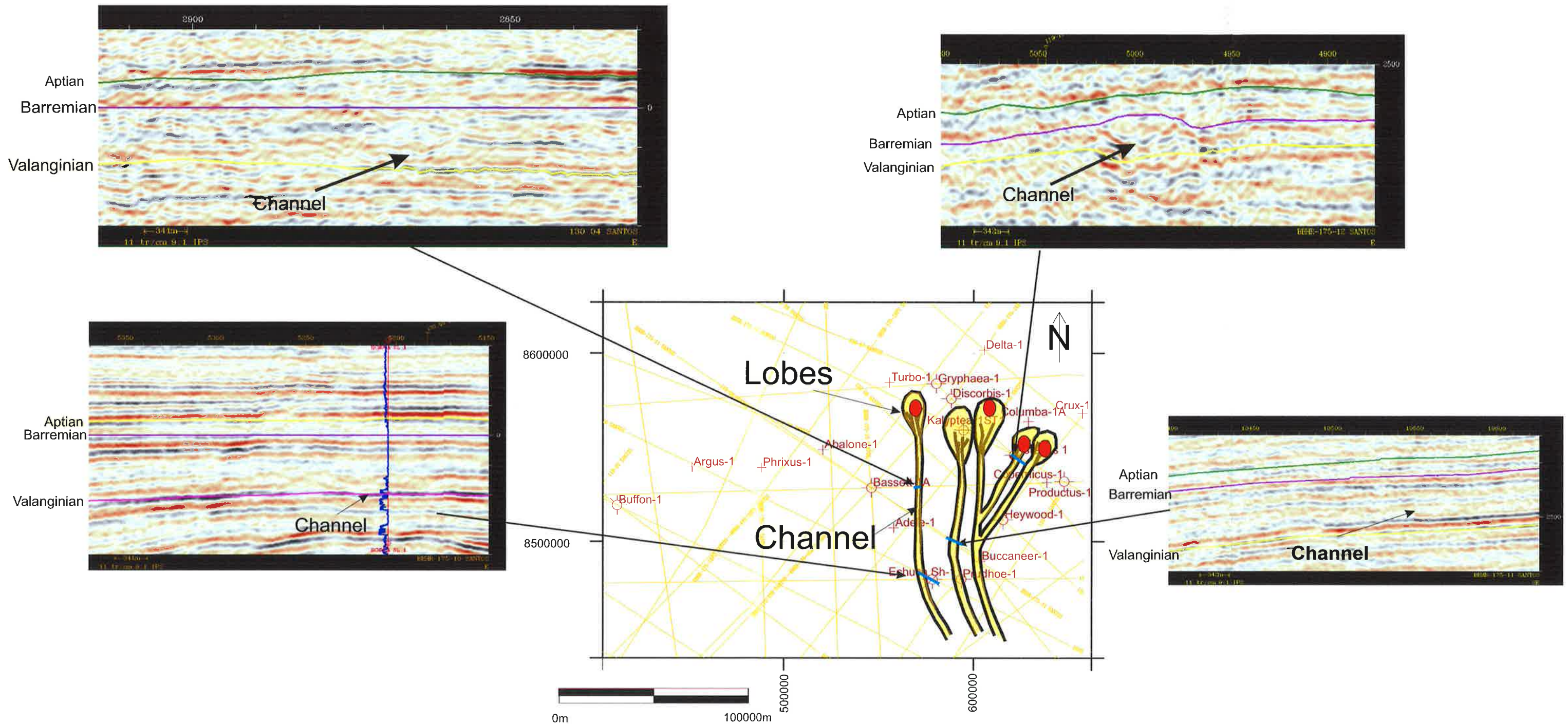


Figure 6.6 Sequence 1 channel-levees and lobes based on seismic facies interpretation, Red circles show potential stratigraphic traps.

6.2 Sequence 2

Seismic and Electric-log Facies Analysis

Log motif interpretations of sand in Asterias-1 at a depth of 3395 – 3480 m indicated that the sand was deposited in the inner fan of a mud/sand rich system (Figure 6.1). The interpretation of sand in Kalyptea-1 ST1 at a depth of 4135 - 4172 m indicated that the sand was deposited in outer fan lobes (Figure 6.1). Four channels and four lobes were interpreted in the study area (Figure 6.7). The average width to thickness ratio of the channel sands in Sequence 2 based on seismic data interpretation is 1:21 and the width of the channels ranges from 771 to 1529 m (Table 6.1). The channel shape in the mud/sand rich systems tends to be sinuous (Weimer and Slatt, 2004). The width of the lobes in the study area ranges from 1800 to 4100 m, with width to thickness ratio is between 1:32 to 1:59.

Depositional System and Paleogeography

The isochron map of the Barremian interval shows that the thickest area is located to the south and thins to the north, east and west of the study area (Figure 5.6). This isochron map also indicates that paleodirection of the sediment was from southeast to northwest. The clinoforms feature present in the southern part of the study area indicate that this area was deposited in the lowstand wedge (Figure 6.4). The clinoforms range from 50-100 msec, which assuming a velocity of 2700 m/sec, gives an approximate thickness is 67-135m. The presence of lobes in the northern part of the study area indicates that the sediment in this area was deposited as a lowstand fan. Figure 6.9 shows the schematic depositional model in the study area.

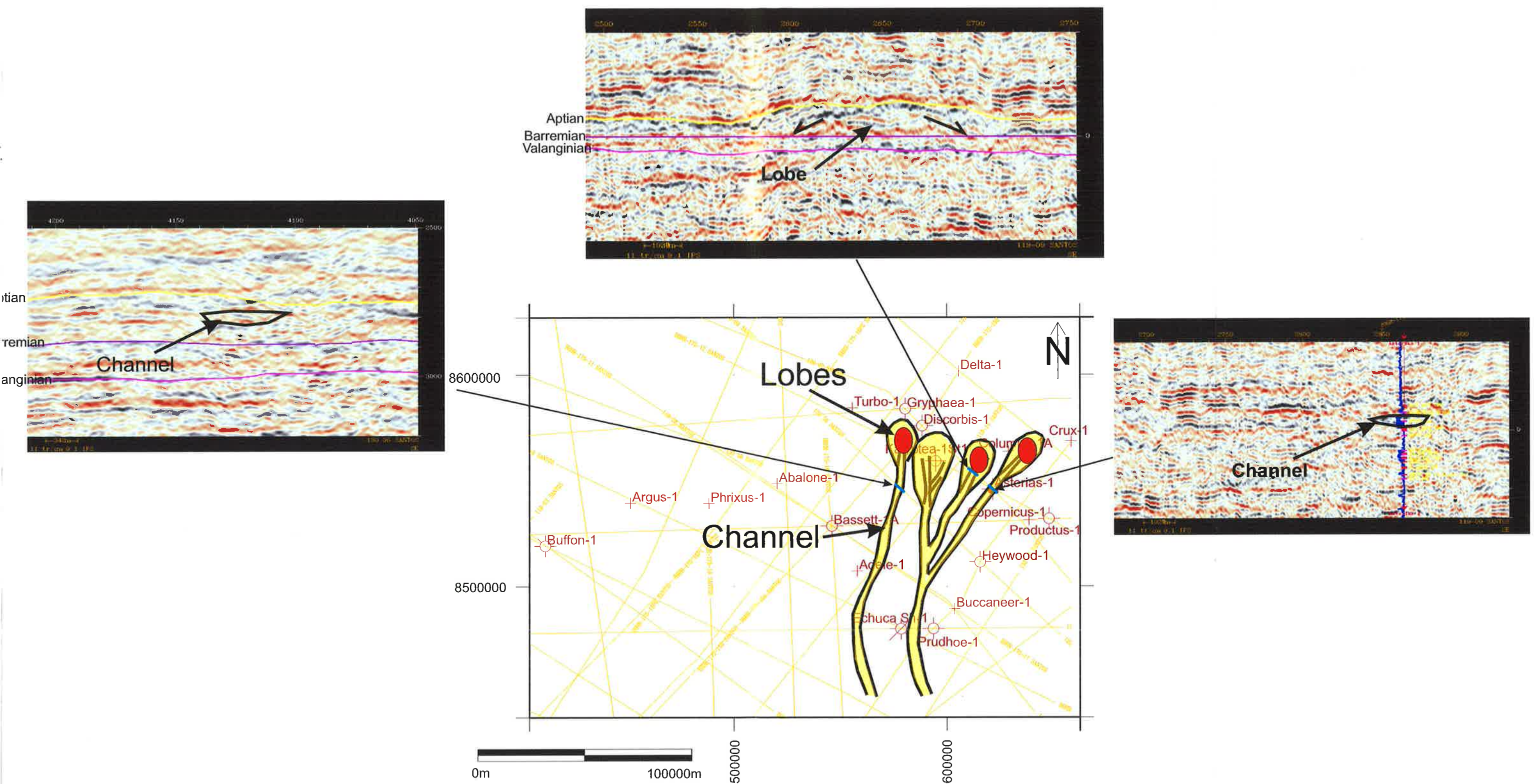


Figure 6.7 Sequence 2 channel-levees and lobes based on seismic facies interpretation. Red circles show potential stratigraphic traps.

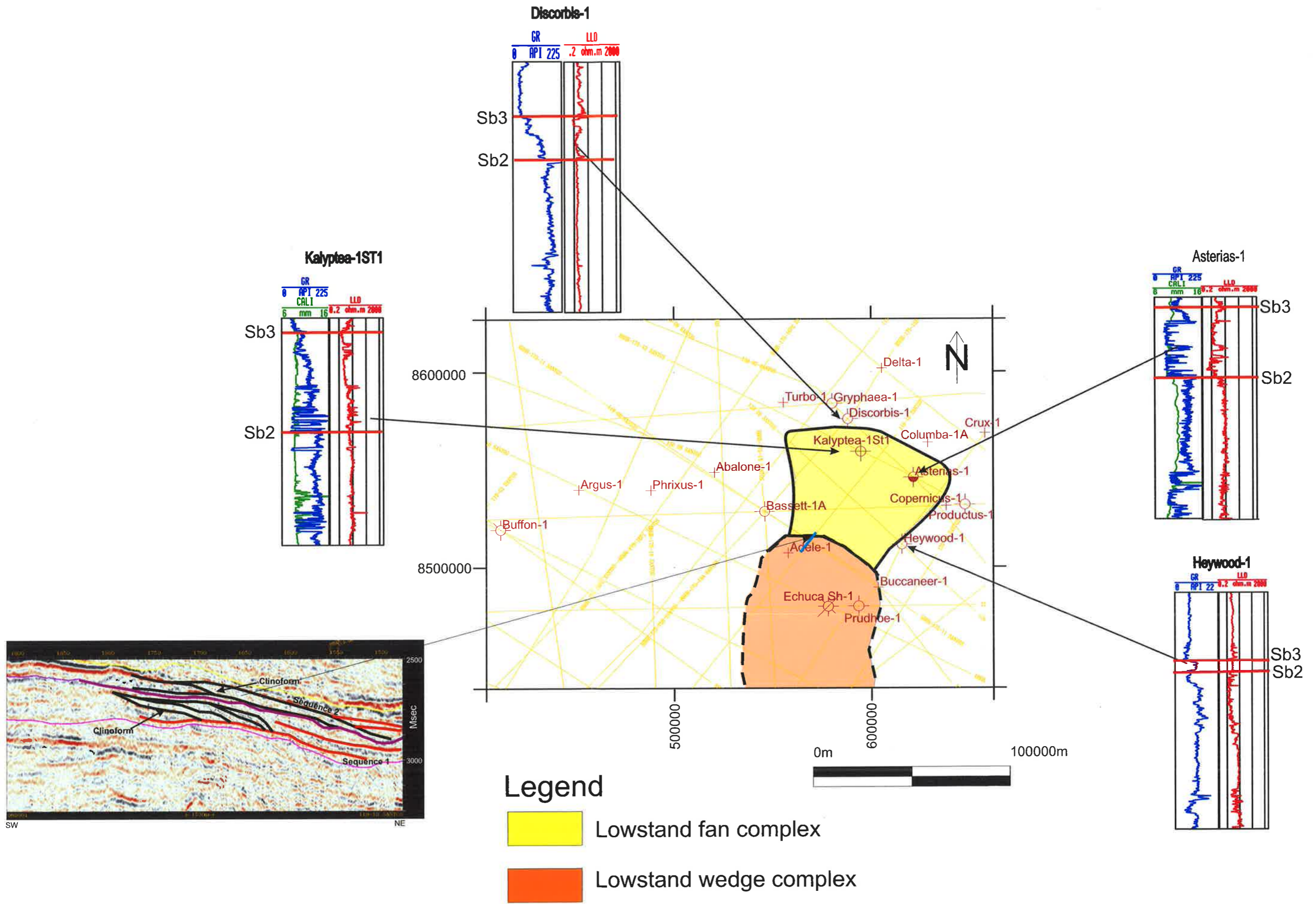


Figure 6.8 Paleogeographic map of Sequence 2

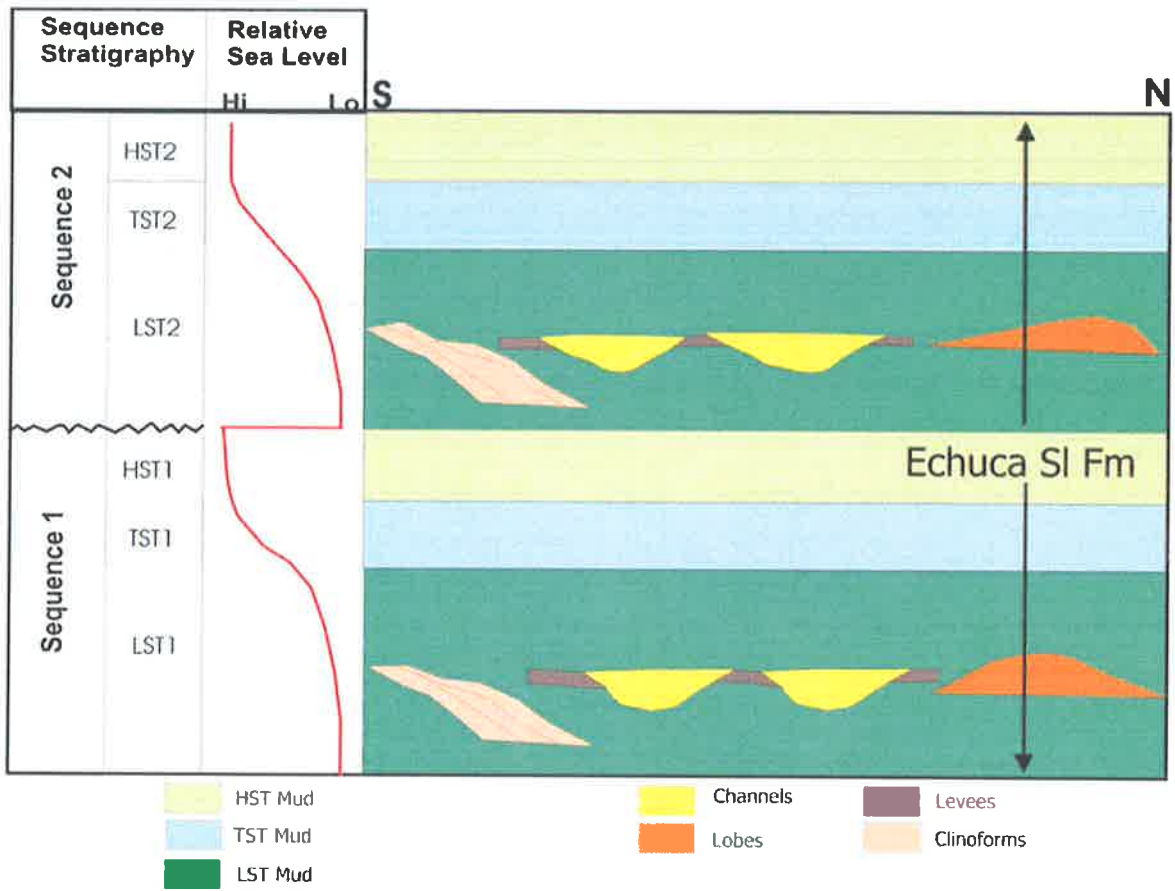


Figure 6.9 Schematic depositional model of the study area.

CHAPTER 7 PLAY ANALYSIS

7.1 Sequence 1

Trapping Mechanisms

Structural traps

There are no structural traps in the study area, even though two normal faults have been interpreted from the Base Valanginian and Base Barremian interval. Fault 1 is located to the east of the Heywood-1 and has 150 msec (approximately 187 m) throw and heads to the west (Figure 5.2). Fault 2 is located to the west of the Basset-1 well and has 100 msec (approximately 150 m) throw and also heads to the west (Figure 5.2). The fault did not form the traps because the dip of the bed was not steep enough to create a closure. The deepest structural contour is 3800 msec (approximately 4800 m) and the shallowest structural contour is 1000 msec (approximately 1200 m) (Figure 5.2). The formation is absent in Sequence 1 in the west of the study area to the east of Phrixus-1 well since that there was no deposition of sediment due to the presence of the Scott Reef-Brecknock structural high (Figure 7.1).

Stratigraphic traps

In Sequence 1, four from five lobes are potential candidates for stratigraphic traps. The traps are formed by the pinchout of channels in the distal part of the fans (Figure 6.6). The channel pinchouts can be recognized by mound shapes in the seismic sections (Figure 6.2). Kalyptea-1ST1 penetrated one of these lobes in this sequence but the sand was wet. One of the possible reasons is that the well penetrated the sand below the hydrocarbon water contacts. To find the hydrocarbon, it is recommended to drill the lobes to the north of Kalyptea-1ST1 to chase up-dip stratigraphic traps (Table 7.1).

Table 7.1 The coordinates of the potential stratigraphic traps

Stratigraphic Traps	Latitude	Longitude
	X	Y
Sequence 1		
1	568800	8571460
2	608436	8563060
3	627037	8528950
4	637450	8490550
Sequence 2		
1	577545	8568600
2	616767	8562580
3	639107	8564340

Hydrocarbon Source and Migration

The source of the hydrocarbons is from the shales adjacent to the reservoir sands and also from the shales that were deposited during the highstand systems tracts above the reservoir sands. The average hydrogen index is 190 mg hydrocarbons/g TOC (Blevin et al., 1998b). The thermal subsidence in the Early Cretaceous caused hydrocarbons to be expelled from the source rock and migrate to the channel sand adjacent to the source rock (Figure 7.2). Geohistory modelling has shown that the source rock in the Valanginian to Aptian rocks entered the oil window during the latest Cretaceous in the mid-basin area (Blevin et al., 1998a). Even though no hydrocarbon has been found in the Echuca Shoals Formation in the northern Caswell Sub-basin, the oil that is present in this formation at Gwydion-1 in Yampi Shelf Sub-basin is believed to be from this source rock (Spry and Ward, 1997). The Jurassic and Cretaceous age faults are a conduit for migration (Blevin et al., 1998b). The hydrocarbon may also have migrated laterally in the Cretaceous interval (Spry and Ward, 1997).

Reservoir rock

The sandstone that was deposited in the lowstand systems tracts in Sequence 1 is potentially a reservoir rock. The facies is a proven reservoir sand in another adjacent sub-basin (Yampi Shelf) in the Londonderry-1 and Gwydion-1 wells. The sand in the Echuca Shoals Formation is comprised of quartzose and greensand (Spry and Ward, 1997). In Sequence 1, the sand is present in Asterias -1 where it is 55 m thick, Kalyptea-1ST1 where it is 20 m thick, and Gryphaea-1 where it is 25 m thick (Figure 4.5). All of these sands are wet and the reason

according to the well completion reports is because there were no structural traps present in the study area. Hence to locate stratigraphic traps is very important in this area.

Potential Seals

The shale that was deposited during the highstand systems tract in Sequence 1 has potential to be a seal. The shale thickness varies between the wells. The thickest shale in Sequence 1 exists at the Echuca Shoals-1 well where it is 160 m thick. The shale thins to the west and north of the study area.

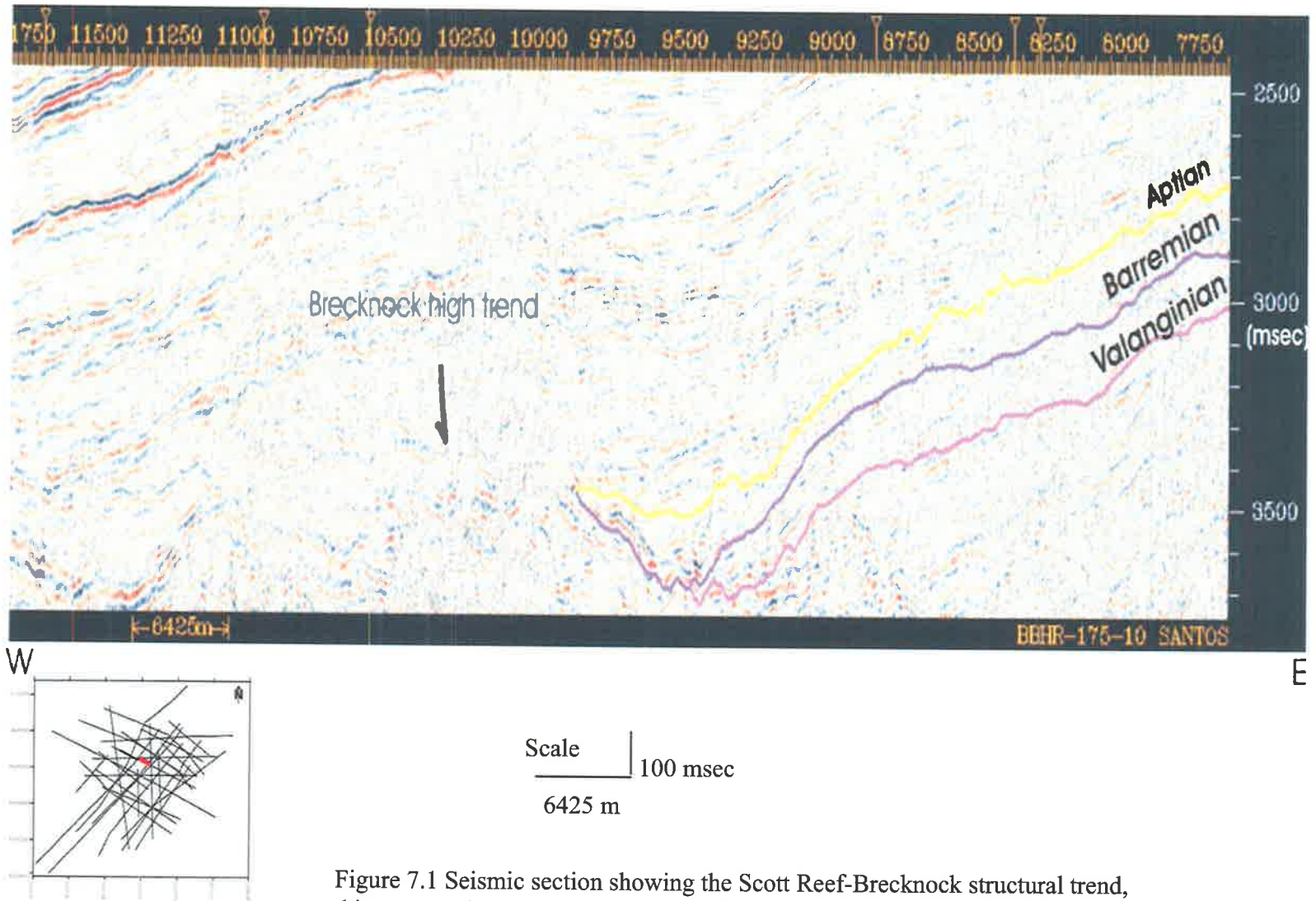


Figure 7.1 Seismic section showing the Scott Reef-Brecknock structural trend, this structural trend is the boundary of the Echuca Shoals Formation.

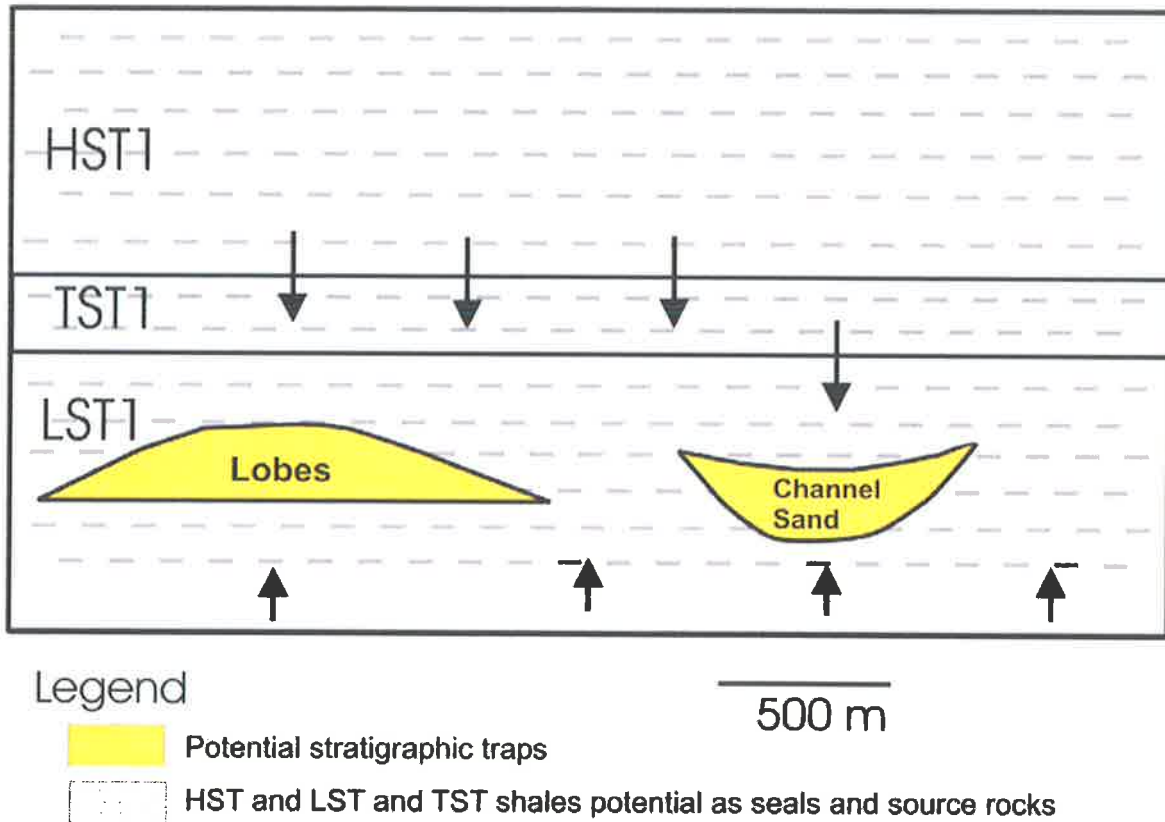


Figure 7.2 Schematic of seal and hydrocarbon migration in Sequence 1. Black arrows show the migration direction.

7.2 Sequence 2

Trapping Mechanisms

Structural traps

Similar to Sequence 1, there are no potential structural traps observed in Sequence 2. Fault 1 as indicated in Sequence 1 is still present in this sequence (Figure 5.5). The throw of the Fault 1 in Sequence 2 is 100 msec (approximately 125 m). The structure is a homocline so no anticline trap exists in the study area. The deepest contour structure in Sequence 2 is at 3500 ms (approximately 4500 m) and the shallowest contour is at 1000 ms (approximately 1200 m) (Figure 5.2).

Stratigraphic traps

Three potential stratigraphic traps were identified from four lobes in Sequence 2 (Figure 6.7). One from four lobes has been penetrated by Kalyptea-1ST1 well but there is no indication of hydrocarbon in this sequence. One of the possible reasons is the well penetrated the sand down-dip of the hydrocarbon water contact. The bed is dipping to the south, therefore it is recommended to drill a new well north of Kalyptea-1ST1 to chase the updip end of the stratigraphic trap (Table 7.1).

Hydrocarbon source and Migration

The highstand systems tracts shales in Sequence 1 and Sequence 2 and the transgressive systems tracts shales in Sequence 2 can be potential source rocks. The average initial Hydrogen Index values range from 130 to 330 mg hydrocarbons/g TOC, suggesting that the shales have a fair to good oil potential (Blevin et al., 1998b).

Reservoir Rock

The sandstone that was deposited in the lowstand systems tracts in Sequence 2 has the potential to be a reservoir rock. In this sequence, the sand is present at Kalyptea-1ST1 where it is 45 m thick (Figure 4.6), Asterias-1 where it is 85 m thick (Figure 4.6) and at Crux-1 where it is 10 m thick (Figure 4.8). From the well completion report for Asterias-1, the porosity of the sand ranges from 17 to 29 %. All of these sands were wet and one of the possible reasons is the lack of a structural trap in the area.

Potential Seals

The shale that was deposited within the transgressive systems tracts and highstand systems tracts has the potential to act as vertical seals. The shale is thick in the middle of the study area and thins to the east. The thickest shale recorded is at Adele-1 where it is 280 m thick (Figure 4.7).

7.3 Summary

- Seven potential stratigraphic traps were identified in Sequence 1 and Sequence 2 in the study area. The dip direction of the traps is to the south. To recover potential hydrocarbons it is suggested to drill new well to the north of Kalyptea-1ST1.

- The ranges average initial hydrogen index in Sequence 1 and Sequence 2 ranges from 130-330 mg hydrocarbons/g TOC suggest that the shales have fair to good oil potential (Blevin et al., 1998b). Modelling indicate that these source rocks would have generated oil in the Late Cretaceous to Early Tertiary intervals (Blevin et al., 1998b).
- Potential seals are the highstand and transgressive systems tracts shales in Sequence 1 and Sequence 2.
- The quality of reservoir rocks is good with porosity ranging from 17 to 29%.

CHAPTER 8 CONCLUSIONS AND RECOMMENDATIONS

8.1 Conclusions

1. Base on core analysis, log facies interpretation and seismic facies interpretation, the Echuca Shoals Formation in the northern Caswell Sub-basin was deposited in a deepwater environment as a lowstand wedge and fan.
2. The Echuca Shoals Formation can be divided into two sequences: Sequence 1 which is Valanginian-Hauterivian in age and Sequence 2 which was deposited in the Barremian. Each sequence consists of a lowstand systems tract, transgressive systems tract and highstand systems tract.
3. Five channels and five lobes have been identified in Sequence 1 with the average width to thickness ratio of the channels being 1:17. Four channels and four lobes have been identified in Sequence 2 with average width to thickness ratios of the channels being 1:21. The terminal lobes that feature in Sequence 1 and Sequence 2 have the potential to be stratigraphic traps due to sand pinchouts. The structural dip direction of the potential reservoir layers are to the south.
4. Isochron mapping indicates that the paleodirection of sediment supply for both Sequence 1 and Sequence 2 was from the southeast. The source of the sediment was most likely from the Asterias Delta.
5. Seismic mapping shows that the Echuca Shoals Formation was not deposited to the west of Abalone-1 due to the presence of the Scott Reef-Brecknock high trend. Two faults have been identified within Sequence 1 and Sequence 2. However, the faults did not form closures due to the subdued regional structural dip to the west.

8.2 Recommendations

1. More detailed seismic facies interpretation to check the connectivity and the geometry of the channel sands.
2. Detailed 2D and/or 3D seismic mapping to identify potential structural traps in the study area.
3. 3D seismic attribute mapping to help delineate reservoir sand distribution.
4. Combined with candidate reservoir objectives from other formations, the stratigraphic traps that are potentially present in the Echuca Shoals Formation in this study area can be potential targets for wildcat wells.

REFERENCES

- Bertram, G. T., and Milton, N. J., 1996, Seismic stratigraphy: In Emery D. and Myers, K.J. (eds), Sequence stratigraphy, 45-60.
- BHP Petroleum, 1987, Asterias-1 well completion report, BHP Petroleum (unpublished).
- Bishop, M. G., 1999, A total petroleum system of the Browse Basin, Australia: Late Jurassic, Early Cretaceous-Mesozoic, U.S. Department of the interior, U.S. Geological Survey, Open-File Report 99-50-1.
- Blevin, J. E., Boreham, C. J., Summons, R. E., Struckmeyer, H. I. M., and Loutit, T. S., 1998b, An effective Lower Cretaceous petroleum system on the North West Shelf: evidence from the Browse Basin. In: Purcell, P.G. and R.R. (eds), The Sedimentary basins of Western Australia 2: Proceedings of Petroleum Exploration Society of Australia Symposium, Perth, 397-420.
- Blevin, J. E., Struckmeyer, H. I. M., Cathro, D. L., Totterdell, J. M., Boreham, C. J., Romine, K. K., Loutit, T. S., and Sayers, J., 1998a, Tectonostratigraphic framework and petroleum systems of the Browse Basin, North West Shelf. In: Purcell, P.G. and R.R. (eds), The Sedimentary basins of Western Australia 2: Proceedings of Petroleum Exploration Society of Australia Symposium, Perth, 370-396.
- Bradshaw, J., Sayers, J., Bradshaw, M., Kneale, R., Ford, C., Spencer, L., and Lisk, M., 1998, Palaeogeography and its impact on the petroleum systems of the North West Shelf, Australia. In: Purcell, P.G. and R.R. (eds), The Sedimentary basins of Western Australia 2: Proceedings of Petroleum Exploration Society of Australia Symposium, Perth, 95-120.
- Brincat, M. P., Lisk, M., Kennard, J. M., Bailey, W. R., and Eadington, P. J., 2004, Evaluating the oil potential of the gas-prone Caswell Sub-basin: Insights from fluid inclusion studies. In: Ellis, G.K., Baillie, P.W. and Munson, T.J. (eds), Timor Sea Petroleum Geoscience. Proceedings of Timor Sea Symposium, Darwin, 19-20 June 2003. Northern Territory Geological Survey, Special Publication 1, 437-455.
- Brown Jr, L. F., and Fisher, W. L., 1977, Seismic stratigraphic interpretation of depositional systems: Examples from Brazilian rift and pull-apart basin, AAPG Memoir 24, 213-248.
- Catuneanu, O., 2006, Principles of sequence stratigraphy, Elsevier, 375 p
- Clark, J. D., and Pickering, K. T., 1996, Submarine channels: Process and architecture, London, Vallis Press, 231 p.
- Geoscience Australia, 2006, Oil and Gas Resources of Australia 2004, Geoscience Australia, Canberra.

- Hocking, R. M., Mory, A. J., and Williams, I. R., 1994, An Atlas of Neoproterozoic and Phanerozoic basins of Western Australia. In: Purcell, P. G. and R. R. (eds), *The Sedimentary basins of Western Australia: Proceedings of Petroleum Exploration Society of Australia Symposium*, Perth 1994, 21-43.
- Hoffman, N., and Hill, K. C., 2004, Structural-stratigraphic evolution and hydrocarbon prospectivity of the deep-water Browse Basin, North West Shelf, Australia. In: Ellis, G.K., Baillie, P.W. and Munson, T.J. (eds), *Timor Sea Petroleum Geoscience. Proceedings of the Timor Sea Symposium*, Darwin, 19-20 June 2003. Northern Territory Geological Survey, Special Publication 1, 373-409.
- Kennard, J. M., Deighton, I., Ryan, D., Edwards, D. S., and Boreham, C. J., 2004, Subsidence and thermal history modeling: New insights into hydrocarbon expulsion from multiple petroleum systems in the Browse Basin. In: Ellis, G.K., Baillie, P.W. and Munson, T.J. (eds), *Timor Sea Petroleum Geoscience. Proceedings of Timor Sea Symposium*, Darwin, 19-20 June 2003. Northern Territory Geological Survey, Special Publication 1, 411-436
- Longley, I. M., Buessenschuett, C., Clydsdale, L., Cubitt, C. J., Davis, R. C., Johnson, M. K., Marshall, N. M., Murray, A. P., Somerville, R., Spry, T. B., and Thompson, N. B., 2002, The North West Shelf of Australia – a Woodside perspective. In: Keep, M. and Moss, E.J. (eds), 2002, *The Sedimentary Basins of Western Australia 3: Proceedings of the Petroleum Exploration Society of Australia Symposium*, Perth, WA, 2002, 27-88.
- Maung, T. U., Cadman, S., and West, B., 1994, A review of the petroleum potential of the Browse Basin. In: Purcell, P.G. and R.R. (eds), *The Sedimentary basins of Western Australia: Proceedings of Petroleum Exploration Society of Australia Symposium*, Perth 1994, 333-346.
- McQuillin, R., Bacon, M., and Barclay, W., 1984, *An introduction to seismic interpretation*, Graham and Trotman, 287 p.
- Mitchum Jr, R. M., Vail, P. R., and Thompson III, S., 1977, Seismic stratigraphy and global changes of sea level. Part 2: The depositional sequence as a basic unit for stratigraphic analysis. In *Seismic Stratigraphy-application to hydrocarbon exploration*, AAPG Memoir 26, 53-62.
- Myers, K. J., and Milton, N. J., 1996, Concepts and principles of sequence stratigraphy: In Emery D. and Myers, K.J. (eds), *Sequence stratigraphy*, 11-41.
- Posamentier, H. W., and Vail, P. R., 1988, Eustatic controls on clastic deposition II-Sequence and system tract models: SEPM Special Publication 42, 125-154.
- Posamentier, H. W., and Erskine, R. D., 1991, Seismic expression and recognition criteria of ancient submarine fans. In Weimer, P. and Link, M. H., (eds), 1991, *Seismic facies and sedimentary processes of submarine fans and turbidite systems*, 197-222.
- Posamentier, H. W., and Allen, G. P., 1999, *Siliciclastic sequence stratigraphy: concepts and applications*, SEPM Concepts in Sedimentology and Paleontology No.7, 204 p.

- Reading, H. G., and Richards, M., 1994, Turbidite systems in deep-water basin margins classified by grain size and feeder system, *AAPG Bulletin*, V.78, 792-822.
- Richards, M., and Bowman, M., 1998, Submarine fans and related depositional system II: Variability in reservoir architecture and wireline log character, *Marine and petroleum geology*, Elsevier, 821-839.
- Richards, M., Bowman, M., and Reading, H., 1998, Submarine-fan systems I: Characterization and stratigraphic prediction, *Marine and petroleum geology*, Elsevier, 689-717.
- Richards, M. T., 1996, Deep-marine clastic system: In Emery D. and Myers, K.J. (eds), *Sequence stratigraphy*, 178-210.
- Rider, M., 1996, *The geological interpretation of well logs*, Whittles Publishing, 280 p.
- Sandwell, D. T., and Smith, W. H. F., 1995, Marine gravity from satellite altimetry (poster), The geological data center, Scripps Institute of Oceanography, La Jolla, CA 92093 (digital file, Version 7.2)
- Sloss, L. L., 1963, Sequences in the cratonic interior of North America, *Geological Society of America Bulletin*, V. 74, 93-114.
- Spry, T. B., and Ward, I., 1997, The Gwydion discovery: a new play fairway in the Browse basin, *The APPEA Journal*, 37 (1) 87-104.
- Struckmeyer, H. I. M., Blevin, J. E., Sayers, J., Totterdell, J. M., Baxter, K., and Cathro, D. L., 1998, Structural evolution of the Browse Basin, North West Shelf: New concepts from deep-seismic data. In: Purcell, P.G. and R.R. (eds), *The Sedimentary basins of Western Australia 2*, 345-367.
- Symonds, P. A., Collins, C. D. N., and Bradshaw, J., 1994, Deep structure of the Browse Basin: Implications for the basin development and petroleum exploration. In Purcell, P.G. and R.R. (eds), *The Sedimentary Basins of Western Australia: Proceedings of Petroleum Exploration Society of Australia Symposium, Perth 1994*, 315-331.
- Vail, P. R., 1987, Seismic stratigraphy interpretation using sequence stratigraphy, part 1, in A.W. Bally, ed., *Atlas of seismic stratigraphy: AAPG Studies in Geology no. 27*, 1-10.
- Van Wagoner, J. C., Posamentier, H. W., Mitchum, R. M., Vail, P. R., Sarg, J. F., Loutit, T. S., and Hardenbol, J., 1988, An overview of the fundamentals of sequence stratigraphy and key definitions. In Wilgus, C.K., Hastings, B.S., Kendall, C.G.St.C., Posamentier, H.W., Ross, C.A., and Van Wagoner, J.C. (Eds.), *Sea-level changes: An integrated approach*, SEPM (Society of Economic and Paleontologists and Mineralogists), Tulsa, Oklahoma, Special Publication, 39-45.
- Van Wagoner, J. C., Mitchum, R. M., Campion, K. M., and Rahmanian, V. D., 1990, Siliciclastic sequence stratigraphy in well logs, cores, and outcrops, *AAPG Methods in Exploration Series*, No. 7, 55 p.

- Weimer, P., 1991, Seismic, Facies, Characteristics, and Variations in Channel Evolution, Mississippi Fan (Plio-Pleistocene), Gulf of Mexico. In Weimer, P and Link, M.H. (eds), Seismic Facies and Sedimentary Processes of submarine Fans and Turbidite systems, 323-347.
- Weimer, P., and Slatt, R. M., 2004, Petroleum System of deepwater settings, 2004, Distinguished Instructor Short Course, Society of Exploration Geophysicists, Series No 7.
- Yeates, A. N., Bradshaw, M. T., Dickins, J. M., Brakel, A. T., Exon, N. F., Langford, R. P., Mulholland, S. M., Totterdell, J. M., and Yeung, M., 1987, The Westralian Superbasin: an Australian link with Tethys, International Symposium on Shallow Tethys, 2, A.A. Balkema, Rotterdam, 199-213.